

Submitted to *The Astrophysical Journal*

A Comparison of the Afterglows of Short- and Long-Duration Gamma-Ray Bursts

M. Nysewander^{1,2}, A.S. Fruchter¹ & A. Pe'er^{1,3}

ABSTRACT

We present a comparative study of the observed properties of the optical and X-ray afterglows of short- and long-duration γ -ray bursts (GRBs). Using a large sample of 37 short and 421 long GRBs, we find a strong correlation between the afterglow brightness measured after 11 hours and the observed fluence of the prompt emission. Both the optical (R band) and X-ray flux densities (F_R and F_X) scale with the γ -ray fluence, F_γ . For bursts with a known redshift, a tight correlation exists between the afterglow flux densities at 11 hours (rest-frame) and the total isotropic γ -ray energy, $E_{\gamma,\text{ISO}}$: $F_{R,X} \propto E_{\gamma,\text{ISO}}^\alpha$, with $\alpha \simeq 1$. The constant of proportionality is nearly identical for long and short bursts, when $E_{\gamma,\text{ISO}}$ is obtained from the Swift data. Additionally, we find that for short bursts with $F_\gamma \gtrsim 10^{-7}$ erg cm $^{-2}$, optical afterglows are nearly always detected by reasonably deep early observations. Finally, we show that the ratio F_R/F_X has very similar values for short and long bursts. These results are difficult to explain in the framework of the standard scenario, since they require that either (1) the number density of the surrounding medium of short bursts is typically comparable to, or even larger than the number density of long bursts; (2) short bursts explode into a density profile, $n(r) \propto r^{-2}$ or (3) the prompt γ -ray fluence depends on the density of the external medium. We therefore find it likely that either basic assumptions on the properties of the circumburst environment of short GRBs or else the standard models of GRB emission must be re-examined. We believe that the most likely solution is that the ambient density surrounding typical short bursts is higher than has generally been expected: a typical value of ~ 1 per cm $^{-3}$ is indicated. We discuss recent modifications to the standard binary merger model for short bursts which may be able to explain the implied density.

¹Space Telescope Science Institute, 3700 San Martin Dr, Baltimore, MD, 21218

²Alion Science & Technology, 1000 Park Forty Plaza, Durham, NC 27713; mnysewander@alionscience.com

³Giacconi Fellow

Subject headings: gamma rays: bursts — radiation mechanism: nonthermal

1. Introduction

Although the past decade has seen great progress in characterizing the afterglows of long-duration GRBs (LGRBs), the afterglows of short-duration GRBs (SGRBs) remain elusive. The average fluence of an SGRB is an order of magnitude fainter than that of an LGRB, and thus while SGRBs have been localized by *Swift*, about ten long bursts are localized for every short burst. Optical afterglows of SGRBs have been detected, but are notoriously dim, and large-aperture telescopes are generally required to detect them. Nearly half of all SGRBs have a fluence less than 10^{-7} ergs cm $^{-2}$ and none of these have a detected optical afterglow. SGRB X-ray afterglows are commonly detected, but are faint and less likely to be rapidly localized with their positions distributed in real-time, further complicating optical ground-based observations. As a result, only a few well-sampled, robust optical SGRB light curves exist that span a wide range of time or frequency.

The faintness of the afterglows of short GRBs (compared to the long GRBs) has been attributed to properties of the progenitor and circumburst environment. While the LGRB-SN connection is strong, the progenitors of SGRBs are less certain. Observations have shown that long-duration GRBs are associated with the deaths of massive stars (Stanek et al. 2003; Hjorth et al. 2003a; see Woosley & Bloom 2006 for a comprehensive review). However, a number of models exist for the progenitors of SGRBs. The leading model is a binary pair of compact objects, dual neutron stars, or a neutron star and black hole, which merge in a dramatic explosion causing a burst of γ -rays (Eichler et al. 1989; Narayan et al. 1992; Lee et al. 2005) powered by accretion onto the newly formed compact object.

It is commonly believed that the difference in the long and short progenitors implies that they reside in different environments (for a recent review, see Nakar 2007). Because LGRBs are associated with massive stars, they will lie in or near dense regions of active star-formation. SGRBs progenitors can have long lifetimes and do not need to be in galaxies with active star-formation, nor be associated with dense regions. In fact, the observed diverse host galaxy morphology is roughly consistent with the expected wide range of progenitor lifetimes (Belczynski et al. 2006a).

Two of the first detected SGRB afterglows, those of GRB 050509B (Gehrels et al. 2005) and GRB 050724 (Berger et al. 2005), were found near bright, giant elliptical galaxies. GRB 050709 (Hjorth et al. 2005) and GRB 051221A (Soderberg et al. 2006a) both occurred in late-type galaxies with ongoing star-formation. However, within these late-type galaxies,

SGRBs do not necessarily trace areas of active star-formation as is the case with LGRBs (Bloom et al. 2002; Fruchter et al. 2006), rather, they can occur in low luminosity outer regions of the galaxy (e.g. GRB 050709; Fox et al. 2005, GRB 060121; Levan et al. 2006b). Some theories of the formation of compact object binaries include a violent supernova-induced *kick* that can offset them from their host galaxy (Belczynski et al. 2006b) and may place them in these low density environments.

The low environmental densities into which SGRBs occur have an observational implication. Within the context of the standard afterglow model (e.g. Mészáros & Rees 1997; Sari et al. 1998) for observing frequencies below the cooling frequency (and above the peak frequency), the afterglow flux is proportional to the density of the external medium to the power 1/2. Well-sampled, multiwavelength observations of LGRB afterglows have suggested that at half a day, the cooling frequency generally lies between the optical and X-ray frequencies (e.g. Galama et al. 1998b; Harrison et al. 1999; Panaiteescu & Kumar 2002; Soderberg et al. 2006a). It is therefore expected that the differences in the density of the circumburst medium between the long and short bursts would affect the late time optical emission, which is below the cooling break. (Note that according to the standard model, the flux above the cooling break is independent of the external medium density, n . Thus, the flux at the X-ray frequency may not be affected by the difference in densities. See discussion in §4 below).

In addition to depending on the environment, we also expect the absolute afterglow brightnesses to be proportional to the total energy released in the burst. The intrinsic energy release of short burst progenitors is not well-known because the current redshift distribution of SGRBs is fragmentary. The average redshift of the SGRB distribution is $\langle z \rangle = 0.5$ with $E_{ISO} \sim 10^{48} - 10^{51}$, compared to $\langle z \rangle = 1.9$ and $E_{ISO} \sim 10^{49} - 10^{53.5}$ for LGRBs. However, it is unclear to what extend these differences are a result of observational biases and/or true intrinsic differences in luminosity or collimation in comparison with LGRBs. No SGRB absorption redshifts have been measured, which is likely due to the lower afterglow brightness and possibly a less dense external medium on which to imprint strong absorption lines. Therefore, because all SGRB redshifts have been measured from optical emission lines in host galaxies, the current sample of redshifts is limited to $z \lesssim 1$. Berger et al. (2007a) have noted that the lack of bright galaxies in the error circles of a number of XRT localizations may suggest that a number of short bursts without optical identifications may lie at $z > 1$. Finally we note that the E_{ISO} values presented here are either based upon the γ -ray fluence observed by the Swift Burst Alert Telescope (BAT) or for the smaller non-Swift sample, scaled to the BAT sensitivity. Because the BAT is only sensitive up to 150 keV, these values underestimate the total prompt emission of all bursts. However, this is most severe on short bursts, which tend to have a harder spectrum than long bursts. We return to this point in

more detail later.

In this paper we compare the optical and X-ray afterglows measured after 11 hours (a standard *Swift* timescale) with the prompt energy emission of both long- and short-duration γ -ray bursts, and compare these results with afterglow theory. We test the predictions of the standard model with a large data set that spans over six decades in energy. We find that SGRBs afterglows are very similar to low-luminosity LGRBs afterglows. Surprisingly, we find that the afterglow brightnesses depend little upon the classification of long or short; rather, the bursts scale primarily with the high-energy prompt emission. Our result is difficult to reconcile with standard afterglow theory, and contradicts previous claims that SGRB optical afterglows are dim due to the density of their surrounding medium (Panaitescu et al. 2001; Nakar 2007; Berger 2007a).

This paper is organized as follows: In §2 we detail the steps taken to gather the data presented herein. We compare the prompt and afterglow emission of the two populations in §3. In §4, we explore the assumptions of the standard model, under what conditions the results are valid, and implications related to host galaxies and intrinsic SGRB energies. We show that the afterglow data implies that either (1) the environment of short GRBs is comparable to that of long GRBs, (2) SGRBs explode into a wind profile, or (3) the prompt emission fluence depends on the environment. In §5 we discuss the statistical significance of our data sample. We summarize and draw final conclusions in §6.

2. Data

In this study, we include GRBs detected by all satellites, beginning with GRB 970111, the first localization with follow-up observations capable of detecting an afterglow, and ending over a decade later, with GRB 071227. To be included in the analysis, a GRB must have published values of the prompt emission and had optical or X-ray afterglow follow-up observations within a few days of the burst. 421 LGRBs and 37 SGRBs have been included in the sample, out of which 408 LGRB and 37 SGRB have optical and 299 LGRBs and 27 SGRB have X-ray follow-up observations. For each GRB, Tables 1 and 2 present the short and long prompt gamma-ray fluence, X-ray afterglow flux at eleven hours, and optical *R*-band magnitude at eleven hours (times here are measured in the observer’s frame). We also include basic properties of the burst: the satellite and frequency range of the prompt data and the redshift, if known. The data come from over 700 unique sources; these sources are listed in the tables. We thoroughly searched the literature to provide the most accurate values. Only the first page of Table 2 is presented in the printed version of this paper. The entire table can be found in the Electronic Supplement.

The decision of whether a burst is classified as *short* or *long* is based upon many factors in the prompt emission and not merely on the burst duration. When a burst’s sub-type is questionable, we adopt the classification published by the instrument team. Formal measures of T_{90} do not always accurately distinguish long from short, such as in cases where we observe a short hard spike followed by a long, soft tail of emission (e.g. GRB 050724 or GRB 051227; Barthelmy et al. 2005a,b). Some bursts, notably GRB 040924 and GRB 050925, have short durations but soft emission, hence are likely the tail-end of the long-duration population (Huang et al. 2005; Holland et al. 2005). GRB 050911 has a complex BAT γ -ray light curve that may be interpreted as short, but because it is not conclusively in either category (Page et al. 2006a), it is not included.

Our primary sources for GRB fluence and duration are published catalogues, such as those for *Swift* (Sakamoto et al. 2008) or *HETE* (Sakamoto et al. 2005), however some are taken from refereed papers or, if no other source is available, from GCN Circulars. If no error is given in the original publication, we assume that the GRB is detected at the 3σ level. Because this data set includes bursts discovered by many satellites, we list in tables 1 and 2 the frequency range in which the prompt emission is observed.

All fluences have been transformed into the *Swift* 15–150 keV fluence range by determining empirical transformations derived from bursts that were detected by multiple satellites. For all bursts with detections by more than one satellite, we calculate the fluence ratio between the two detectors, and the deviation about this ratio. Due to sparse data and lack of overlap in mission lifetimes, in many instances it is necessary to perform multiple transformations to arrive at the final *Swift* BAT fluence (e.g. using the *Ulysses* to *Swift* ratio in order to relate *INTEGRAL* and *Swift*). However, the additional scatter introduced in doing so is included in the final ratio error. We jointly calculate the transformation for the similar *HETE* 25–100 keV, *Ulysses* 25–100 keV, and *BATSE* 20–100 keV bands, and find the ratio to *Swift* to be 1.65 ± 0.31 . The high-energy *Konus-Wind* (typically 20–2000 or 20–10000 keV) and *RHESSI* (30–10000 keV) fluences were similarly grouped and found to have a rough transformation ratio of 0.37 ± 0.23 into the *Swift* range. Few bursts (seven) had joint detections with *INTEGRAL* (20–200 keV); these indicate a ratio of 0.95 ± 0.68 . The *HETE* (30–400 keV) ratio is calculated to be 0.63 ± 0.32 , and the *BeppoSAX* ratio is 0.67 ± 0.45 . The scaling and large additional errors introduced by this method compensate for the additional scatter caused by comparing bursts between different detectors. If we restrict our analysis to *Swift* bursts only, our results do not significantly change.

X-ray fluxes, corrected for Galactic extinction, are primarily taken from large-scale uniform studies that fit light curves to estimate the flux at eleven hours, such as those for *Swift* (Gehrels et al. 2008) or *BeppoSAX* (de Pasquale et al. 2006) GRBs. For bursts not

included in these studies, we obtained data from refereed papers, the *Swift* XRT Lightcurve Repository (Evans et al. 2007), or GCN Circulars. Nearly all X-ray afterglow fluxes are given in the 0.3–10 keV range, however a few were reported in a different energy range and these are noted in Tables 1 and 2. For the few bursts with no reported Galactic extinction, we estimated the extinction from the neutral hydrogen column density using the Chandra Colden and PIMMS online calculators. These bursts are noted in Tables 1 and 2. In a few instances where no error is given, we assume that the source is detected at the 3σ level. We choose detections or limits as close to eleven hours as possible that we then extrapolated using temporal slopes of $\alpha_{S,X} = -1.22 \pm 0.37$ and $\alpha_{L,X} = -1.17 \pm 0.30$ for SGRBs and LGRBs respectively. These slopes are averages derived from power-law fits that we performed of the light curves of all bursts observed by XRT until December 31st 2007 that have a well-defined temporal slope based on data that extend from minutes until at least eleven hours after the burst. Figure 1 presents a histogram of these slopes and corresponding Gaussian least-squares fit to the scatter in the population. The original measurement error and the error associated with the extrapolation are added in quadrature to determine the final error reported in the tables.

Optical magnitudes are obtained from refereed papers when available and from GCN Circulars when not. We chose observations taken as close to eleven hours as possible, preferably in the *R*-band. All optical magnitudes have been corrected for Galactic extinction using the method presented in Schlegel et al. (1998). If no error is given, as is often the case for GCN derived magnitudes, we again assume that the source is detected at the 3σ level. These data are extrapolated in time using a temporal slope of $\alpha_{L,opt} = -0.85 \pm 0.35$ for long and $\alpha_{S,opt} = -0.68 \pm 0.20$ for short GRBs, and in frequency using a spectral slope of $\beta = -1.0$. Because of a lack of early optical data, the optical indices are averages based on all afterglow observations with data that extend from at least three hours until after eleven hours following the burst. We fit power-laws to the afterglows of the five SGRBs and 81 LGRBs that fit this selection criteria. Figure 2 presents a histogram of these slopes and Gaussian least-squares fit to the scatter. The original measurement error and the error associated with the extrapolation are added in quadrature to determine the final error.

Often, multiple optical limiting magnitudes exist for a given GRB, and in that case, we took care to choose the one that is most constraining. This sometimes can be arbitrary since the level of constraint depends upon the intrinsic shape of the light curve and redshift of the progenitor, both of which are unknowns given a non-detection. At early times, optical afterglows are often not simple power-laws so we avoided limiting magnitudes taken in the first few minutes. Additionally, we require that >95% of the satellite-localized error circle be covered by optical observations, and we assume that the limiting magnitude of the DSS is $R = 20$.

The computed average optical indices are significantly shallower than the X-ray indices. One may expect an observational bias to be introduced because we may be preferably selecting afterglows with shallower temporal decays, because afterglows are typically more difficult to observe in the optical than in the X-ray. In order to show that our analysis is unbiased, we made the following test. We selected X-ray indices by the criteria of the GRB having an optical detection, and through this, we applied the same optical selection effect to the X-ray. When making this selection, we found that the average X-ray temporal slopes remain nearly unchanged (-1.19 versus -1.16). Therefore, we conclude that the difference between the optical and X-ray temporal indices is real and is not an observational effect.

3. Data Analysis

The entire sample of 421 long and 37 short bursts are presented in Tables 1 and 2 and are plotted in Figures 3 and 4. Figure 3 presents the optical brightness at eleven hours (observer frame) versus the prompt high-energy fluence; Figure 4 presents the X-ray brightness at eleven hours (observer frame) versus the prompt fluence. In both figures, we see the same trend: GRBs with high fluence or energy have greater brightness in both optical and X-ray. Not unexpectedly, at both high and low afterglow wavelengths, there is a large intrinsic scatter in the data; the full width in the optical distribution spans nearly four orders of magnitude. A portion of the scatter is certainly intrinsic to the population – we do not expect tight linear correlations. However, the scatter in the optical is larger than in the X-ray, and this may be partially due to observational effects. The optical data comes from a wider variety of sources: different telescopes, filters, instruments, observing teams, reduction and calibration methods, etc. Line-of-sight source-frame absorption may also play a role in the large optical scatter.

The 126 long and 15 short bursts with measured redshift are presented in the rest-frame in Figures 5 and 6. Figure 5 plots the optical, while Figure 6 plots the X-ray luminosities versus the prompt γ -ray energy, $E_{\gamma,\text{ISO}}$. As discussed above, these plots exhibit a clear correlation between the afterglow brightness at eleven hours and the prompt GRB fluence (note that in figures 5, 6 and 7 the time is measured in the source frame, and thus is redshift corrected with respect to the observed time). Eight of the short bursts have redshifts derived from hosts found with accurate optical positions or are associated with Abell clusters, while seven have hosts determined by XRT error circles only. These seven bursts are differentiated from the bursts with secure redshifts in Figures 5 and 6, but are included in the fit detailed below. In calculating the isotropic equivalent energy emitted in γ -rays, $E_{\gamma,\text{ISO}} = 4\pi F_\gamma d_L^2(1+z)^{-1}$, the luminosity distance, d_L is determined assuming $H_o = 71 \text{ km s}^{-1} \text{ Mpc}^{-1}$, $\Omega_M = 0.27$,

$\Omega_\Lambda = 0.73$. We transformed the optical data from observer frame filters to rest-frame R -band using an assumed spectral slope of $\beta = -1$. The unabsorbed X-ray fluxes have been transformed to 5 keV in the source frame assuming the integrated flux has a spectral slope of $\beta = -1$ between 0.2–10 keV in the observer frame.

While the existence of correlations for each of the two populations by themselves is not surprising, it is clear from Figures 5 and 6 that the distributions of the long and short bursts over-lap in both prompt and afterglow energies. In afterglow brightness, both the observed and rest-frame populations overlap such that for a given fluence, the two classes are not significantly different. In each instance, both in optical and X-ray, and in observer and rest-frame, the afterglow brightnesses scale roughly as a power-law with energy. Therefore, we model the data as a one-dimensional Gaussian distribution about a straight line in log-log space: $\log(F_{R,X}) = a + \alpha \log(E_{\gamma,\text{ISO}})$. We take into account errors in both coordinates by minimizing the χ^2 merit function:

$$\chi^2(a, \alpha) = \sum_{i=1}^n \frac{(y_i - a - \alpha x_i)^2}{\sigma_{y_i}^2 + \alpha^2 \sigma_{x_i}^2} \quad (1)$$

where we have fit to the line $y(x) = a + \alpha x$. We note that physically, $y(x) \equiv \log(F_{R,X})$, $x \equiv \log(E_{\gamma,\text{ISO}})$, and σ_{x_i} and σ_{y_i} are the x and y standard deviations for the i th point. The errors alone over-constrain the linear fit and produce poor χ^2 merit values. Therefore, in order to compensate for the intrinsic width of the distribution, we add a constant 1/3 dex error to each error bar to mimic the scatter effect. Increasing the assumed population width past 1/3 dex does not significantly affect the final best fits. Our fits using this technique can be found in Table 3. The slopes and intercepts of the long and short burst distributions are equivalent, within our ability to fit them. While the small number of short bursts means that the errors on a combined slope and intercept fit are large, if we restrict the slope to $\alpha = 1$, then the intercepts (*i.e.* the brightnesses) of the two distributions are found to be the same well within the error of ~ 0.2 dex.

The X-ray sample is dominated by observations performed by *Swift*, and therefore provides a largely homogeneous sample for our analysis. However, the interpretation of the optical data is hindered by the vast diversity of follow-up programs and typical depths of searches. Many optical limits exist for bursts which do not constrain the distribution, while some are deeply constraining. Without knowing the intrinsic source-frame extinction, it is not possible to determine whether these reflect the intrinsic scatter in the distribution or if they are a result of line-of-sight effects. Limits of X-ray afterglows are rare and often due to a delayed follow-up program rather than intrinsic dimness of the afterglows. Therefore, we do not fit to limits in our analysis in either optical or X-ray. However, ignoring limits may introduce a selection bias to the fits.

Figures 3 and 4 plot observer-frame quantities and therefore have not been corrected for distance. Given a broadly homogeneous population, we expect the effect of distance to dominate the slope of the populations. In a Euclidean universe we would expect the slope imposed to be $\alpha = 1$. The real universe, of course, is expanding, and there is a factor of $1 + z$ difference between the correction of a bolometric luminosity and a flux. However, if, as is frequently found, the spectral slope of the afterglow is $\beta \sim -1$, this factor of $1 + z$ is largely canceled by the k-correction. And this may largely be responsible for the excellent consistency between the populations seen in the Figures and Table 3.

In Figures 5 and 6 we show the subset of bursts with published redshifts. Compared to the previous plots, the scatter in both figures has been reduced. It is clear from both figures, that the dominant predictor of afterglow brightness is the prompt energy emission. The fits to the optical and X-ray flux, given in Table 4 are quite consistent between long and short bursts. If we again assume that the afterglow luminosities scale directly with energy, and impose a slope of $\alpha = 1$ on the rest-frame distributions, we find that the long bursts are only brighter on average than the short bursts for a given $E_{\gamma,\text{ISO}}$ by about a factor of two, while the long bursts themselves vary in brightness in the X-ray and optical by orders of magnitude for a given $E_{\gamma,\text{ISO}}$. However, this difference is only at the $\sim 1\sigma$ level and thus may be entirely statistical rather than real. We note here that similar results to those discussed so far have been derived by two other groups working contemporaneously, Gehrels et al. (2008) and Kann et al. (2009).

Readers may be concerned by the fact that we have not corrected the Swift data for the loss of total fluence in the γ -ray due to the rather low high-energy cutoff of the Swift BAT – 150 keV. This is well below the peak of the spectral energy distribution of most short bursts, although it is above the peak for most LGRBs with $E_{\gamma,\text{ISO}} \lesssim 10^{52.5}$ ergs (Amati 2006). Thus we may be underestimating the true γ -ray fluence of the short burst compared to the long bursts in some cases by up to a factor several (Kann et al. 2009), particularly at low values of $E_{\gamma,\text{ISO}}$ where the two types of bursts overlap. However, this correction would affect the plots of the afterglow flux density in the optical and X-ray versus $E_{\gamma,\text{ISO}}$ similarly. As we will show in the next section, it is the ratio of the optical afterglow flux density to that in the X-ray which provides this paper’s real insight into the density of the media surrounding the bursts, and this ratio is unaffected by corrections to E_{γ} or $E_{\gamma,\text{ISO}}$.

4. A Comparison of Theory with Observations

4.1. The Standard Model

In order to compare the results presented in the previous section to the predictions of the standard model of GRB afterglow emission, we first give a short description of the model’s predictions (For a much more detailed introduction to the theory see, e.g., Sari et al. 1998). Afterglow emission follows the propagation of a relativistic shock wave that moves through the cold ambient medium, whose density is assumed constant, $n = 1n_0 \text{ cm}^{-3}$. A canonical value of $n_0 = 1$ is often used in the literature for LGRBs, but values fitted from afterglow light curves and spectra of long GRBs range from $\sim 10^{-3}$ to $\sim 10^2$ (e.g., Panaiteescu & Kumar 2002; Soderberg et al. 2006a). The shock wave moves in a self-similar motion (Blandford & McKee 1976), which implies shocked fluid Lorentz factor $\Gamma(E, n, R) = (17E/16\pi nm_p c^2 R^3)^{1/2}$. Here, $E \equiv E_{\text{ISO}}$ is the total explosion energy¹, and R is the radius of the shock wave, which is related to the observed time via $t \approx R/4\Gamma^2 c$ (Waxman 1997).

The shock wave accelerates electrons and generates magnetic field. The accelerated electrons assume power law distribution $n_{el}(\gamma)d\gamma \propto \gamma^{-p}d\gamma$ above $\gamma_m = \epsilon_e(m_p/m_e)g(p)\Gamma$. Here, ϵ_e is the fraction of post-shock thermal energy that goes into the electrons, Γ is the Lorentz factor of the shocked fluid, and $g(p)$ is a function of the power law index of the accelerated electrons, $g(p) = (p - 2)/(p - 1)$ for $p > 2$, $g(p) = \log(\gamma_{\max}/\gamma_m)^{-1} \approx 1/7$ for $p = 2$, where γ_{\max} is the maximum Lorentz factor in which power law distribution of the electrons exist (e.g., Pe’er & Waxman 2005). A fraction ϵ_B of the post shock thermal energy is assumed to be converted to the magnetic field. With these definitions, synchrotron flux peaks at observed frequency

$$\nu_m^{ob} = \frac{3}{4\pi} \Gamma \gamma_m^2 \frac{qB}{m_e c} = 7.8 \times 10^{12} g(p)^2 (1+z)^{1/2} E_{52}^{1/2} \epsilon_{e,-1}^2 \epsilon_{B,-2}^{1/2} t_d^{-3/2} \text{ Hz}, \quad (2)$$

where $Q = 10^x Q_x$ in cgs units was used, and the observed time is measured in days.

The peak of the observed spectral flux at ν_m is

$$F_{\nu, \text{max}}^{ob} = \frac{1}{4\pi d_L^2} N_e P_{\nu_m} \approx \frac{N_e}{4\pi d_L^2} \frac{P_{tot}}{\nu_m^{ob}} = 7.3 (1+z) d_{L,28}^{-2} E_{52} \epsilon_{B,-2}^{1/2} n_0^{1/2} \text{ mJy}, \quad (3)$$

where $P_{tot} = \Gamma^2(4/3)c\sigma_T\gamma_m^2(B^2/8\pi)$ is the total synchrotron power radiated by electrons at γ_m , σ_T is Thomson cross section, and $N_e = 4\pi R^3 n/3$ is the total number of radiating electrons. In estimating the observed flux, luminosity distance $d_L = 10^{28} d_{L,28} \text{ cm}$ is assumed.

¹Note the difference between the total explosion energy E_{ISO} , and the energy emitted in γ -rays, $E_{\gamma, \text{ISO}}$.

The synchrotron peak flux frequency is below the break frequency ν_c , the characteristic synchrotron emission frequency of electrons for which the synchrotron cooling time, $6\pi m_e c / B^2 \sigma_T \gamma_c (1 + Y)$ is comparable to the ejecta (rest frame) expansion time, $\sim r/\Gamma c$,

$$\nu_c^{ob} = 4.0 \times 10^{15} (1 + Y)^{-2} (1 + z)^{-1/2} E_{52}^{-1/2} \epsilon_{B,-2}^{-3/2} n_0^{-1} t_d^{-1/2} \text{ Hz.} \quad (4)$$

Here, Y is the Compton parameter. As we show below, for the canonical parameters values used here, after 11 hours $Y \ll 1$. Therefore, the inclusion of Y does not change the parametric dependence of ν_c .

The results in equation 2 indicate that the peak frequency is below the optical band ($\nu_R = 5 \times 10^{14}$ Hz) after 11 hours, even for equipartition values of ϵ_e and ϵ_B . Since $\nu_c > \nu_m$, (the “slow cooling” regime), the flux at frequencies above ν_m is given by

$$F_\nu^{ob} = \begin{cases} F_{\nu,\max}^{ob} (\nu/\nu_m)^{-(p-1)/2}, & \nu_m < \nu < \nu_c, \\ F_{\nu,\max}^{ob} (\nu_c/\nu_m)^{-(p-1)/2} (\nu/\nu_c)^{-p/2}, & \nu_c < \nu. \end{cases} \quad (5)$$

4.2. The Comparison

Two of the primary observational results obtained in this paper, summarized in figures 5 and 6, can now be compared to the predictions in equations 2 – 5. For bursts with known redshift, E_{ISO} and observed time $t_d = 11/24$, adopting the assumption that $2 \leq p \leq 2.5$, there are 3 free parameters whose values are unknown: the ambient medium number density n and the parameters ϵ_e and ϵ_B . In order to remove some of the degeneracy, we look at the ratio of the fluxes at the R and the X bands. This ratio for the long and short GRBs is presented in Figure 7.

While the peak flux frequency is below the optical (R) band, the value of the cooling break depends on the density of the ambient medium and on ϵ_B . Thus, three options exist:

1. The break frequency is above the observed X-ray frequency, $\nu_R < \nu_X = 1.25 \times 10^{18}$ Hz $< \nu_c^{ob}$. In this case the ratio of the fluxes at the R and X-ray bands is predicted by equation 5 to be $F_R/F_X = (\nu_x/\nu_R)^{(p-1)/2} = 50$ (for $p=2$). This ratio is inconsistent with the results presented in Figure 7, which clearly indicate a ratio $F_R/F_X \simeq 1 - 2 \times 10^3$ for both the short and long bursts. The flux ratio increases with p , and for $p = 2.5$ it is ~ 350 . Still, this is lower than that observed for the vast majority of bursts, and is more than an order of magnitude below the ratio of many.
2. The break frequency is in between the optical and the X-ray bands, $\nu_R < \nu_c^{ob} < \nu_X$. As noted earlier many studies of afterglows from long GRBs have found this to be

the case (e.g. Galama et al. 1998b; Harrison et al. 1999; Panaiteescu & Kumar 2002; Soderberg et al. 2006a). Indeed, in this situation, the expected ratio of the fluxes, $F_R/F_X = (\nu_x/\nu_R)^{(p-1)/2}(\nu_x/\nu_c)^{1/2} = 720 E_{52}^{1/4} \epsilon_{B,-2}^{3/4} n_0^{1/2}$ (calculated for ν_c after 11 hours and for $p = 2$) is consistent with the results obtained in Figure 7 for the long bursts. For $p = 2.5$, this ratio is somewhat higher $\approx 5 \times 10^3 E_{52}^{1/4} \epsilon_{B,-2}^{3/4} n_0^{1/2}$, which is slightly above the results in Figure 7.

On the other hand, for characteristic energy $E \simeq 10^{50}$ erg typical for the short bursts, this ratio is $F_R/F_x \simeq 130 E_{50}^{1/4} \epsilon_{B,-2}^{3/4} n_0^{1/2}$ (for $p = 2$), nearly an order of magnitude lower than the result obtained in Figure 7 for the short bursts. For $p = 2.5$, the obtained value is $F_R/F_x \simeq 1600 E_{50}^{1/4} \epsilon_{B,-2}^{3/4} n_0^{1/2}$, consistent with the results in this figure. The value of $F_R/F_X \approx 1600$ is obtained for values of the ambient number density of short bursts which are comparable to that expected for long bursts, $n_0 = 1$. Lower values of the number density would be inconsistent with the results in Figure 7, unless the value of ϵ_B is larger for short bursts than for the long ones. This discrepancy is further aggravated by observed F_R/F_x values around 10^4 for several short bursts. It is hard to make these consistent with the theory using any set of parameters consistent with standard expectations.

3. The third possibility is that the cooling frequency is below the R band, i.e., $\nu_c^{ob} < \nu_R < \nu_X$. Using equation 5 one obtains the ratio of the R to X-ray fluxes to be $F_R/F_X = (\nu_x/\nu_R)^{p/2} = 2500$ (for $p = 2$), which is consistent with the results presented in Figure 7. On the other hand, the requirement that $\nu_c^{ob} < \nu_R$ for short GRBs for which $E = 10^{30}$ erg implies $n_0 > 130\epsilon_{B,-2}^{-3/2}$. Even for equipartition value of the magnetic field this requirement implies value of n which is at least as high for short GRBs as for the long GRBs.

The analysis presented above implies that under the assumption of the synchrotron emission model, the characteristic values of the number densities of short GRBs are required to be at least similar to the characteristic values obtained for long GRBs, $n \gtrsim 1 \text{ cm}^{-3}$. Lower values of the number density in short bursts require stronger magnetic field. Moreover, the results hint toward power law index $p \simeq 2.5$ in short bursts.

The ratios calculated above are done in the framework of the standard model, which assumes knowledge of total explosion energy E_{ISO} , while for bursts with measured redshift we only measure the energy emitted in γ rays, $E_{\gamma,\text{ISO}}$. However, as we show in §4.3 below, the efficiency in converting the explosion energy into γ rays is very high, $E_{\gamma,\text{ISO}}/\epsilon_e E_{\text{ISO}} \simeq 1$ for both the long and short bursts. We note that in principle it is possible that the average values of the microphysical parameter ϵ_e , ϵ_B and the power law index p are different for short and long GRBs, which may affect our result. However, we find this possibility unlikely, since

after 11 hours both types of bursts are well in the self-similar phase, in which the properties of the blast wave - that determines the values of these parameters - are well defined.

The basic results found do not change if one assumes that the flux at the X-ray band is dominated by Compton scattering (see, e.g., Sari & Esin 2001; Zhang & Mészáros 2001). For $\nu_c^{ob} < \nu_X$ and $\nu_m^{ob}\gamma_m^2 < \nu_X < \nu_c^{ob}\gamma_m^2$, one obtains the ratio of the Compton to the synchrotron flux at the X-band to be $F_{X,IC}/F_{X,syn} \approx (16/3)\sigma_T n r \gamma_m^{p-1} (\nu_x/\nu_c)^{1/2} = 2.8 \times 10^{-2} g(p) E_{52}^{5/8} \epsilon_{e,-1}^{3/4} \epsilon_{B,-2}^{9/8} n_0^{9/8} t_d^{1/8}$, where $p = 2$ is assumed. This ratio clearly indicates that inverse Compton emission does not dominate the flux at the X band unless the number density is significantly higher than $n_0 = 1$. Therefore, addition of IC component does not ease the requirement for high values of the number density in short GRBs.

We have so far assumed that the density of the ambient medium is constant, i.e. independent of radius from the burst. This, however, may not be the case. Motivated by the association of long GRBs to the deaths of massive stars, some authors (c.f. Woosley 1993; Paczynski 1998) have proposed that the explosion producing a GRB may occur into a wind, ejected by the progenitor prior to its explosion. This scenario results in an ambient matter density profile, $\rho(r) = Ar^{-2}$, with characteristic value $A = 5 \times 10^{11} A_* \text{ gr cm}^{-2}$ typical for Wolf-Rayet star (Chevalier & Li 2000).

In an explosion into density profile, the evolution of the Lorentz factor of the flow in its similar expansion phase is $\Gamma(E, r) = (9E/16\pi\rho c^2)^{1/2}r^{-3/2}$, and the relation between the radius of the shock front and the observed time is $t \approx r/2\Gamma^2 c$ (Pe'er & Wijers 2006). Similar calculations to the ones presented in equations 2 – 4 results in (see, e.g., Panaitescu & Kumar 2001)

$$\begin{aligned} \nu_m^{ob.} &= 1.6 \times 10^{11} g(p)^2 (1+z)^{1/2} E_{52}^{1/2} \epsilon_{e,-1}^2 \epsilon_{B,-2}^{1/2} t_d^{-3/2} \text{ Hz}, \\ \nu_c^{ob.} &= 1.4 \times 10^{14} (1+Y)^{-2} (1+z)^{-3/2} E_{52}^{1/2} A_*^{-2} \epsilon_{B,-2}^{-3/2} t_d^{1/2} \text{ Hz}, \\ F_{\nu, \text{max}}^{ob.} &\simeq 45(1+z) d_{L,28}^{-2} E_{52}^{1/2} A_* \epsilon_{B,-2}^{1/2} t_d^{-1/2} \text{ mJy}. \end{aligned} \quad (6)$$

Focusing on the case $\nu_m^{ob} < \nu_R < \nu_c^{ob} < \nu_X$, using similar arguments to the ones presented for the constant density scenario discussed above imply that the observed ratio $F_R/F_X \simeq 10^3$ is obtained for combination of the parameters which fulfill $E_{52}^{1/2} A_*^{-2} \epsilon_{B,-2}^{-3/2} \approx 33$. For long GRBs characterized by $E \simeq 10^{52}$ erg and canonical value of $\epsilon_B = 0.01$, the obtained value of A_* is $A_* \approx 0.15$. For short GRBs for which $E \approx 10^{49}$ erg, the obtained value is lower, $A_* \lesssim 0.03$. The assumption $\nu_c^{ob} > \nu_X$ is inconsistent with the results presented in Figure 7 and the assumption $\nu_c^{ob} < \nu_R$ leads to higher values of A_* .

We thus find it possible to explain the results found for short GRBs in a scenario in which the explosion that produces short GRBs occurs into a wind profile, with wind density which is ~ 30 times lower than the typical value for Wolf-Rayet stars. There are both strong theoretical (c.f. Chevalier & Li 2000) and observational (Starling et al. 2008)

reasons to believe that a substantial fraction of long GRBs would explode into a medium with a wind structure. However, the standard models of SGRB production involve the merger of compact binaries. The mass loss from the supernovae producing the compact remnants should, however, impart velocities to the binaries that would take them far outside of any remnant stellar winds long before they merge. Therefore, if a wind density profile is indeed a key to understanding the emission of SGRBs, a novel progenitor system will be required.

4.3. A Further Limit on Emission Mechanisms

The results presented here also place strong constraints on the efficiency of γ -ray production during prompt emission, significantly extending the limits derived in earlier works (Freedman & Waxman 2001; Berger et. al. 2003). For $\nu_c^{ob} < \nu_X$ and assuming power law index $p = 2$, equations 2 – 5 predict the flux at the X-ray band after 11 hours to be $F_X^{ob} \simeq 0.3(1+z)d_{L,28}^{-2}E_{52}\epsilon_{e,-1}\mu\text{Jy}$. This result depends only on the energy in the lepton component, which is a fraction ϵ_e of the total explosion energy E . For bursts with known luminosity distance, the rest-frame brightness is thus

$$F_{\nu,X} \simeq 3 \times 10^{26} E_{52}\epsilon_{e,-1} \text{erg s}^{-1} \text{Hz}^{-1} \quad (7)$$

(note that an order unity uncertainty may exist due to the approximations used in deriving the equations, as well as the assumption that $p = 2$). Comparison with the results presented in Table 4 and Figure 6 shows that for a given X-ray brightness, the energy emitted in γ rays is similar to the energy carried by the leptons. Thus, we can conclude that the γ ray production is efficient, $E_{\gamma,\text{ISO}}/\epsilon_e E_{\text{ISO}} \simeq 1$. This result holds for at least the seven orders of magnitude in energies considered in this work.

The similarity found between the X-ray fluxes of short and long GRBs implies that the high efficiency in γ ray production is a property of both types. This result is consistent with the tentative conclusion of Bloom et al. (2006), who studied a single SGRB, namely GRB050509b.

5. Systematic biases and possible caveats

Our sample includes total of 37 short GRBs, out of which 16 (43%) have measured redshift. From those bursts, seven have measured optical and X-ray fluxes at 11 hours and thus the fluence ratio at 11 hours (rest frame) can be obtained, and nine have only upper limits on the observed optical fluence, and thus only upper limits on the ratio at 11 hours are known (see figures 5, 7). Therefore, a question may arise as to whether our conclusions

could be biased by selection effects, and in particular, whether bursts in low density regions might be excluded from our sample because their afterglows would be expected to be too weak.

Consider, however, all bursts with γ -ray fluence larger than 10^{-7} erg cm $^{-2}$ (see figure 3 and tables 1, 2). Essentially all long GRBs are in this group, as are more than half of the short bursts (22 out of 37). Furthermore, above this fluence, 8 out of 9 short bursts which have reasonably deep ($< 3\mu Jy$ or $AB = TBD$) mag early searches, have identified optical counterparts. Indeed, with one exception, GRB 061210, all the optical upper limits lie above detections with comparable E_γ .

If the standard model is correct and the prompt gamma-ray fluence arises from an internal process, then choosing this sample in no way selects bursts by the properties of their external medium. However, because an optical ID has been necessary to get a secure redshift for a short GRB, this is the prime sample used to derive a relationship between the fluxes F_R , F_x and $E_{\gamma,\text{ISO}}$ in Figures 5 – 7. Our fits then (in particular Figure 5) depend on a sample which is essentially complete, and which does not depend upon the properties of the external medium, unless the external medium influences the observed E_γ .

Of course, if $E_{\gamma,\text{ISO}}$ depends upon the external medium, and in particular its density, then our conclusions would be biased. But this bias only arises if perhaps the most interesting (and potentially controversial) of our possible conclusions is true: the initial gamma-ray fluence is not entirely due to an internal process but is also regulated by the medium external to the exploding object.

A further comparison of optical and X-ray fluxes is presented in figure 8. In this figure, we plot the ratio of the observed fluxes for bursts, using the full sample of bursts for which detections or upper limits exist. Since the redshift, and thus $E_{\gamma,\text{ISO}}$, is in most cases unknown, we plot a histogram of the optical to X-ray flux ratio at 11 hours observed time. The histogram clearly shows that the two distributions exhibit a Gaussian-like behavior, with very similar means, $\langle F_R/F_X \rangle = 770$ for the long bursts and $\langle F_R/F_X \rangle = 1130$ for the short bursts, where only those bursts with optical and X-ray detections (no upper limits) were used in this calculation. The similar Gaussian shapes and similar means of the SGRB and LGRB populations also suggests that contaminations, in particular incorrect identification of a long burst as short, does not significantly affect the distribution (otherwise a bi-modal distribution would likely have been seen - unless, of course both distributions have the same ratio, which is the main conclusion here).

Again, it is the fact that the values $\langle F_R/F_X \rangle$ for the short bursts are near 1000 (and comparable or larger than those of long bursts) which is surprising. It is then interesting

that three very clear, well studied short bursts, 050709, 050724 and 051221A have values of $\langle F_R/F_X \rangle$ of about 7000, 10,000 and 500 respectively. Examination of the table by the reader will show that even if some of the short bursts in our sample are falsely identified short bursts, the bursts which are clearly short agree with the claims presented here.

Additionally, it is possible that the ratio of f_R/f_X could be affected absorption of photons in the host galaxy. While many long GRBs show substantial X-ray columns Campana et al. (2006); Schady et al. (2007); Galama & Wijers (2001), the large majority of the observed 10 keV passband of the XRT is unaffected, and thus our X-ray fluxes should be fairly accurate. The measured optical absorption of long gamma-ray burst afterglows often suggests lower column densities than the X-ray, with typical optical absorptions in the range of one-tenth to one magnitude Schady et al. (2007); Cenko et al. (2009). The effect of host absorption on short bursts has not yet been well studied. But again, the main danger would be a suppression of the optical relative to the X-ray. However, our main result is that the short bursts have brighter optical emission relative to the X-ray than expected by the standard model and typically assumed environmental densities.

6. Summary and discussion

In this work, we present a comprehensive study of the optical and X-ray afterglows obtained after 11 hours of 37 short and 421 long GRBs, and compared the results to the energy emitted in γ -rays during the prompt emission phase. This sample is the largest used so far for this type of study. We find a strong correlation between the optical and X-ray afterglow brightnesses and prompt γ -ray fluence of GRBs, a result similar to one reported contemporaneously by Gehrels et al. (2008) Kann et al. (2009). However, we also show that the ratio of the optical to X-ray emission in the short burst afterglows is comparable to that of the long-bursts. This equivalence between burst types, and the absolute ratio we find can only be understood in the framework of the standard theory if the circumburst density of SGRBs is typically comparable to, or even higher than the circumburst density of LGRBs. We point out that in a wind-like scenario for SGRBs can also explain this result if the average mass loss rate of the SGRB progenitor is ~ 30 times lower than the characteristic mass loss rate from a Wolf-Rayet star. Finally, we have shown that in the framework of the standard model, in which the prompt emission fluence is independent of the environmental density, by selecting bursts with γ -ray fluence larger than 10^{-7} erg cm $^{-2}$ we obtain for short bursts above this fluence an essentially complete sample for analysis.

These results indicate that SGRB afterglows are not necessarily dim due to a lower density in the circumburst environment. While the average SGRB afterglow is significantly

dimmer than the average LGRB afterglow, this appears to be largely due to the lower total energy release of the burst, as indicated by the fainter prompt γ -ray emission. We can thus conclude that if the prompt emission is a result of internal shocks, then either the external density of long and short bursts is similar, or the afterglow flux is less sensitive to the density of the surrounding medium than predicted. On the other hand, if the prompt emission is due to an external shock, both quantities the gamma-ray fluence and afterglow intensity will depend on the external density and may scale accordingly. In this case we could attribute the faintness of *both* the prompt and afterglow emission to the external medium density.

Due to the short lifetimes of the massive star progenitors of long-duration GRBs, they have been traditionally expected to occur in or near giant molecular clouds ($n \sim 10^{2.5} \text{ cm}^{-3}$; Shu et al. 1987). Some observational evidence supports this hypothesis. The hosts of LGRBs are typically blue and actively forming massive stars (Fruchter et al. 1999; Sokolov et al. 2001; Le Floc'h et al. 2003; Christensen et al. 2004; Gorosabel et al. 2005). Fruchter et al. (2006) find that LGRBs are preferentially located on the brightest regions of these galaxies, which they interpret as evidence that GRBs frequently occur on or near massive OB associations. X-ray observations of GRB afterglows show neutral hydrogen column densities consistent those of Galactic giant molecular clouds (Galama & Wijers 2001; Jakobsson et al. 2006; Schady et al. 2007). At optical wavelengths, moderate extinction characteristic of dense regions is seen in some bursts (Kann et al. 2007), while in others the afterglow appears significantly extinguished (Djorgovski et al. 2001; Levan et al. 2006a; Watson et al. 2006; Pellizza et al. 2006; Rol et al. 2007), and at high redshifts where Ly α absorption can be found in the optical spectrum, large hydrogen column densities (up to 10^{23} cm^{-3}) are frequently found (c.f. Jakobsson et al. 2007). Nonetheless, as noted earlier, the density of the medium into which the relativistic flow of the GRB expands may be dominated by an earlier wind from the progenitor star rather than the ISM.

In contrast, SGRBs are found in both elliptical and star-forming galaxies, a fact consistent with merger scenarios. The ISM of elliptical galaxies is sparse and has a typical density of only $n \sim 10^{-2.5} \text{ cm}^{-3}$ (Fukazawa et al. 2006). Panaiteescu (2006), however, estimates a circumburst density of $10^{-1} < n < 10^3 \text{ cm}^{-3}$ for GRB 050724, a burst in an E/S0 galaxy (Berger et al. 2005). At the same time circumburst densities of $10^{-4} < n < 10^{-1} \text{ cm}^{-3}$ Panaiteescu (2006) and 10^{-3} to 10^{-1} cm^{-3} Soderberg et al. (2006a) are found for GRBs 050709 and 051221A, respectively, both of which occurred in apparently star-forming galaxies. As we have shown here, the lower ranges of these two latter densities are inconsistent with the distribution of ratios of F_X/F_R seen in Figure 7. These estimates of the SGRB circumburst density, however, assume a locally uniform medium. If the SGRBs were to typically form in a windlike structure, this ratio would be acceptable. Still, the common presence of a wind structure around SGRBs would rule out the standard merger models.

The velocity by mass loss during the supernovae, let alone any kicks by the supernovae, would easily move the compact remnants by more than 100 pc from their natal region before a binary merger occurred (Belczynski et al. 2006a).

A potentially simple explanation of the results presented here is that both the afterglow and the prompt emission are due to an external interaction (e.g., Dermer 2008). In this case, both the afterglow and prompt emission might be expected to scale similarly. However, it is difficult to explain the strong variability observed in many bursts in such a model (see, e.g., Mészáros 2006). Furthermore, observational evidence for a correlation between the density of a circumburst medium and $E_{\gamma, \text{ISO}}$ is so far either weak or potentially damaging. Troja et al. (2008) have suggested that SGRBs far from the center of their host may be fainter than those closer in. However, this work uses a number of associations based on the brightest galaxy in a rather large Swift XRT error circle, and therefore may in some cases assign an incorrect offset, and thus will need to be confirmed on larger, better samples. In contrast, the only work to examine this issue for long bursts has found a positive correlation between the brightness of the burst and the distance of the burst from the center of the host (Ramirez-Ruiz et al. 2002). This is, to first order, the opposite of one would predict if the external medium played a role in the gamma-ray emission. It has, however, been noted that the bursts GRBG 050509b and 050724, both of which were in early type galaxies were intrinsically weaker than bursts found in star-forming hosts Rhoads (2009). Nonetheless, we note again that the work by Panaiteescu (2006) suggests that the circumburst medium around at GRB 0507024 was reasonably dense.

Several recent advances in the theory and modelling of the binary merger process and the local interstellar medium could potentially explain our results. van den Heuvel (2007) has pointed out that the large majority of known double neutron-star binaries have low eccentricities, suggesting that the second born neutron stars in binaries, unlike single neutron stars, typically did not receive substantial “kick” velocities at birth. Lower kicks will lead to lower systemic velocities, and a higher probability that the system remains in a moderately dense ISM when the binary merges. Furthermore, the time to merger may often be relatively short. Belczynski et al. (2009) estimate that up to 70% of NS-NS and NS-BH binaries may merge with 100 Myr after formation. Indeed, one burst that appears to have likely been a short burst, GRB 060505, lies in an [HII] region on the outskirts of its spiral host (Fynbo et al. 2006; Ofek et al. 2007; Levesque & Kewley 2007). Some short bursts, however, occur in early-type galaxies. Here recent result could also provide an explanation for an apparent ISM density of 1 cm^{-3} . Binary mergers in early-type galaxies are almost certainly dominated by the evolving binaries in globular clusters (Grindlay et al. 2006), and the most rapid evolution is likely to occur in the densest clusters. These clusters however, could have ionized gas densities of the required magnitude due to the colliding winds of giants contained

in the cluster (Parsons, Ramirez-Ruiz & Lee 2009).

Although we may not fully understand the mechanism, we cannot escape the conclusion that SGRBs are fundamentally similar in emission properties to LGRBs – particularly the fainter LGRBs that have typically been found at low redshift. It has been suggested that low-luminosity LGRBs (e.g. GRB 980425, GRB 031203 and GRB 060218) have large, and perhaps nearly quasi-spherical, opening angles when compared to traditional LGRBs (Soderberg et al. 2004b, 2006b; Liang et al. 2007). Similarly, of the three SGRBs with estimated opening angles, GRB 050709 and GRB 050724 have large measured angles, $\Theta \sim 14^\circ$ (Fox et al. 2005) and $\sim 25^\circ$ (Grupe et al. 2006; Malesani et al. 2007) respectively, while GRB 051221 has $4^\circ < \Theta < 8^\circ$ (Burrows et al. 2006; Soderberg et al. 2006a), which is more typical of traditional high $E_{\gamma,\text{ISO}}$ LGRB opening angles. Yet both long and short populations appear to largely fall on a simple log-linear relationship between afterglow intensity and gamma-ray luminosity over six orders of magnitude in energy. Within this relationship there may be strong hints as to the nature of the progenitors of SGRBs, or perhaps a new more fundamental understanding of the GRB emission mechanism.

This work made use of data supplied by the UK *Swift* Science Data Centre at the University of Leicester. We gratefully acknowledge J. Racusin, N. Gehrels, D. Burrows, and the *Swift* team for generously sharing pre-published XRT values. We also thank A. Levan, N. Gehrels, E. Waxman, K. Belczynski, E. Ramirez-Ruiz, E. van den Heuvel, R. Sari and J. Graham for helpful discussions, J. Greiner for his online GRB Table and R. Quimby, E. McMahon and J. Murphy for the GRBlog. AP wishes to acknowledge the support of the Riccardo Giacconi fellowship award of the Space Telescope Science Institute.

REFERENCES

- Amati, L. 2006 MNRAS, 372, 233
Antonelli, L. A., et al. 1999, A&AS, 138, 435
Barbier, L., et al. 2007, GRB Coordinates Network, 6623, 1
Barthelmy, S. D., et al. 2005a, Nature, 438, 994
Barthelmy, S., Gehrels, N., Norris, J., & Sakamoto, T. 2005b, GRB Coordinates Network, 4401, 1
Belczynski, K., Perna, R., Bulik, T., Kalogera, V., Ivanova, N., & Lamb, D. Q. 2006a, ApJ, 648, 1110

- Belczynski, K., Sadowski, A., Rasio, F. A., & Bulik, T. 2006b, ApJ, 650, 303
- Belczynski, K., Stanek, K. Z., & Fryer, C. L. 2009, ApJ, submitted astro-ph/0712.3309
- Berger, E., Kulkarni, S.R. & Frail, D.A. 2003, ApJ, 590, 379
- Berger, E. 2005, GRB Coordinates Network, 3801, 1
- Berger, E., & Boss, A. 2005, GRB Coordinates Network, 4323, 1
- Berger, E., & Fox, D. 2005, GRB Coordinates Network, 4316, 1
- Berger, E., et al. 2005a, Nature, 438, 988
- Berger, E. 2006a, GRB Coordinates Network, 5965, 1
- Berger, E. 2007a, ApJ, 670, 1254
- Berger, E. 2007b, GRB Coordinates Network, 5995, 1
- Berger, E., & Kaplan, D. L. 2007, GRB Coordinates Network, 6680, 1
- Berger, E., et al. 2007b, ApJ, 664, 1000
- Berger, E., Morrell, N., & Roth, M. 2007b, GRB Coordinates Network, 7154, 1
- Bikmaev, I., et al. 2005a, GRB Coordinates Network, 3797, 1
- Blandford, R.D., & McKee, C.F. 1976, Phys. Fluids, 19, 1130
- Bloom, J. S., Kulkarni, S. R., & Djorgovski, S. G. 2002, AJ, 123, 1111
- Bloom, J. S., et al. 2006, ApJ, 638, 354
- Bloom, J. S., et al. 2007, ApJ, 654, 878
- Burrows, D. N., et al. 2006, ApJ, 653, 468
- Campana et al. 2006, A&A, 449, 61
- Castro-Tirado, A. J., et al. 1997, IAU Circ., 6598, 2
- Castro-Tirado, A., Alises, M., & Greiner, J. 2000, GRB Coordinates Network, 870, 1
- Castro-Tirado, A. J., Bond, I., Kilmartin, P., de Ugarte Postigo, A., Gorosabel, J., Jelinek, M., & Yock, P. 2005, GRB Coordinates Network, 3018, 1

- Cenko, S. B., Fox, D. B., & Price, P. A. 2006, GRB Coordinates Network, 5912, 1
- Cenko, S. B., Rau, A., Berger, E., Price, P. A., & Cucchiara, A. 2007, GRB Coordinates Network, 6664, 1
- Cenko, S. B. et al. 2009 ApJ693 1484
- Chevalier, R. A., Li, Z.-Y. 2000, ApJ, 536, 195
- Christensen, L., Hjorth, J., & Gorosabel, J. 2004, A&A, 425, 913
- Cobb, B. E. 2006, GRB Coordinates Network, 5935, 1
- Connaughton, V., et al. 1997, IAU Circ., 6683, 1
- Cucchiara, A., Fox, D. B., Berger, E., & Price, P. A. 2006, GRB Coordinates Network, 5470, 1
- Cucchiara, A., Fox, D. B., Cenko, S. B., Berger, E., Price, P. A., & Radomska, J. 2007, GRB Coordinates Network, 6665, 1
- Cusumano, G., Burrows, D. N., Hunsberger, S., Pagani, C., La Parola, V., & Mangano, V. 2005, GRB Coordinates Network, 4326, 1
- D'Avanzo, P., et al. 2008, in preparation
- de Pasquale, M., et al. 2006, A&A, 455, 813
- Dermer, C.d. 2008, ApJ, in press (astro-ph/0703223)
- Diercks, A. H., et al. 1998, ApJ, 503, L105
- Djorgovski, S. G., et al. 1997, Nature, 387, 876
- Djorgovski, S. G., Kulkarni, S. R., Goodrich, R., Frail, D. A., & Bloom, J. S. 1998, GRB Coordinates Network, 137, 1
- Djorgovski, S. G., Kulkarni, S. R., Bloom, J. S., & Frail, D. A. 1999, GRB Coordinates Network, 289, 1
- Djorgovski, S. G., Frail, D. A., Kulkarni, S. R., Bloom, J. S., Odewahn, S. C., & Diercks, A. 2001, ApJ, 562, 654
- Djorgovski, S. G., Bloom, J. S., & Kulkarni, S. R. 2003, ApJ, 591, L13

- Donaghy, T. Q., et al. 2006, ArXiv Astrophysics e-prints, arXiv:astro-ph/0605570
- Eichler, D., Livio, M., Piran, T., & Schramm, D. N. 1989, Nature, 340, 126
- Evans, P. A., et al. 2007, A&A, 469, 379
- Fox, D. B., et al. 2005, Nature, 437, 845
- Freedman, D.L., & Waxman, E. 2001, ApJ, 547, 922
- Fruchter, A. S., et al. 1999, ApJ, 519, L13
- Fruchter, A. S., et al. 2006, Nature, 441, 463
- Fukazawa, Y., Botoya-Nonesa, J. G., Pu, J., Ohto, A., & Kawano, N. 2006, ApJ, 636, 698
- Fynbo, J. P. U. et al. 2006, Nature, 444, 1047
- Galama, T., et al. 1997, Nature, 387, 479
- Galama, T., et al., 1998a, GRB Coordinates Network, 62, 1
- Galama, T., et al., 1998b, ApJ, 500L, 101
- Galama, T. J., & Wijers, R. A. M. J. 2001, ApJ, 549, L209
- Gehrels, N., et al. 2005, Nature, 437, 851
- Gehrels, N., et al. 2008, ApJ, 189, 1161
- Grindlay, J., Portegies Zwart, S. & McMillan, S., Nature Physics, 2, 116
- Golenetskii, S., Aptekar, R., Mazets, E., Pal'Shin, V., Frederiks, D., & Cline, T. 2007, GRB Coordinates Network, 6671, 1
- Gorosabel, J., et al. 1999, A&AS, 138, 455
- Gorosabel, J., et al. 2005, A&A, 444, 711
- Graham, J. F., Fruchter, A. S., Levan, A. J., Nysewander, M., Tanvir, N. R., Dahlen, T., Bersier, D., & Pe'Er, A. 2007, GRB Coordinates Network, 6836, 1
- Groot, P. J., et al. 1997a, IAU Circ., 6616, 2
- Groot, P. J. et al. 1997b, GRB Coordinates Network, 17, 1
- Groot, P. J., et al. 1998a, ApJ, 493, L27

- Groot, P. J., et al. 1998b, ApJ, 502, L123
- Grupe, D., Burrows, D. N., Patel, S. K., Kouveliotou, C., Zhang, B., Mészáros, P., Wijers, R. A. M., & Gehrels, N. 2006, ApJ, 653, 462
- Guidorzi, C., et al. 2005, GRB Coordinates Network, 4356, 1
- Guidorzi, C., et al. 2007, GCNR, 77, 1 (2007), 77, 1
- Halpern, J. P., Tonnesen, S., Tuttle, S., & Mirabal, N. 2005a, GRB Coordinates Network, 4202, 1
- Harrison, F. A., et al. 1999, ApJ, 523, L121
- Hjorth, J., et al. 2002, ApJ, 576, 113
- Hjorth, J., et al. 2003a, Nature, 423, 847
- Hjorth, J., et al. 2005, Nature, 437, 859
- Holland, S. T., Barthelmy, S., Beardmore, A., Gehrels, N., Kennea, J., Page, K., Palmer, D., & Rosen, S. 2005, GRB Coordinates Network, 4034, 1
- Holland, S. T., de Pasquale, M., & Markwardt, C. B. 2007, GRB Coordinates Network, 7145, 1
- Huang, K. Y., et al. 2005, ApJ, 628, L93
- Hurley, K., Cline, T., Frontera, F., Guidorzi, C., Montanari, E., Mazets, E., & Golenetskii, S. 2000a, GRB Coordinates Network, 895, 1
- Hurley, K., Cline, T., Mazets, E., & Golenetskii, S. 2000b, GRB Coordinates Network, 865, 1
- Hurley, K., Cline, T., Mazets, E., & Golenetskii, S. 2001, GRB Coordinates Network, 916, 1
- Hurley, K., et al. 2002a, GRB Coordinates Network, 1409, 1
- Hurley, K., et al. 2002b, GRB Coordinates Network, 1719, 1
- Jakobsson, P., et al. 2006, A&A, 460, L13
- Jakobsson, P., et al. 2007, A&A, 406, 13
- Johnson, S., et al. 2007, GRB Coordinates Network, 6218, 1

- Kann, D. A., et al. 2007, ArXiv e-prints, 712, arXiv:0712.2186
- Kann, D. A., *et al.* 2008, ApJ, submitted (arXiv:0804.1959)
- Kocevski, D., & Bloom, J. S. 2007, GRB Coordinates Network, 7107, 1
- Lamb, D. Q., et al. 2002, GRB Coordinates Network, 1403, 1
- Le Floc'h, E., et al. 2003, A&A, 400, 499
- Lee, W. H., Ramirez-Ruiz, E., & Granot, J. 2005, ApJ, 630, L165
- Levan, A., et al. 2006a, ApJ, 647, 471
- Levan, A. J., et al. 2006b, ApJ, 648, L9
- Levan, A. J., et al. 2007, GRB Coordinates Network, 6603, 1
- Levan, A. J., et al. 2008, MNRAS, 384, 541
- Levesque, E. M., & Kewley, L. J., 2007 ApJ667, 121
- Liang, E., Zhang, B., Virgili, F., & Dai, Z. G. 2007, ApJ, 662, 1111
- Malesani, D., et al. 2007, A&A, 473, 77
- Marshall, F. E., Takeshima, T. 2000, GRB Coordinates Network, 58, 1
- Marshall, F. E., Barthelmy, S. D., Burrows, D. N., Chester, M. M., Cummings, J., Evans, P. A., Roming, P., & Gehrels, N. 2007a, GCNR, 80, 1 (2007), 80, 1
- Marshall, F. E., Barthelmy, S. D., Brown, P. J., Burrows, D. N., Cummings, J., Roming, P., Starling, R., & Gehrels, N. 2007b, GCNR, 81, 1 (2007), 81, 1
- McBreen, S., et al. 2007, GCNR, 46, 2 (2007), 46, 2
- Mészáros, P. 2006, Rep. Prog. Phys., 69, 2259
- Mészáros, P., & Rees, M.J. 1997, ApJ, 476, 232
- Metzger, M. R., Djorgovski, S. G., Kulkarni, S. R., Steidel, C. C., Adelberger, K. L., Frail, D. A., Costa, E., & Frontera, F. 1997, Nature, 387, 878
- Mineo, T., Tagliaferri, G., Malesani, D., Giommi, P., Burrows, D., Fox, D., Chincarini, G., & Page, K. 2005, GRBCoordinates Network, 4195, 1

- Mirabal, N., Halpern, J. P., Gotthelf, E. V., & Mukherjee, R. 2005, ApJ, 620, 379
- Murakami, T., Ueda, Y., Yoshida, A., Kawai, N., Marshall, F. E., Corbet, R. H. D., & Takeshima, T. 1997, IAU Circ., 6732, 1
- Nakar, E. 2007, Phys. Rep., 442, 166
- Narayan, R., Paczynski, B., & Piran, T. 1992, ApJ, 395, L83
- Nysewander, M., Moran, J., Johnson, L., Moschler, D., Reichart, D., & Henden, A. 2002, GRB Coordinates Network, 1760, 1
- Ofek, E. O.. et al. 2007, ApJ, 662 11290
- Paciesas, W. S., et al. 1999, ApJS, 122, 465
- Paczyński, B. 1998, ApJ, 494, L45
- Pagani, C., La Parola, V., & Burrows, D. N. 2005, GRB Coordinates Network, 3934, 1
- Page, K. L., et al. 2006a, ApJ, 637, L13
- Panaiteescu, A. 2006, MNRAS, 367, L42
- Panaiteescu, A. & Kumar, P. 2000, ApJ, 543, 66
- Panaiteescu, A. & Kumar, P. 2002, ApJ, 571, 779
- Panaiteescu, A., Kumar, P., & Narayan, R. 2001, ApJ, 561, L171
- Parson, R. K., Ramirez-Ruiz, E. & Lee, W. H., 2009, ApJ, submitted (astro-ph/0904.1768)
- Pe'er, A., & Waxman, E. 2005, ApJ, 633, 1018
- Pe'er, A., & Wijers, R.A.M.J. 2006, ApJ, 643, 1036
- Pellizza, L. J., et al. 2006, A&A, 459, L5
- Perley, D. A., Thoene, C. C., & Bloom, J. S. 2007a, GRB Coordinates Network, 6774, 1
- Perri, M., Stratta, G., Fenimore, E., Schady, P., Barthelmy, S. D., Burrows, D. N., Roming, P., & Gehrels, N. 2007a, GCNR, 103, 1 (2007), 103, 1
- Piranomonte, S., Covino, S., Malesani, D., Tagliaferri, G., Chincarini, G., & Stella, L. 2006, GRB Coordinates Network, 5392, 1

- Piranomonte, S., Vergani, S., D'Avanzo, P., & Tagliaferri, G. 2007, GRB Coordinates Network, 6612, 1
- Perley, D. A., Bloom, J. S., Modjaz, M., Poznanski, D., & Thoene, C. C. 2007, GRB Coordinates Network, 7140, 1
- Price, P. A., Axelrod, T. S., & Schmidt, B. P. 2000, GRB Coordinates Network, 898, 1
- Price, P. A., Morrison, G., & Bloom, J. S. 2001a, GRB Coordinates Network, 919, 1
- Price, P. A., Axelrod, T. S., Schmidt, B. P., & Reichart, D. E. 2001b, GRB Coordinates Network, 1020, 1
- Price, P. A., Schmidt, B. P., & Axelrod, T. S. 2002, GRB Coordinates Network, 1410, 1
- Price, P. A., Berger, E., Fox, D. B., Cenko, S. B., & Rau, A. 2006, GRB Coordinates Network, 5077, 1
- Ramirez-Ruiz, E., Lazzati, D., & Blain, A. 2002, ApJ, 565, 9
- Reichart, D. E., et al. 1999, ApJ, 517, 692
- Rhoads, J. 2009, ApJ, in press (astro-ph/0807.2642)
- Rol, E., et al. 2007, ApJ, 669, 1098
- Sakamoto, T., et al. 2005, ApJ, 629, 311
- Sakamoto, T., et al. 2008, ApJS, 175, 179
- Sari, R., & Esin, A. 2001, ApJ, 548, 787
- Sari, R., Piran, T., & Narayan, R. 1998, ApJ, 497, L17
- Schady, P., et al. 2007, MNRAS, 377, 273
- Schlegel, D. J., Finkbeiner, D. P., & Davis, M. 1998, ApJ, 500, 525
- Shu, F. H., Adams, F. C., & Lizano, S. 1987, ARA&A, 25, 23
- Sokolov, V. V., et al. 2001, A&A, 372, 438
- Soderberg, A., Djorgovski, S. G., Halpern, J. P., & Mirabal, N. 2004a, GRB Coordinates Network, 2837, 1
- Soderberg, A. M., et al. 2004b, Nature, 430, 648

- Soderberg, A. M., et al. 2006a, ApJ, 650, 261
- Soderberg, A. M., et al. 2006b, Nature, 442, 1014
- Stanek, K. Z., et al. 2003, ApJ, 591, L17
- Starling, R., Osborne, J. P., Page, K. L., & Marshall, F. E. 2007, GRB Coordinates Network, 6852, 1
- Starling, R. L. C., et al. 2008, A&A, 481, 319
- Stratta, G., et al. 2007a, A&A, 461, 485
- Stratta, G., et al. 2007b, A&A, 474, 827
- Stratta, G., Perri, M., Conciatore, M., Burrows, D., & Sato, G. 2007c, GRB Coordinates Network, 6119, 1
- Tinney, C., et al. 1998, IAU Circ., 6896, 1
- Troja, E., King, A. R., O'Brien, P. T., Lyons, N., & Cusumano, G. 2008, MNRAS, L5
- van den Heuvel, E. P. J. 2007, AIP Conf. Proceedings, 924, 598 (astro-ph/0704.1215)
- Villasenor, J. S., et al. 2005, Nature, 437, 855
- Vrba, F. J., et al. 2000, ApJ, 528, 254
- Vreeswijk, P. M., et al. 1999, ApJ, 523, 171
- Watson, D., et al. 2006, ApJ, 652, 1011
- Waxman, E. 1997, ApJ, 491, L19
- Wiersema, K., et al. 2008, in preparation
- Woosley, S. 1993, ApJ, 405, 273
- Woosley, S. E., & Bloom, J. S. 2006, ARA&A, 44, 507
- Xin, L. P., Zhai, M., Qiu, Y. L., Wei, J. Y., Hu, J. Y., Deng, J. S., Urata, Y., & Zheng, W. K. 2007, GRB Coordinates Network, 6747, 1
- Zhang, B., & Mésáros, P. 2001, ApJ, 559, 110
- Zheng, W. K., et al. 2007, GRB Coordinates Network, 6250, 1

Ziaeepour, H., Barthelmy, S. D., Parsons, A., Page, K. L., de Pasquale, M., & Schady, P.
2007a, GCNR, 74, 2 (2007), 74, 2

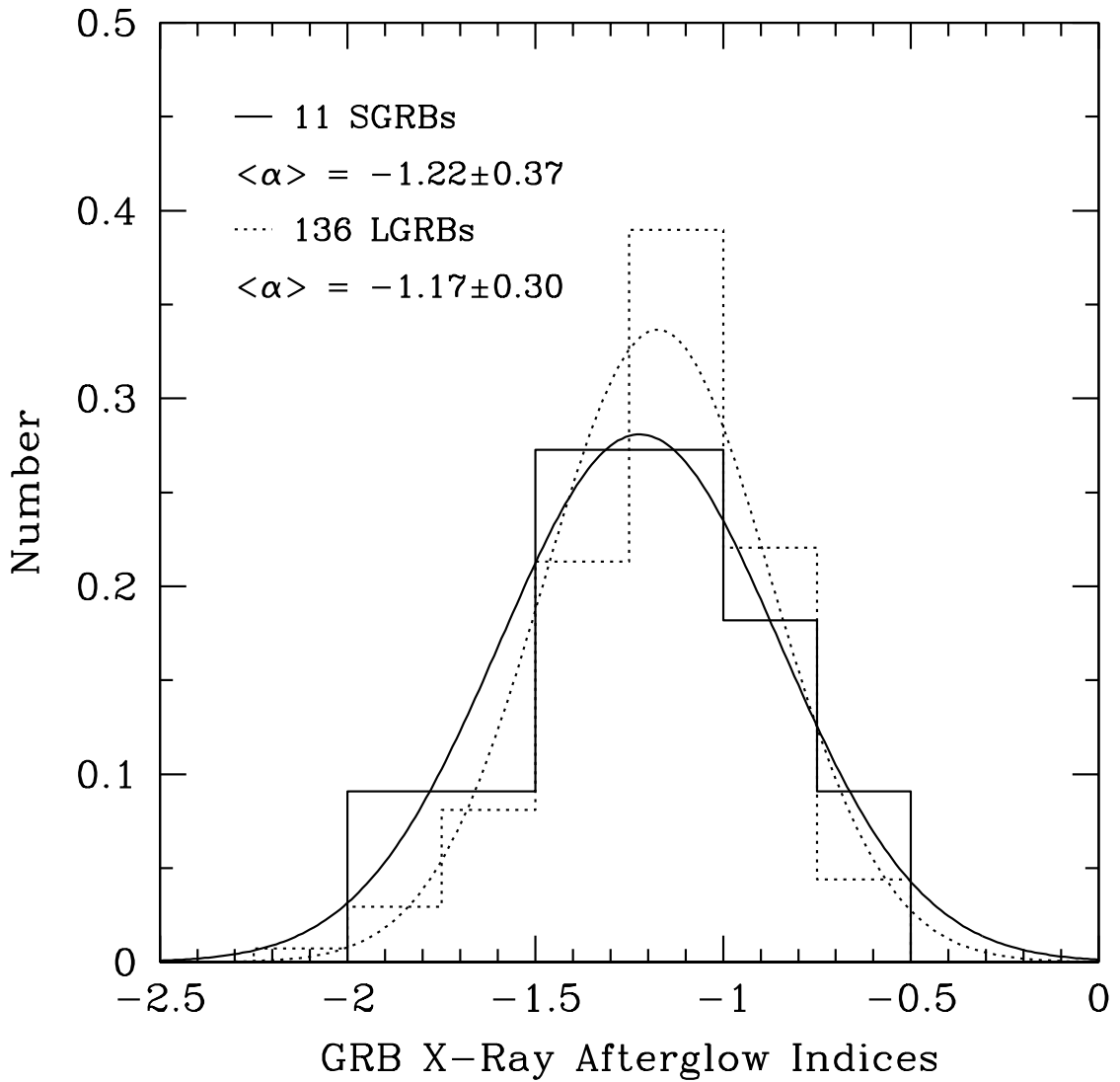


Fig. 1.— A compilation of the X-ray afterglow temporal indices of the two populations and presents the best-fit Gaussian distribution to each data set. We include only afterglow indices of bursts with a rapid XRT detection and with data extending to at least 11 hours. The solid line indicates SGRBs; the dashed indicates LGRBs. The plot has been normalized by the sum of the bursts used: 11 short and 136 long bursts.

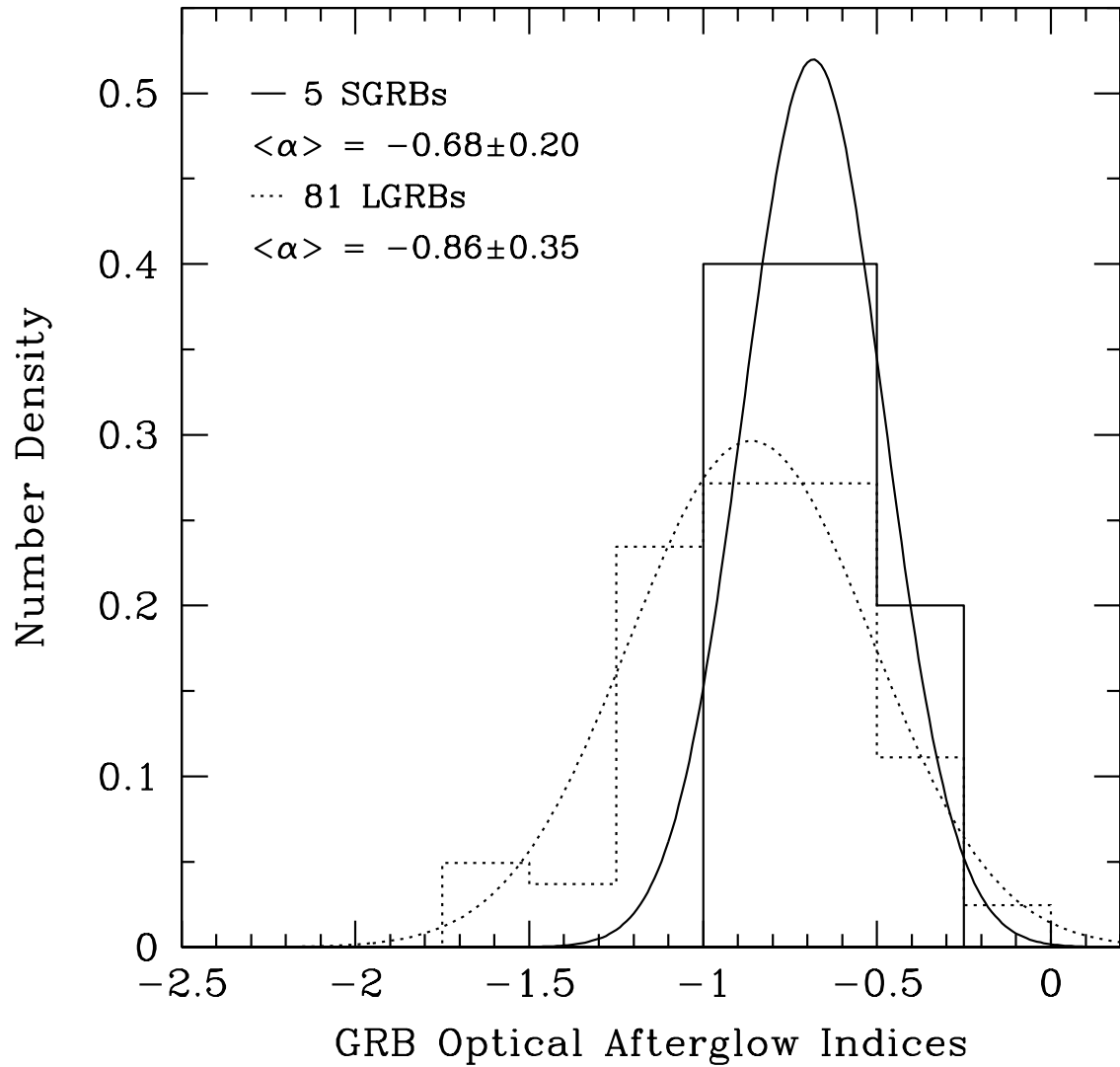


Fig. 2.— A compilation of all short and long burst optical afterglow indices and the best Gaussian fits to the distributions. We include only afterglow data that have light curves extending from at most three hours to at least eleven hours. The solid line indicates SGRBs; the dashed indicates LGRBs. The plot has been normalized by the sum of bursts used: 5 short and 81 long.

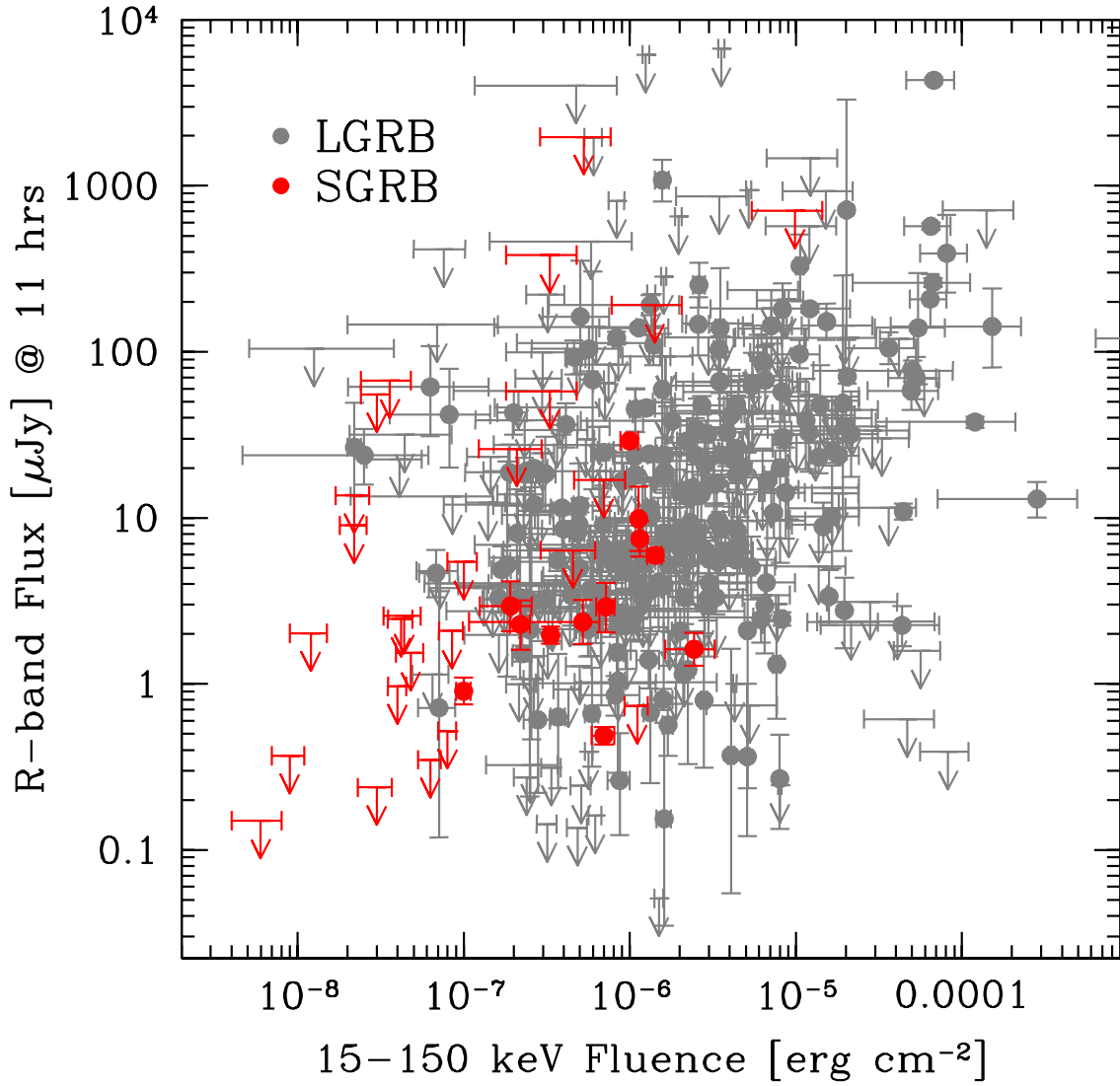


Fig. 3.— A plot of the optical R -band flux (corrected for Galactic extinction) at eleven hours (observed frame) versus prompt 15–150 keV γ -ray fluence for both long (grey) and short (red) bursts. Note that below a fluence of 10^{-7} ergs cm^{-2} , no optical afterglow of an SGRB has been discovered, while above 10^{-7} , all reasonably deep observing campaigns but one (GRB 061210) have detected an optical afterglow.

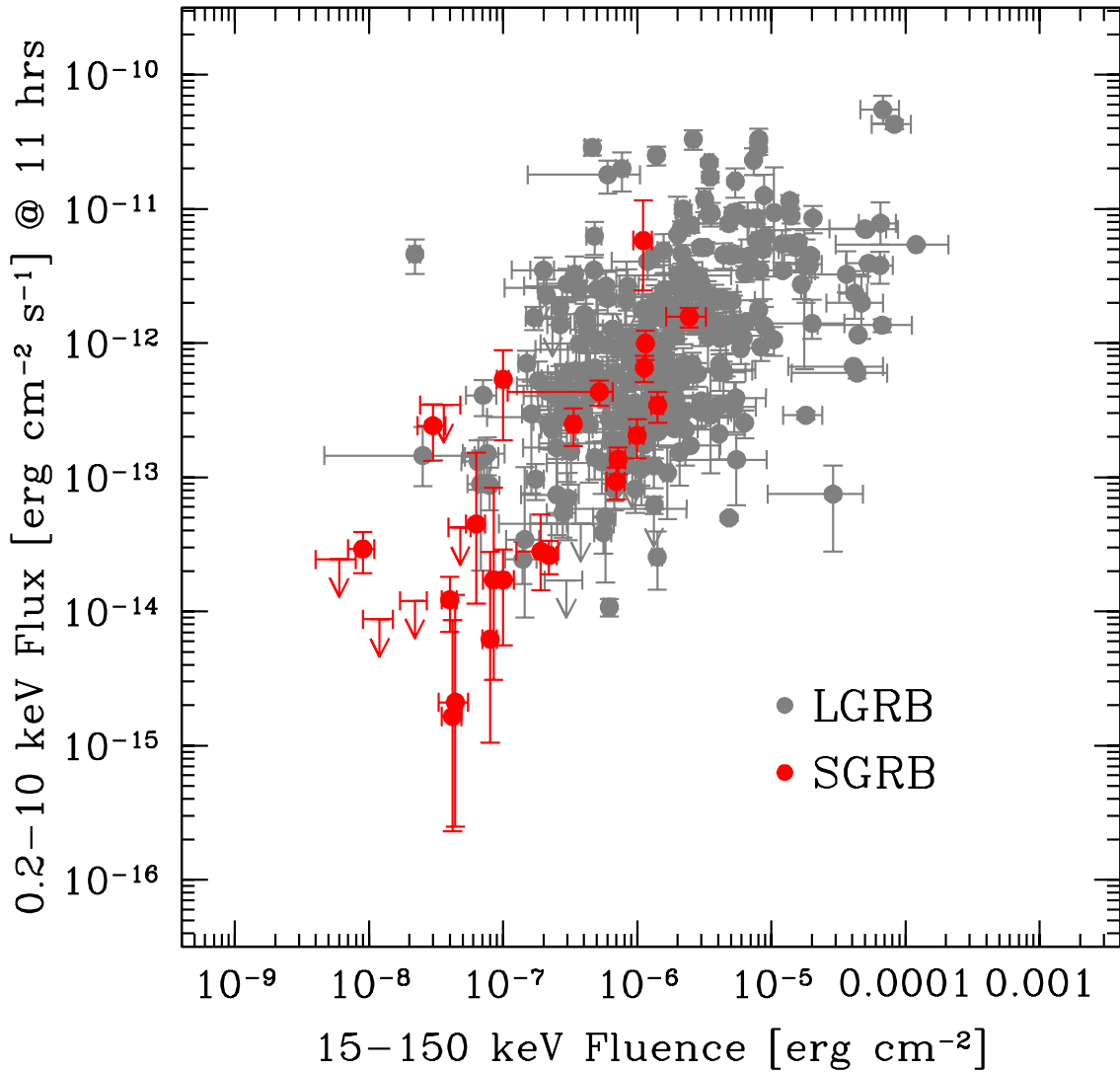


Fig. 4.— A plot of the X-ray flux at eleven hours (observed frame) versus the prompt 15–150 keV γ -ray fluence for both long (grey) and short (red) bursts.

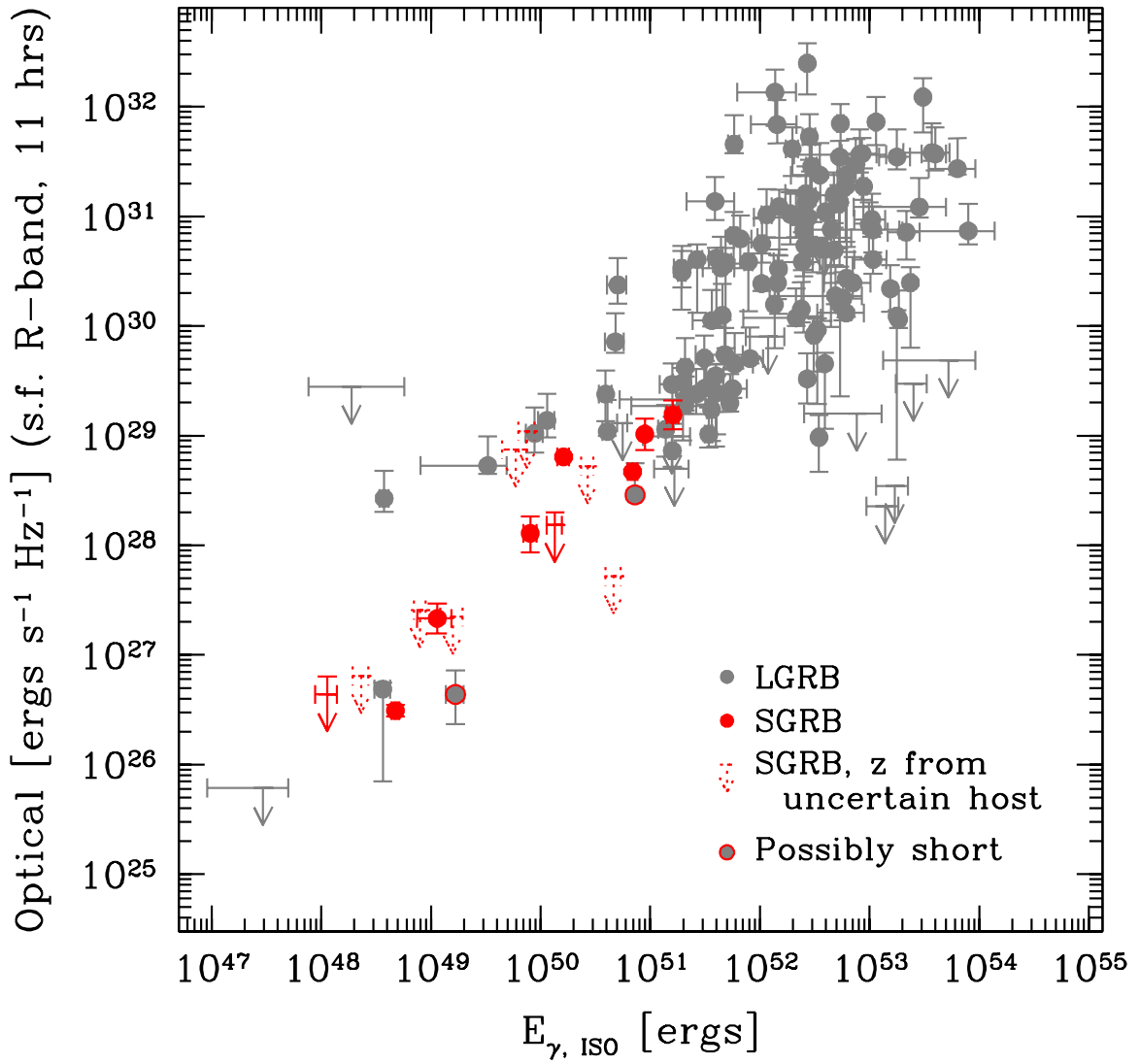


Fig. 5.— A plot of the rest-frame optical R -band (corrected for Galactic extinction) afterglow brightness at eleven hours (in the source frame) versus $E_{\gamma, \text{ISO}}$, the total prompt emission of the burst in gamma-rays. Dashed upper limits represent SGRBs with a host galaxy determined by XRT error circle only. The classification of GRB 060614 and GRB 060505 is uncertain, therefore they are labeled as “Possibly short”.

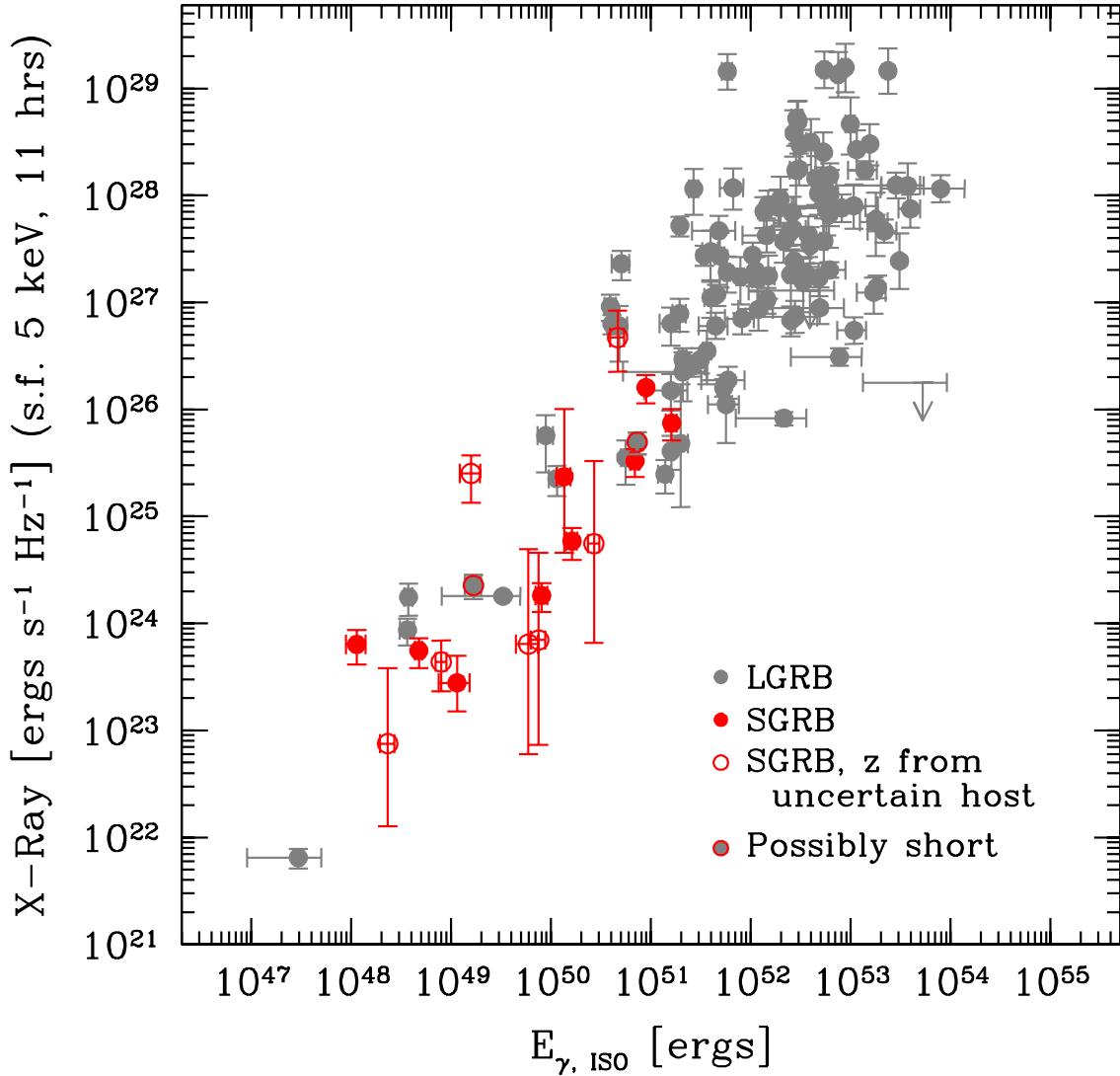


Fig. 6.— A plot of the rest-frame 5 keV X-ray afterglow brightness at eleven hours (rest frame) versus $E_{\gamma, \text{ISO}}$. The open circles represent SGRBs with a host galaxy determined by XRT error circle only. The classification of GRB 060614 and GRB 060505 is uncertain, therefore they are labeled as “Possibly short.”

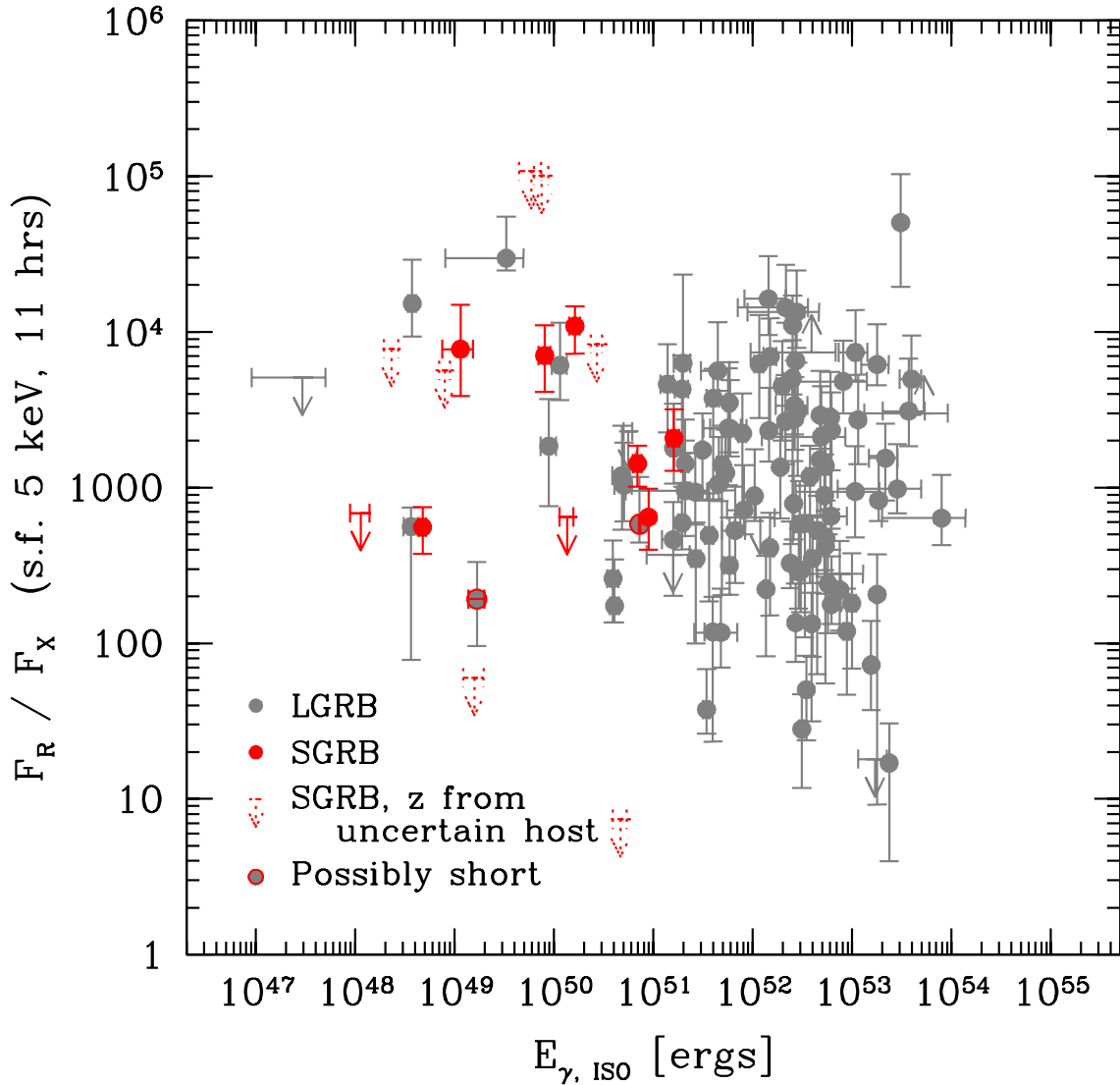


Fig. 7.— The ratio of the total fluence in the optical over that in the x-ray versus the $E_{\gamma, \text{ISO}}$, measured at 11 hours (source frame). Once again the short and long bursts do not appear to differ, except in their typical $E_{\gamma, \text{ISO}}$. There is no evidence in a suppression of this ratio either by a low density medium surrounding the short bursts or their lower typical $E_{\gamma, \text{ISO}}$, as would be expected from the standard theory if the synchrotron frequency of the bursts were typically between the optical and X-ray. However, the observed absolute values of this ratio are hard to explain by the standard theory if this is not the case.

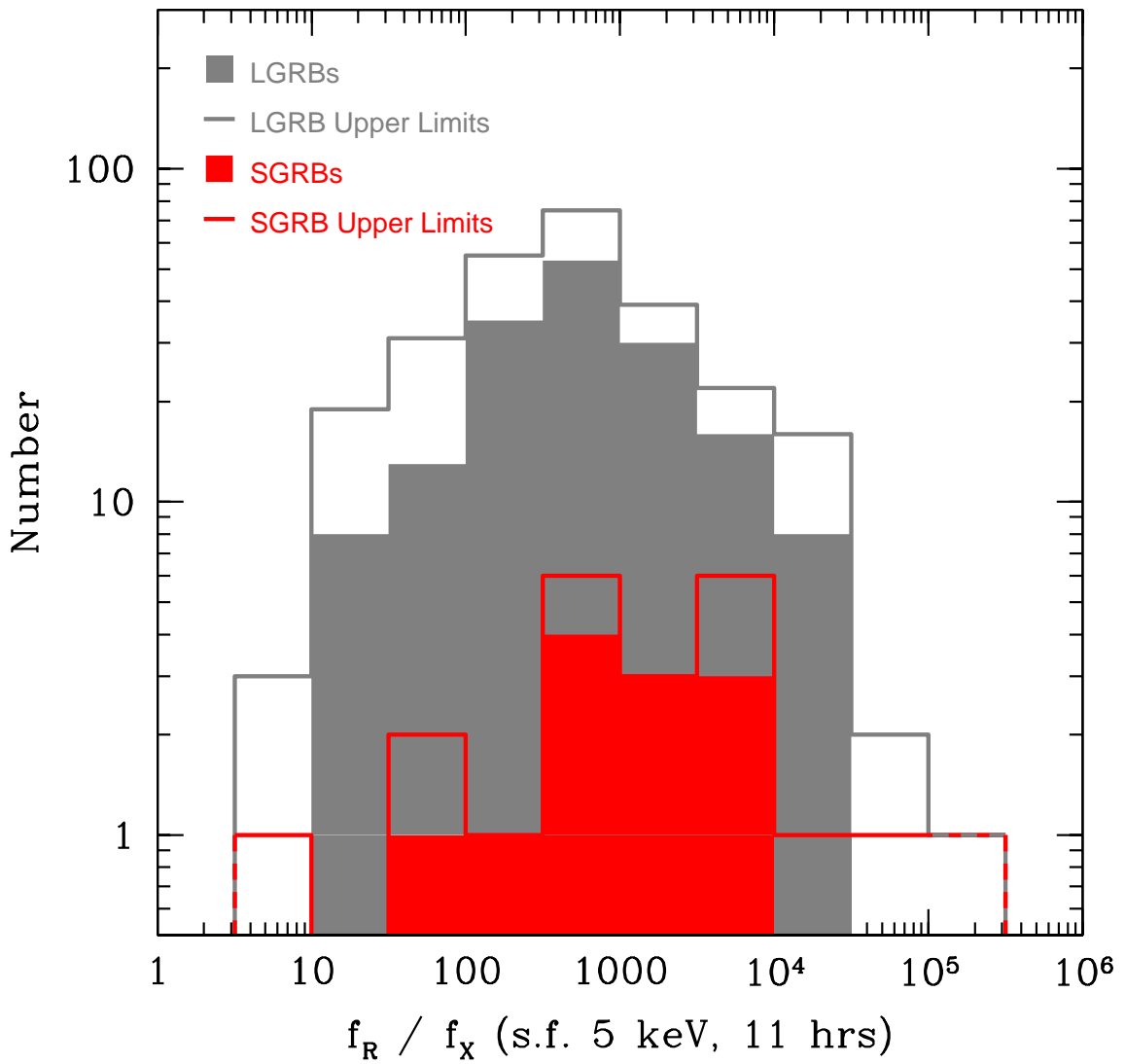


Fig. 8.— Histogram of the ratio of the observed fluxes at the optical and X-band after 11 hours (observed time). Long GRBs are marked in gray, and short ones in red. When only upper limits are known, empty boxes are drawn. Clearly, both samples show a nearly Gaussian shape in a log-normal plot, with similar means.

Table 1:: Observed Prompt and Afterglow Properties of Short-Duration GRBs

GRB	Satellite	Channel	z	Fluence [10^{-7} keV] erg cm^{-2}]	Log $E_{\gamma, ISO}$ [erg]	11 hr R -band [μJy]	11 hr keV [10^{-14} $\text{erg cm}^{-2} \text{s}^{-1}$]	Log F_R / F_X	Ref.
001025B	<i>Ulysses</i>	25–100		2.0		< 382.6			1,2
001204	<i>Ulysses</i>	25–100		8.6		< 190.9			3,4
010119	<i>Ulysses</i>	25–100		3.2		< 1970.3			5,6
010326B	<i>HETE</i>	30–400		3.3 ± 0.8		< 26.0			7,8
020531	<i>HETE</i>	30–400		$11.1^{+1.4}_{-1.3}$		< 16.9			9,10
020603	<i>Ulysses</i>	25–100		60.0		< 708.7			11,12
021201	<i>Ulysses</i>	25–100		2.0		< 58.0			13,14
050202	<i>Swift</i>	15–150		0.3 ± 0.1		< 55.3			15, 16
050509B	<i>Swift</i>	15–150	0.225	0.09 ± 0.02	$48.05^{+0.09}_{-0.11}$	< 0.4	2.9 ± 1.0	< 2.93	15, 17, 18
050709	<i>HETE</i>	30–400	0.161	3.0 ± 0.4	$49.06^{+0.13}_{-0.18}$	$2.9^{+1.2}_{-0.9}$	$2.8^{+2.5}_{-1.4}$	$3.85^{+0.31}_{-0.33}$	19, 20
050724	<i>Swift</i>	15–150	0.257	10.0 ± 1.2	$50.21^{+0.05}_{-0.06}$	29.1 ± 1.1	20.5 ± 6.6	$3.98^{+0.12}_{-0.17}$	15, 21, 22, 23
050813	<i>Swift</i>	15–150	0.722 [†]	0.4 ± 0.1	$49.77^{+0.10}_{-0.12}$	< 2.6	$0.21^{+1.12}_{-0.18}$	< 4.92	15, 24, 25, 26
050906	<i>Swift</i>	15–150		0.06 ± 0.02		< 0.1	< 2.44 ^a		15, 27, 28
051105A	<i>Swift</i>	15–150		0.22 ± 0.04		< 9.0			15, 29, 30
051210	<i>Swift</i>	15–150	0.114 ^C	0.9 ± 0.1	$48.36^{+0.07}_{-0.08}$	< 2.1	$1.72^{+6.66}_{-1.41}$	< 3.91	15, 24, 31, 32
051211	<i>HETE</i>	30–400		7.2 ± 1.2		< 6.4			7, 33, 34
051221A	<i>Swift</i>	15–150	0.546	11.5 ± 0.4	50.95 ± 0.01	$7.5^{+2.1}_{-1.6}$	99.4 ± 24.5	$2.71^{+0.14}_{-0.16}$	15, 21, 35
051227	<i>Swift</i>	15–150		7.0 ± 1.1		0.5 ± 0.1	9.3 ± 2.5		15, 21, 36
060121	<i>HETE</i>	30–400		38.7 ± 2.7		$1.6^{+0.4}_{-0.3}$	157.0 ± 26.4		7, 21, 37
060313	<i>Swift</i>	15–150		11.3 ± 0.5		$9.9^{+5.5}_{-3.6}$	65.5 ± 14.6		15, 21, 36
060502B	<i>Swift</i>	15–150	0.287 [†]	0.4 ± 0.1	$48.90^{+0.05}_{-0.06}$	< 1.0	$1.2^{+0.6}_{-0.5}$	< 3.73	15, 24, 38, 39
060801	<i>Swift</i>	15–150	1.131 [†]	0.8 ± 0.1	$50.43^{+0.05}_{-0.06}$	< 0.5	$0.6^{+2.2}_{-0.5}$	< 3.75	15, 24, 40, 41
061006	<i>Swift</i>	15–150	0.438	14.2 ± 1.4	$50.84^{+0.04}_{-0.05}$	6.0 ± 0.4	34.4 ± 8.9	$3.07^{+0.10}_{-0.13}$	15, 21, 36, 42
061201	<i>Swift</i>	15–150	0.084 ^C	3.3 ± 0.3	$48.68^{+0.03}_{-0.04}$	2.0 ± 0.2	24.9 ± 7.7	$2.73^{+0.13}_{-0.17}$	15, 21, 43, 44

Continued on Next Page...

Table 1 – Continued

GRB	Satellite	Channel	z	Fluence [10^{-7} erg cm $^{-2}$]	Log $E_{\gamma, ISO}$ [erg]	11 hr R -band [μ Jy]	11 hr keV [10^{-14} erg cm $^{-2}$ s $^{-1}$]	Log $F_R /$ F_X	Ref.
061210	<i>Swift</i>	15–150	0.410 [†]	11.1±1.8	$50.67^{+0.06}_{-0.07}$	< 0.7	$580.8^{+581.3}_{-335.2}$	<0.93	15, 24, 36, 45
061217	<i>Swift</i>	15–150	0.827 [†]	0.4±0.1	$49.88^{+0.07}_{-0.08}$	< 2.5	$0.2^{+0.7}_{-0.1}$	<5.00	15, 24, 46, 47
070209	<i>Swift</i>	15–150		0.2±0.1		< 13.6	<1.2		15, 48, 49
070406	<i>Swift</i>	15–150		0.4±0.1		< 67.2	< 34.6		15, 50, 51
070429B	<i>Swift</i>	15–150	0.904	0.6±0.1	$50.13^{+0.06}_{-0.08}$	< 0.3	$4.5^{+10.7}_{-3.4}$	<2.72	15, 24, 52, 53
070707	<i>Konus-Wind</i>	20–2000			$14.1^{+1.6}_{-10.7}$	$2.4^{+0.8}_{-0.6}$	43.3 ± 9.3		54, 24, 55
070714B	<i>Swift</i>	15–150	0.922	7.2±0.9	$51.21^{+0.05}_{-0.06}$	$2.9^{+1.1}_{-0.9}$	13.6 ± 3.0	$3.16^{+0.17}_{-0.19}$	56, 21, 57, 58
070724A	<i>Swift</i>	15–150	0.457 [†]	0.3±0.1	$49.20^{+0.09}_{-0.12}$	< 0.2	24.2 ± 10.9	<1.82	59, 21, 60, 61
070729	<i>Swift</i>	15–150		1.0±0.2		< 5.4	1.7 ± 1.2		62, 24, 63
070809	<i>Swift</i>	15–150		1.0±0.1		0.9 ± 0.2	13.6 ± 3.0		64, 21, 65
070810B	<i>Swift</i>	15–150		0.12±0.03		< 2.0	< 0.9 ^a		66, 67, 68
071112B	<i>Swift</i>	15–150		0.5±0.1		< 1.5	< 4.2		69, 70
071227	<i>Swift</i>	15–150	0.384	2.3±0.3	49.91 ± 0.06	$2.2^{+0.9}_{-0.7}$	2.6 ± 0.7	$3.77^{+0.18}_{-0.21}$	71, 21, 72, 73

[†]: probable redshift, ^C: cluster redshift, ^a Uses estimated N_H , 1. Hurley et al. (2000b), 2. Castro-Tirado et al. (2000), 3. Hurley et al. (2000a), 4. Price et al. (2000), 5. Hurley et al. (2001), 6. Price et al. (2001a), 7. Donaghy et al. (2006), 8. Price et al. (2001b), 9. Sakamoto et al. (2005), 10. Lamb et al. (2002), 11. Hurley et al. (2002a), 12. Price et al. (2002), 13. Hurley et al. (2002b), 14. Nysewander et al. (2002), 15. Sakamoto et al. (2008), 16. Castro-Tirado et al. (2005), 17. Gehrels et al. (2005), 18. Bloom et al. (2006), 19. Villasenor et al. (2005), 20. Fox et al. (2005), 21. Gehrels et al. (2008), 22. Malesani et al. (2007), 23. Berger et al. (2005), 24. Evans et al. (2007), 25. Bikmaev et al. (2005), 26. Berger (2005), 27. Levan et al. (2008), 28. Pagani et al. (2005), 29. Halpern et al. (2005a), 30. Mineo (2005), 31. Berger & Boss (2005), 32. Berger & Fox (2005), 33. Cusumano et al. (2005), 34. Guidorzi et al. (2005), 35. Soderberg et al. (2006a), 36. Berger et al. (2007a), 37. Levan et al. (2006b), 38. Price et al. (2006), 39. Bloom et al. (2007), 40. Piranomonte et al. (2006), 41. Cucchiara et al. (2006), 42. D' Avanzo et al. (2008), 43. Stratta et al. (2007b), 44. Berger (2007b), 45. Cenko et al. (2006), 46. Cobb (2006), 47. Berger (2006a), 48. Stratta et al. (2007c), 49. Johnson et al. (2007), 50. McBreen et al. (2007), 51. Zheng et al. (2007), 52. Holland et al. (2007), 53. Perley et al. (2007), 54. Golenetskii et al. (2007), 55. Piranomonte et al. (2007), 56. Barbier et al. (2007), 57. Levan et al. (2007), 58. Graham et al. (2007)

59. Ziaeepour et al. (2007a) 60. Cenko et al. (2007), 61. Cucchiara et al. (2007), 62. Guidorzi et al. (2007), 63. Berger & Kaplan (2007), 64. Marshall et al. (2007a), 65. Perley et al. (2007a), 66. Marshall et al. (2007b), 67. Starling et al. (2007), 68. Xin et al. (2007), 69. Perri et al. (2007a), 70. Kocevski & Bloom (2007), 71. Stratta et al. (2007a), 72. Wiersema et al. (2008), 73. Berger et al. (2007b)

Table 2:: Observed Prompt and Afterglow Properties of Long-Duration GRBs

GRB	Satellite	Channel	z	Fluence [10^{-7} keV] [erg cm^{-2}]	Log E_{ISO} [erg]	11 hr <i>R</i> -band [μJy]	11 hr keV [10^{-14} $\text{erg cm}^{-2} \text{s}^{-1}$]	$F_R /$ F_X	Ref.
970111	<i>BeppoSAX</i>	40–700		430 ± 30		<33.6	7.5 ± 4.7^a		1, 2
970228	<i>BeppoSAX</i>	40–700	0.695	64.5	$51.91^{+0.12}_{-0.17}$	$22.0^{+4.0}_{-3.5}$	208.0 ± 27.0^a	$2.86^{+0.29}_{-0.15}$	1, 3, 4
970402	<i>BeppoSAX</i>	40–700		82.0 ± 9.0		<44.0	13.5 ± 7.3^a		1, 5
970508	<i>BeppoSAX</i>	40–700	0.835	14.5	$51.42^{+0.12}_{-0.17}$	$6.5^{+1.6}_{-1.3}$	57.2 ± 9.0^a	$2.97^{+0.25}_{-0.21}$	1, 6, 7
970616	<i>BATSE</i>	20–100		109.7 ± 0.6		<14.0	$385.8^{+208.3b,d}_{-186.8}$		8, 9, 10
970815	<i>BATSE</i>	20–100		52.5 ± 0.6		$14.2^{+12.3}_{-6.7}$	$498.9^{+471.8b}_{-286.4}$		8, 11, 12
970828	<i>BATSE</i>	20–100	0.958	700.0	$53.23^{+0.12}_{-0.17}$	<0.6	$198.8^{+113.5b,d}_{-91.1}$	<1.26	13, 14, 15
971214	<i>BeppoSAX</i>	40–700	3.42	64.9	$53.03^{+0.24}_{-0.60}$	$5.6^{+0.5}_{-0.4}$	63.5 ± 9.1^a	2.97 ± 0.29	1, 16
971227	<i>BeppoSAX</i>	40–700		6.6 ± 0.7		<5.8	$40.4^{+14.3a}_{-6.2}$		1, 17, 18
980326	<i>BeppoSAX</i>	40–700		7.5 ± 1.5		$11.9^{+1.2}_{-1.1}$	$<152.6^{b,d}$		1, 19, 20
980329	<i>BeppoSAX</i>	40–700		650 ± 50		$2.3^{+0.7}_{-0.6}$	59.9 ± 5.6^a		1, 21
980425	<i>BeppoSAX</i>	40–700	0.009	28.5 ± 5.0	$47.47^{+0.23}_{-0.51}$	<24.6	28.2 ± 5.9^a	<3.71	1, 22, 23
980515	<i>BeppoSAX</i>	40–700		23.0 ± 3.0			56.0 ± 22.0^a		1
980519	<i>BeppoSAX</i>	40–700		81.0 ± 5.0		$62.4^{+10.1}_{-9.0}$	$39.0^{+12.0a}_{-11.0}$		1, 24
980613	<i>BeppoSAX</i>	40–700	1.097	9.9	$51.31^{+0.24}_{-0.60}$	$2.9^{+0.7}_{-0.6}$	$26.0^{+12.0a}_{-11.0}$	$2.98^{+0.32}_{-0.29}$	1, 25, 26
980703	<i>BeppoSAX</i>	40–700	0.966	300 ± 100	$52.69^{+0.24}_{-0.60}$	$35.5^{+11.3}_{-9.2}$	$139.9^{+69.9a}_{-32.0}$	$3.33^{+0.33}_{-0.17}$	1, 27, 28

A complete version of this Table can be found in the Electronic Supplement.

^a: 1.6–10.0 keV, ^b: 2–10 keV, ^c: 0.5–6.0 keV, ^d: Uses estimated N_H , 1. de Pasquale et al. (2006) 2. Castro-Tirado et al. (1997) 3. Galama et al. (1997), 4. Djorgovski et al. (1999), 5. Groot et al. (1997a), 6. Djorgovski et al. (1997), 7. Metzger et al. (1997), 8. Paciesas et al. (1999), 9. Connaughton et al. (1997), 10. Gorosabel et al. (1999), 11. Mirabal et al. (2005), 12. Soderberg et al. (2004a), 13. Groot et al. (1998a), 14. Murakami et al. (1997), 15. Djorgovski et al. (2001), 16. Diercks et al. (1998), 17. Antonelli et al. (1999), 18. Groot et al. (1997b), 19. Marshall et al. (1998), 20. Groot et al. (1998b), 21. Reichart et al. (1999), 22. Tinney et al. (1998), 23. Galama et al. (1998a), 24. Vrba et al. (2000), 25. Djorgovski et al. (2003), 26. Hjorth et al. (2002), 27. Djorgovski et al. (1998), 28. Vreeswijk et al. (1999)

Table 3: Best-fit Results of the Observed Properties of Long and Short GRBs

	slope α	zero-point a	χ^2/dof	zero-point, w/ $\alpha = 1$	χ^2/dof
Short, optical	1.63±0.91	10.66±7.52	0.65	6.74±0.17	0.73
Long, optical	0.97±0.11	6.58±0.62	1.30	6.78±0.05	1.30
Short, X-ray	1.06±0.30	-5.94±2.02	0.67	-6.33±0.16	0.66
Long, X-ray	1.10±0.09	-5.59±0.54	1.05	-6.18±0.04	1.06

Table 4: Best-fit Results of the Rest-Frame Properties of Long and Short GRBs

	slope α	zero-point a	χ^2/dof	zero-point, w/ $\alpha = 1$	χ^2/dof
Short, optical	1.05±0.26	-24.42±13.20	0.31	-21.90±0.22	0.31
Long, optical	0.93±0.09	-19.20±4.44	0.90	-21.68±0.07	0.90
Short, X-ray	1.00±0.21	-25.18±10.54	0.71	-25.04±0.19	0.71
Long, X-ray	1.05±0.07	-27.32±3.73	1.09	-24.74±0.07	1.10

Table 1:: Observed Prompt and Afterglow Properties of
Short-Duration GRBs

GRB	Satellite	Channel	z	Fluence $[10^{-7}$ [keV] $\text{erg cm}^{-2}]$	Log $E_{\gamma, ISO}$ [erg]	11 hr <i>R</i> -band $[\mu\text{Jy}]$	11 hr keV $[10^{-14}$ $\text{erg cm}^{-2} \text{s}^{-1}]$	Log $F_R /$ F_X	Ref.
001025B	<i>Ulysses</i>	25–100		2.0		< 382.6			1,2
001204	<i>Ulysses</i>	25–100		8.6		< 190.9			3,4
010119	<i>Ulysses</i>	25–100		3.2		< 1970.3			5,6
010326B	<i>HETE</i>	30–400		3.3 ± 0.8		< 26.0			7,8
020531	<i>HETE</i>	30–400		$11.1^{+1.4}_{-1.3}$		< 16.9			9,10
020603	<i>Ulysses</i>	25–100		60.0		< 708.7			11,12
021201	<i>Ulysses</i>	25–100		2.0		< 58.0			13,14
050202	<i>Swift</i>	15–150		0.3 ± 0.1		< 55.3			15, 16
050509B	<i>Swift</i>	15–150	0.225	0.09 ± 0.02	$48.05^{+0.09}_{-0.11}$	< 0.4	2.9 ± 1.0	< 2.93	15, 17, 18
050709	<i>HETE</i>	30–400	0.161	3.0 ± 0.4	$49.06^{+0.13}_{-0.18}$	$2.9^{+1.2}_{-0.9}$	$2.8^{+2.5}_{-1.4}$	$3.85^{+0.31}_{-0.33}$	19, 20
050724	<i>Swift</i>	15–150	0.257	10.0 ± 1.2	$50.21^{+0.05}_{-0.06}$	29.1 ± 1.1	20.5 ± 6.6	$3.98^{+0.12}_{-0.17}$	15, 21, 22, 23
050813	<i>Swift</i>	15–150	0.722 [†]	0.4 ± 0.1	$49.77^{+0.10}_{-0.12}$	< 2.6	$0.21^{+1.12}_{-0.18}$	< 4.92	15, 24, 25, 26
050906	<i>Swift</i>	15–150		0.06 ± 0.02		< 0.1	< 2.44 ^a		15, 27, 28
051105A	<i>Swift</i>	15–150		0.22 ± 0.04		< 9.0			15, 29, 30
051210	<i>Swift</i>	15–150	0.114 ^C	0.9 ± 0.1	$48.36^{+0.07}_{-0.08}$	< 2.1	$1.72^{+6.66}_{-1.41}$	< 3.91	15, 24, 31, 32
051211	<i>HETE</i>	30–400		7.2 ± 1.2		< 6.4			7, 33, 34
051221A	<i>Swift</i>	15–150	0.546	11.5 ± 0.4	50.95 ± 0.01	$7.5^{+2.1}_{-1.6}$	99.4 ± 24.5	$2.71^{+0.14}_{-0.16}$	15, 21, 35
051227	<i>Swift</i>	15–150		7.0 ± 1.1		0.5 ± 0.1	9.3 ± 2.5		15, 21, 36
060121	<i>HETE</i>	30–400		38.7 ± 2.7		$1.6^{+0.4}_{-0.3}$	157.0 ± 26.4		7, 21, 37
060313	<i>Swift</i>	15–150		11.3 ± 0.5		$9.9^{+5.5}_{-3.6}$	65.5 ± 14.6		15, 21, 36
060502B	<i>Swift</i>	15–150	0.287 [†]	0.4 ± 0.1	$48.90^{+0.05}_{-0.06}$	< 1.0	$1.2^{+0.6}_{-0.5}$	< 3.73	15, 24, 38, 39
060801	<i>Swift</i>	15–150	1.131 [†]	0.8 ± 0.1	$50.43^{+0.05}_{-0.06}$	< 0.5	$0.6^{+2.2}_{-0.5}$	< 3.75	15, 24, 40, 41
061006	<i>Swift</i>	15–150	0.438	14.2 ± 1.4	$50.84^{+0.04}_{-0.05}$	6.0 ± 0.4	34.4 ± 8.9	$3.07^{+0.10}_{-0.13}$	15, 21, 36, 42
061201	<i>Swift</i>	15–150	0.084 ^C	3.3 ± 0.3	$48.68^{+0.03}_{-0.04}$	2.0 ± 0.2	24.9 ± 7.7	$2.73^{+0.13}_{-0.17}$	15, 21, 43, 44

Continued on Next Page...

Table 1 – Continued

GRB	Satellite	Channel	z	Fluence [10^{-7} erg cm $^{-2}$]	Log $E_{\gamma, ISO}$ [erg]	11 hr R -band [μ Jy]	11 hr keV [10^{-14} erg cm $^{-2}$ s $^{-1}$]	Log $F_R /$ F_X	Ref.
061210	<i>Swift</i>	15–150	0.410 [†]	11.1±1.8	$50.67^{+0.06}_{-0.07}$	< 0.7	$580.8^{+581.3}_{-335.2}$	<0.93	15, 24, 36, 45
061217	<i>Swift</i>	15–150	0.827 [†]	0.4±0.1	$49.88^{+0.07}_{-0.08}$	< 2.5	$0.2^{+0.7}_{-0.1}$	<5.00	15, 24, 46, 47
070209	<i>Swift</i>	15–150		0.2±0.1		< 13.6	<1.2		15, 48, 49
070406	<i>Swift</i>	15–150		0.4±0.1		< 67.2	< 34.6		15, 50, 51
070429B	<i>Swift</i>	15–150	0.904	0.6±0.1	$50.13^{+0.06}_{-0.08}$	< 0.3	$4.5^{+10.7}_{-3.4}$	<2.72	15, 24, 52, 53
070707	<i>Konus-Wind</i>	20–2000			$14.1^{+1.6}_{-10.7}$	$2.4^{+0.8}_{-0.6}$	43.3 ± 9.3		54, 24, 55
070714B	<i>Swift</i>	15–150	0.922	7.2±0.9	$51.21^{+0.05}_{-0.06}$	$2.9^{+1.1}_{-0.9}$	13.6 ± 3.0	$3.16^{+0.17}_{-0.19}$	56, 21, 57, 58
070724A	<i>Swift</i>	15–150	0.457 [†]	0.3±0.1	$49.20^{+0.09}_{-0.12}$	< 0.2	24.2 ± 10.9	<1.82	59, 21, 60, 61
070729	<i>Swift</i>	15–150		1.0±0.2		< 5.4	1.7 ± 1.2		62, 24, 63
070809	<i>Swift</i>	15–150		1.0±0.1		0.9 ± 0.2	13.6 ± 3.0		64, 21, 65
070810B	<i>Swift</i>	15–150		0.12±0.03		< 2.0	< 0.9 ^a		66, 67, 68
071112B	<i>Swift</i>	15–150		0.5±0.1		< 1.5	< 4.2		69, 70
071227	<i>Swift</i>	15–150	0.384	2.3±0.3	49.91 ± 0.06	$2.2^{+0.9}_{-0.7}$	2.6 ± 0.7	$3.77^{+0.18}_{-0.21}$	71, 21, 72, 73

[†]: probable redshift, ^C: cluster redshift, ^a Uses estimated N_H , 1. Hurley et al. (2000c), 2. Castro-Tirado et al. (2000), 3. Hurley et al. (2000b), 4. Price et al. (2000d), 5. Hurley et al. (2001a), 6. Price et al. (2001a), 7. Donaghy et al. (2006), 8. Price et al. (2001b), 9. Sakamoto et al. (2005b), 10. Lamb et al. (2002), 11. Hurley et al. (2002a), 12. Price et al. (2002c), 13. Hurley et al. (2002j), 14. Nysewander et al. (2002a), 15. Sakamoto et al. (2008), 16. Castro-Tirado et al. (2005), 17. Gehrels et al. (2005), 18. Bloom et al. (2006), 19. Villasenor et al. (2005), 20. Fox et al. (2005), 21. Gehrels et al. (2009), 22. Malesani et al. (2007a), 23. Berger et al. (2005a), 24. Evans et al. (2007), 25. Bikmaev et al. (2005), 26. Berger (2005), 27. Levan et al. (2008), 28. Pagani et al. (2005), 29. Halpern et al. (2005a), 30. Mineo (2005), 31. Berger & Boss (2005), 32. Berger & Fox (2005), 33. Cusumano et al. (2005), 34. Guidorzi et al. (2005a), 35. Soderberg et al. (2006a), 36. Berger et al. (2007c), 37. Levan et al. (2006b), 38. Price et al. (2006), 39. Bloom et al. (2007a), 40. Piranomonte et al. (2006a), 41. Cucchiara et al. (2006a), 42. D' Avanzo et al. (2008), 43. Stratta et al. (2007b), 44. Berger (2007), 45. Cenko et al. (2006a), 46. Cobb (2006), 47. Berger (2006a), 48. Stratta et al. (2007d), 49. Johnson et al. (2007), 50. McBreen et al. (2007a), 51. Zheng et al. (2007), 52. Holland et al. (2007a), 53. Perley et al. (2007c), 54. Golenetskii et al. (2007b), 55. Piranomonte et al. (2007), 56. Barbier et al. (2007), 57. Levan et al. (2007a), 58. Graham et al. (2007)

59. Ziaeepour et al. (2007a), 60. Cenko et al. (2007a), 61. Cucchiara et al. (2007a), 62. Guidorzi et al. (2007a), 63. Berger & Kaplan (2007), 64. Marshall et al. (2007a), 65. Perley et al. (2007a), 66. Marshall et al. (2007b), 67. Starling et al. (2007), 68. Xin et al. (2007a), 69. Perri et al. (2007a), 70. Kocevski & Bloom (2007), 71. Stratta et al. (2007a), 72. Wiersema et al. (2008), 73. Berger et al. (2007b)

Table 2:: Observed Prompt and Afterglow Properties of Long-Duration GRBs (con't)

GRB	Satellite	Channel	z	Fluence [10^{-7} [keV] erg cm^{-2}]	Log $E_{\gamma, ISO}$ [erg]	11 hr <i>R</i> -band [μJy]	11 hr 0.2–10 keV [10^{-14} $\text{erg cm}^{-2} \text{s}^{-1}$]	Log $F_R /$ F_X	Ref.
970111	<i>BeppoSAX</i>	40–700		430 ± 30		< 33.6	7.5 ± 4.7^a		1, 2
970228	<i>BeppoSAX</i>	40–700	0.695	64.5	$51.91^{+0.12}_{-0.17}$	$22.0^{+4.0}_{-3.5}$	208.0 ± 27.0^a	$2.86^{+0.29}_{-0.15}$	1, 3, 4
970402	<i>BeppoSAX</i>	40–700		82.0 ± 9.0		< 44.0	13.5 ± 7.3^a		1, 5
970508	<i>BeppoSAX</i>	40–700	0.835	14.5	$51.42^{+0.12}_{-0.17}$	$6.5^{+1.6}_{-1.3}$	57.2 ± 9.0^a	$2.97^{+0.25}_{-0.21}$	1, 6, 7
970616	<i>BATSE</i>	20–100		109.7 ± 0.6		< 14.0	$385.8^{+208.3b,d}_{-186.8}$		8, 9, 10
970815	<i>BATSE</i>	20–100		52.5 ± 0.6		$14.2^{+12.3}_{-6.7}$	$498.9^{+471.8b}_{-286.4}$		8, 11, 12
970828	<i>BATSE</i>	20–100	0.958	700.0	$53.23^{+0.12}_{-0.17}$	< 0.6	$198.8^{+113.5b,d}_{-91.1}$	< 1.26	13, 14, 15
971214	<i>BeppoSAX</i>	40–700	3.42	64.9	$53.03^{+0.24}_{-0.60}$	$5.6^{+0.5}_{-0.4}$	63.5 ± 9.1^a	2.97 ± 0.29	1, 16
971227	<i>BeppoSAX</i>	40–700		6.6 ± 0.7		< 5.8	$40.4^{+14.3a}_{-6.2}$		1, 17, 18
980326	<i>BeppoSAX</i>	40–700		7.5 ± 1.5		$11.9^{+1.2}_{-1.1}$	$< 152.6^{b,d}$		1, 19, 20
980329	<i>BeppoSAX</i>	40–700		650 ± 50		$2.3^{+0.7}_{-0.6}$	59.9 ± 5.6^a		1, 21
980425	<i>BeppoSAX</i>	40–700	0.009	28.5 ± 5.0	$47.47^{+0.23}_{-0.51}$	< 24.6	28.2 ± 5.9^a	< 3.71	1, 22, 23
980515	<i>BeppoSAX</i>	40–700		23.0 ± 3.0			56.0 ± 22.0^a		1
980519	<i>BeppoSAX</i>	40–700		81.0 ± 5.0		$62.4^{+10.1}_{-9.0}$	$39.0^{+12.0a}_{-11.0}$		1, 24
980613	<i>BeppoSAX</i>	40–700	1.097	9.9	$51.31^{+0.24}_{-0.60}$	$2.9^{+0.7}_{-0.6}$	$26.0^{+12.0a}_{-11.0}$	$2.98^{+0.32}_{-0.29}$	1, 25, 26
980703	<i>BeppoSAX</i>	40–700	0.966	300 ± 100	$52.69^{+0.24}_{-0.60}$	$35.5^{+11.3}_{-9.2}$	$139.9^{+69.9a}_{-32.0}$	$3.33^{+0.33}_{-0.17}$	1, 27, 28
981220	<i>BeppoSAX</i>	40–700		100 ± 20		< 9.6			29, 30
981226	<i>BeppoSAX</i>	40–700		4.0 ± 1.0		$12.0^{+4.4}_{-3.3}$	$28.1^{+21.1a}_{-13.1}$		1, 31
990123	<i>BeppoSAX</i>	40–700	1.6	1790.0	$53.90^{+0.24}_{-0.60}$	$37.8^{+3.1}_{-2.9}$	541.5 ± 17.1^a	$2.80^{+0.28}_{-0.17}$	1, 32
990217	<i>BeppoSAX</i>	40–700		12.7 ± 1.5		< 1.0	$< 28.0^a$		1, 33
990308	<i>BATSE</i>	20–100		21.2 ± 0.5		$65.8^{+34.2}_{-22.7}$			8, 34
990506	<i>BATSE</i>	20–100	1.307	342.6 ± 0.6	$53.40^{+0.12}_{-0.16}$	< 1.6			8, 35, 36
990510	<i>BeppoSAX</i>	40–700	1.619	181.0	$52.91^{+0.24}_{-0.60}$	$181.9^{+8.5}_{-8.2}$	346.7 ± 21.1^a	$3.68^{+0.26}_{-0.21}$	1, 37, 38
990520	<i>BATSE</i>	20–200		8.0 ± 3.0		< 5.8			39, 40

Continued on Next Page...

Table 2 – Continued

GRB	Satellite	Channel	z	Fluence [10^{-7} erg cm $^{-2}$]	Log $E_{\gamma, ISO}$ [erg]	11 hr <i>R</i> -band [μ Jy]	11 hr keV [10^{-14} erg cm $^{-2}$ s $^{-1}$]	Log $F_R /$ F_X	Ref.
990527	<i>Ulysses</i>	25–100		80.0		<28.2			41, 42
990704	<i>BeppoSAX</i>	40–700		10.0 ± 1.0		<2.1	58.9 ± 8.4^a		1, 43
990705	<i>BeppoSAX</i>	40–700	0.842	4230.0	$53.72^{+0.24}_{-0.60}$	$13.0^{+3.5}_{-2.9}$	<46.8 a	>3.48	1, 44, 45
990712	<i>BeppoSAX</i>	40–700	0.434	65.0 ± 3.0	$51.31^{+0.22}_{-0.49}$	26.2 ± 1.0			1, 46, 47
990806	<i>BeppoSAX</i>	40–700		42.0		<2.7	32.0 ± 8.7^a		1, 48
991014	<i>BeppoSAX</i>	40–700		9.0 ± 1.0		<3.6	$54.2^{+19.1^a}_{-15.1}$		1, 49
991105	<i>BATSE</i>	20–100		15.6 ± 0.4		<4.6			8, 50
991208	<i>Ulysses</i>	25–100	0.707	490.0 ± 49.0	$53.02^{+0.12}_{-0.16}$	$392.5^{+276.3}_{-164.9}$			51, 52, 53
991216	<i>BATSE</i>	20–100	1.02	393.9 ± 0.5	$53.25^{+0.12}_{-0.16}$	$571.1^{+27.3}_{-26.1}$	$780.7^{+339.5b}_{-238.1}$	$3.79^{+0.26}_{-0.13}$	8, 54, 55, 56
000115	<i>BATSE</i>	20–100		82.9 ± 0.2		<9.1			8, 57
000126	<i>Ulysses</i>	25–100		100.0		<11.4			58, 59 C ^a
000131	<i>Ulysses</i>	25–100	4.5	100.0	$53.80^{+0.16}_{-0.26}$	$10.2^{+10.6}_{-5.2}$			60, 61
000210	<i>BeppoSAX</i>	40–700	0.846	610 ± 20	$52.89^{+0.22}_{-0.48}$	<2.4	67.0 ± 3.0^a	<2.44	1, 54, 62
000214	<i>BeppoSAX</i>	40–700		61.7		<42.4	$61.9^{+21.0a}_{-18.0}$		1, 63
000301C	<i>Ulysses</i>	25–100	2.03	21.0	$52.55^{+0.16}_{-0.26}$	$66.3^{+34.1}_{-22.6}$			64, 65, 66
000307	<i>Ulysses</i>	25–100		10.0		<94.0			67, 68
000323	<i>Ulysses</i>	25–100		43.0		<235.1			69, 70
000408	<i>Ulysses</i>	25–100		74.0		<1467.3			8, 71, 72
000416	<i>BeppoSAX</i>	40–700		29000.0 ± 0.3		< 120.5			73, 74
000418	<i>Ulysses</i>	25–100	1.118	130.0	$52.85^{+0.16}_{-0.26}$	$32.1^{+25.9}_{-14.3}$			35, 75, 76
000424	<i>BATSE</i>	20–100		11.2 ± 0.3		<11.6			8, 77
000429	<i>BATSE</i>	20–100		51.3 ± 0.5		<204.4			8, 78
000508B	<i>BATSE</i>	20–100		132.5 ± 1.1		<39.8			8, 79
000519	<i>BATSE</i>	20–100		19.4 ± 0.2		<35.0			8, 80
000528	<i>BeppoSAX</i>	40–700		14.4 ± 0.4		<3.4	$30.0^{+41.0a}_{-14.0}$		1, 81
000604	<i>Ulysses</i>	25–100		130.0		<44.8			82, 83

Continued on Next Page...

Table 2 – Continued

GRB	Satellite	Channel	z	Fluence [10^{-7} erg cm $^{-2}$]	Log $E_{\gamma, ISO}$ [erg]	11 hr R -band [μ Jy]	11 hr keV [10^{-14} erg cm $^{-2}$ s $^{-1}$]	Log $F_R /$ F_X	Ref.
000615	<i>BeppoSAX</i>	40–700		9.8±0.9		<19.1	12.9±3.8 ^a		1, 84
000616	<i>Ulysses</i>	25–100		92.0		<928.6			85, 86
000623	<i>Ulysses</i>	25–100		50.0		<138.4			87, 88
000630	<i>Ulysses</i>	25–100		20.0		3.3 $^{+0.8}_{-0.7}$			89, 90
000801	<i>Ulysses</i>	25–100		170.0		<3.1			91, 92
000812	<i>Ulysses</i>	25–100		200.0		<30.2			93, 94
000830	<i>Ulysses</i>	25–100		52.0		<42.5			95, 96
000911	<i>Ulysses</i>	25–100	1.058	50.0	52.39 $^{+0.16}_{-0.26}$	57.3 $^{+28.5}_{-19.3}$			97, 98
000926	<i>Ulysses</i>	25–100	2.038	220.0	53.57 $^{+0.16}_{-0.26}$	105.4 $^{+26.1}_{-20.9}$	325.7 $^{+156.9a}_{-86.9}$	3.49 $^{+0.34}_{-0.23}$	1, 99, 100
001007	<i>Ulysses</i>	25–100		330.0		139.5 $^{+158.0}_{-75.5}$			101, 102
001019	<i>Ulysses</i>	25–100		73.0		<573.1			103, 104
001025A	<i>Ulysses</i>	25–100		32.0		<0.7	33.4 $^{+17.6b}_{-11.6}$		105, 106
001109	<i>BeppoSAX</i>	40–700		49.7±1.9		<2.5	231.8 $^{+58.0a}_{-45.0}$		1, 107
001120	<i>Ulysses</i>	25–100		100.0		<15.1			108, 109
001212	<i>Ulysses</i>	25–100		120.0		<143.7			110, 111
010126	<i>HETE</i>	30–400		29.9		<2.8			112, 113
010213	<i>HETE</i>	30–400		0.7 $^{+0.6}_{-0.3}$		<31.7			114, 115
010214	<i>BeppoSAX</i>	40–700		45.0±0.8		4.0 $^{+1.3}_{-1.1}$	30.6 $^{+7.1a}_{-6.4}$		1, 116
010222	<i>BeppoSAX</i>	40–700	1.477	753.0	53.45 $^{+0.24}_{-0.60}$	76.9 $^{+12.0}_{-10.8}$	705.4±34.0 ^a	2.99 $^{+0.29}_{-0.16}$	1, 117, 118
010324	<i>Ulysses</i>	25–100		18.0		<122.4			119, 120
010326A	<i>HETE</i>	30–400		160.0		<31.7			112, 121
010412	<i>Ulysses</i>	25–100		94.0		<41.7			122, 123
010629B	<i>HETE</i>	30–400		28.6±2.7		38.4 $^{+13.7}_{-10.1}$			114, 124
010921	<i>HETE</i>	30–400	0.45	113.0±9.0	51.56 $^{+0.12}_{-0.17}$	143.7 $^{+40.3}_{-31.6}$			114, 125
011019	<i>HETE</i>	30–400		1.1±1.4		<145.7			114, 126
011030	<i>BeppoSAX</i>	2–28		9.0		<27.5	1800±500 ^b		54, 127, 128

Continued on Next Page...

Table 2 – Continued

GRB	Satellite	Channel	z	Fluence [10^{-7} erg cm $^{-2}$]	Log $E_{\gamma, ISO}$ [erg]	11 hr R -band [μ Jy]	11 hr keV [10^{-14} erg cm $^{-2}$ s $^{-1}$]	Log $F_R /$ F_X	Ref.
011121	<i>BeppoSAX</i>	40–700	0.36	1000.0 ± 20.0	$52.33^{+0.22}_{-0.48}$	$261.1^{+16.2}_{-15.3}$	135.9 ± 15.0^a	$4.16^{+0.27}_{-0.10}$	1, 129, 130
011130	<i>HETE</i>	30–400		1.0 ± 0.6		$61.5^{+47.1}_{-30.5}$			54, 114, 131
011211	<i>BeppoSAX</i>	40–700	2.14	37.0 ± 4.0	$52.44^{+0.23}_{-0.49}$	23.8 ± 0.9	17.2 ± 0.5^b	$4.13^{+0.27}_{-0.23}$	1, 54, 132, 133
011212	<i>HETE</i>	30–400		3.4 ± 2.5		< 58.2			114, 134
020124	<i>HETE</i>	30–400	3.198	61.0 ± 9.0	$52.93^{+0.13}_{-0.18}$	$32.8^{+19.4}_{-12.3}$			114, 135, 136
020127	<i>HETE</i>	30–400	1.9	21.0 ± 5.0	$52.08^{+0.15}_{-0.20}$	< 2.8	$26.9^{+25.6b}_{-14.4}$	< 2.81	54, 114, 137, 138
020305	<i>HETE</i>	30–400		104.0		$67.6^{+42.6}_{-28.0}$			112, 139
020317	<i>HETE</i>	30–400		1.3 ± 0.9		$41.9^{+37.3}_{-21.8}$			114, 140
020321	<i>BeppoSAX</i>	40–700		30.0		< 38.5	$< 34.0^a$		1, 141
020331	<i>HETE</i>	30–400		53.0 ± 9.0		$16.2^{+1.9}_{-1.8}$			114, 142
020405	<i>Ulysses</i>	25–100	0.695	300.0	$52.79^{+0.16}_{-0.26}$	$58.3^{+17.8}_{-13.7}$	710.0 ± 30.0^b	$2.82^{+0.29}_{-0.08}$	54, 143, 144
020410	<i>Konus-Wind</i>	19–1270		130.0		< 34.3	$778.0^{+63.0a}_{-69.0}$		1, 145, 146
020418B	<i>Ulysses</i>	25–100		100.0		< 53.8			147, 148
020427	<i>BeppoSAX</i>	2–28		5.8 ± 0.4			48.2 ± 17.0^a		1, 149
020525	<i>Ulysses</i>	25–100		100.0		< 50.6			150, 151
020604	<i>Ulysses</i>	25–100		30.0		< 17.5			152, 153
020714	<i>Ulysses</i>	25–100		83.0		< 5.1			154, 155
020715	<i>Ulysses</i>	25–100		130.0		< 2.4			156, 157
020801	<i>HETE</i>	30–400		95.0 ± 11.0		< 71.4			114, 158
020812	<i>HETE</i>	30–400		19.0 ± 8.0		< 16.9			114, 159
020813	<i>HETE</i>	30–400	1.25	840.0 ± 12.0	$53.34^{+0.12}_{-0.17}$	$69.7^{+23.7}_{-17.7}$	393.0 ± 8.0^b	$3.19^{+0.22}_{-0.27}$	54, 114, 160, 161
020819B	<i>HETE</i>	30–400	0.41	63.0 ± 8.0	< 4.7	$51.22^{+0.13}_{-0.19}$			114, 162, 163
020903	<i>HETE</i>	30–400	0.25	$0.2^{+0.4}_{-0.1}$	$48.28^{+0.48}_{-0.39}$	< 104.6			114, 164, 165
021004	<i>HETE</i>	30–400	2.3	18.0 ± 7.0	$52.16^{+0.18}_{-0.24}$	$139.3^{+5.4}_{-5.2}$	84.0 ± 5.0^b	$4.21^{+0.27}_{-0.23}$	54, 114, 166, 167
021008	<i>Ulysses</i>	25–100		850.0		< 713.1			168, 169
021016	<i>HETE</i>	30–400		113.0		< 14.8			112, 170

Continued on Next Page...

Table 2 – Continued

GRB	Satellite	Channel	z	Fluence [10^{-7} erg cm $^{-2}$]	Log $E_{\gamma, ISO}$ [erg]	11 hr <i>R</i> -band [μ Jy]	11 hr keV [10^{-14} erg cm $^{-2}$ s $^{-1}$]	Log $F_R /$ F_X	Ref.
021023	<i>Ulysses</i>	25–100		41.0		<13575.8			171, 172
021104	<i>HETE</i>	30–400		6.0 ± 4.0		<46.2			114, 173
021112	<i>HETE</i>	30–400		2.1 ± 1.1		<3.8			114, 174
021113	<i>HETE</i>	8–40		5.0		<4.2			175, 176
021211	<i>HETE</i>	30–400	1.01	23.7 ± 2.0	$51.60^{+0.12}_{-0.17}$	$4.1^{+3.4}_{-1.9}$			114, 177, 178
021219	<i>INTEGRAL</i>	20–200		9.0		<113.2			179, 180
030115A	<i>HETE</i>	30–400		15.0 ± 4.0		$4.8^{+1.4}_{-1.1}$			114, 181
030131	<i>INTEGRAL</i>	20–200		70.0		$4.1^{+2.4}_{-1.7}$			182, 183
030204	<i>Ulysses</i>	25–100		220.0		<11.5			184, 185
030226	<i>HETE</i>	30–400	1.98	43.0 ± 7.0	$52.42^{+0.13}_{-0.19}$	$47.8^{+6.5}_{-5.8}$	135.0 ± 8.0^b	$3.53^{+0.29}_{-0.19}$	54, 114, 186
030227	<i>INTEGRAL</i>	20–200		7.5		$6.4^{+1.3}_{-1.1}$	$89.6^{+30.9b}_{-30.7}$		179, 187, 188 [∞]
030323	<i>HETE</i>	30–400	3.372	9.0 ± 4.0	$52.14^{+0.19}_{-0.35}$	$104.2^{+37.4}_{-27.7}$			114, 189, 190
030324	<i>HETE</i>	30–400		13.0 ± 3.0		$0.9^{+0.3}_{-0.2}$			114, 191
030325	<i>Ulysses</i>	25–100		15.0		<66563.0			192, 193
030328	<i>HETE</i>	30–400	1.52	287.0 ± 14.0	$53.03^{+0.12}_{-0.17}$	$23.7^{+1.3}_{-1.2}$	29.0 ± 2.0^b	$3.87^{+0.27}_{-0.18}$	54, 114, 194, 195
030329	<i>HETE</i>	30–400	0.168	1076 ± 13	$51.65^{+0.12}_{-0.17}$	4328.0 ± 173.4	$5485.9^{+1477.4b}_{-1158.3}$	$3.75^{+0.31}_{-0.13}$	114, 196, 197, 198
030413	<i>Ulysses</i>	25–100		23.0		<148.7			199, 200
030414	<i>Ulysses</i>	25–100		120.0		<14086.9			201, 202
030416	<i>HETE</i>	30–400		3.7 ± 1.9		<38.8			114, 203
030418	<i>HETE</i>	30–400		17.0 ± 7.0		$23.5^{+9.6}_{-7.4}$			114, 204
030429	<i>HETE</i>	30–400	2.66	3.8 ± 1.4	$51.59^{+0.17}_{-0.26}$	$19.1^{+1.4}_{-1.3}$			114, 205
030528	<i>HETE</i>	30–400	0.782	56.0 ± 7.0	$51.75^{+0.13}_{-0.18}$	$8.6^{+2.2}_{-1.9}$	$29.1^{+35.6b}_{-18.4}$	$3.38^{+0.38}_{-0.37}$	114, 206, 207, 208
030723	<i>HETE</i>	30–400		$0.4^{+0.6}_{-0.3}$		$23.9^{+10.6}_{-8.0}$	$14.5^{+9.3b}_{-5.9}$		114, 209, 210
030725	<i>HETE</i>	30–400		167.0 ± 10.0		$96.9^{+20.7}_{-17.1}$			114, 211
030823	<i>HETE</i>	30–400		13.0 ± 4.0		<6.7			114, 212
030824	<i>HETE</i>	30–400		5.8 ± 2.4		<33.9			114, 213

Continued on Next Page...

Table 2 – Continued

GRB	Satellite	Channel	z	Fluence [10^{-7} erg cm $^{-2}$]	Log $E_{\gamma, ISO}$ [erg]	11 hr <i>R</i> -band [μ Jy]	11 hr keV [10^{-14} erg cm $^{-2}$ s $^{-1}$]	Log $F_R /$ F_X	Ref.
030913	<i>HETE</i>	30–400		8.0±3.0		162.6 $^{+192.6}_{-89.2}$			114, 214
031026	<i>HETE</i>	25–100		23.3		<57.2			215, 216
031111A	<i>Ulysses</i>	25–100		21.0		<865.3			217, 218
031203	<i>INTEGRAL</i>	20–200	0.105	14.0	49.52 $^{+0.17}_{-0.61}$	191.5 $^{+28.6}_{-25.0}$	45.0±1.0 ^b	4.47 $^{+0.27}_{-0.08}$	54, 219, 220, 221
031220	<i>HETE</i>	25–100		19.5		<12.2			222, 223
040106	<i>INTEGRAL</i>	20–200		8.2		5.4 $^{+0.8}_{-0.7}$	99.0±1.0 ^b		54, 224, 225
040223	<i>INTEGRAL</i>	20–200		20.0		<2.1	23.0±2.0 ^b		54, 226
040403	<i>INTEGRAL</i>	20–200		5.0		<6.9			227, 228
040422	<i>INTEGRAL</i>	20–200		3.4		<2.7			229
040511	<i>HETE</i>	30–400		100.0		<25.3			230, 231
040624	<i>INTEGRAL</i>	20–200		10.0		<2.9			226, 232 ○
040701	<i>HETE</i>	2–25		4.5±0.8		<83.8			233, 234
040810	<i>HETE</i>	25–100		126.8		<121.7			235, 236
040825B	<i>HETE</i>	30–400		6.3		<8.0			237, 238
040912	<i>HETE</i>	30–400	1.563	4.0	51.20 $^{+0.16}_{-0.27}$	<0.3	7.4 $^{+6.3b}_{-3.7}$	<2.57 $^{+0.29}_{-0.21}$	239, 240, 241
040916	<i>HETE</i>	25–100		5.3±0.6		2.5±0.5			242, 243
040924	<i>HETE</i>	30–400	0.859	26.0	51.50 $^{+0.16}_{-0.27}$	6.9 $^{+1.3}_{-1.1}$			244, 245, 246
041006	<i>HETE</i>	30–400	0.716	70.0	51.77 $^{+0.16}_{-0.27}$	18.1 $^{+2.1}_{-1.9}$	60.7 $^{+21.7c}_{-21.3}$	3.38 $^{+0.31}_{-0.18}$	247, 248, 249
041016	<i>HETE</i>	25–100		46.9		<121.3			250, 251
041211	<i>HETE</i>	30–400		100.0		<3.4			252, 253
041217	<i>Swift</i>	15–150		27.7±1.2		<23.1			254, 255
041219A	<i>INTEGRAL</i>	15–350		1600.0		142.1 $^{+98.9}_{-61.6}$			256, 257
041219C	<i>Swift</i>	15–150		13.1±0.7		<141.5			254, 258
041223	<i>Swift</i>	15–150		167.0±2.8		25.4 $^{+4.5}_{-4.0}$	273.7 $^{+62.5b}_{-61.3}$		254, 259, 260
041224	<i>Swift</i>	15–150		87.3±3.5		<81.0			254, 261
041226	<i>Swift</i>	15–150		3.2±0.8		<220.9			254, 262

Continued on Next Page...

Table 2 – Continued

GRB	Satellite	Channel	z	Fluence [10^{-7} erg cm $^{-2}$]	Log $E_{\gamma, ISO}$ [erg]	11 hr <i>R</i> -band [μ Jy]	11 hr keV [10^{-14} erg cm $^{-2}$ s $^{-1}$]	Log $F_R /$ F_X	Ref.
041228	<i>Swift</i>	15–150		34.9 ± 1.5		<124.1			254, 263
050117	<i>Swift</i>	15–150		88.1 ± 2.3		<207.1	$1259.8^{+535.9}_{-524.9}$		254, 264, 265
050123	<i>HETE</i>	30–400		20.0		<7.1			266, 267
050124	<i>Swift</i>	15–150		11.9 ± 0.7			147.4 ± 30.4		254, 268
050126	<i>Swift</i>	15–150	1.29	8.4 ± 0.8	$51.56^{+0.04}_{-0.04}$	$1.5^{+0.7}_{-0.5}$	27.5 ± 12.7	$2.69^{+0.27}_{-0.42}$	254, 260, 268, 269
050128	<i>Swift</i>	15–150		50.2 ± 2.3		<24.9	448.9 ± 50.4		254, 268, 270
050209	<i>HETE</i>	30–400		20.0		<10.0			271, 272
050215A	<i>Swift</i>	15–150		7.1 ± 1.1		<64.6			254, 273
050215B	<i>Swift</i>	15–150		2.3 ± 0.3		1.5 ± 0.2	44.5 ± 16.1		254, 268, 274
050219A	<i>Swift</i>	15–150		41.1 ± 1.6		<11.7	$69.5^{+19.0}_{-16.8}$		254, 259, 275
050219B	<i>Swift</i>	15–150		158.0 ± 5.0		$3.4^{+1.5}_{-1.1}$	564.2 ± 46.4		254, 268, ¹ 276
050223	<i>Swift</i>	15–150	0.584	6.4 ± 0.7	$50.75^{+0.04}_{-0.05}$	<7.7	18.7 ± 8.0	$<3.36^{+0.26}_{-0.34}$	254, 268, 277, 278
050306	<i>Swift</i>	15–150		115.0 ± 4.3		$38.5^{+30.3}_{-18.8}$			254, 259, 279
050315	<i>Swift</i>	15–150	1.949	32.2 ± 1.5	52.48 ± 0.02	$16.0^{+5.7}_{-4.2}$	515.7 ± 50.7	2.47 ± 0.27	254, 268, 280
050318	<i>Swift</i>	15–150	1.44	10.8 ± 0.8	51.76 ± 0.03	$45.2^{+15.1}_{-12.2}$	115.1 ± 30.0	$3.55^{+0.26}_{-0.32}$	254, 268, 281, 282
050319	<i>Swift</i>	15–150	3.24	13.1 ± 1.5	52.47 ± 0.05	$24.3^{+1.8}_{-1.7}$	442.1 ± 74.3	$2.77^{+0.28}_{-0.32}$	254, 259, 283, 284
050326	<i>Swift</i>	15–150		88.6 ± 1.6		<20.3	133.9 ± 51.8		254, 268, 285
050401	<i>Swift</i>	15–150	2.9	82.2 ± 3.1	53.19 ± 0.02	2.5 ± 0.2	351.0 ± 54.5	$1.86^{+0.28}_{-0.29}$	254, 268, 286
050406	<i>Swift</i>	15–150		0.7 ± 0.1		$4.6^{+1.8}_{-1.3}$	8.9 ± 6.9		254, 268, 287
050408	<i>HETE</i>	30–400	1.2357	19.0	$51.68^{+0.16}_{-0.27}$	5.5 ± 0.4	405.7 ± 107.7	$2.07^{+0.28}_{-0.23}$	268, 288, 289, 290
050410	<i>Swift</i>	15–150		41.5 ± 2.3		<14.3	108.9 ± 49.8		254, 268, 291
050412	<i>Swift</i>	15–150		6.2 ± 0.6		<0.2	$1.1^{+0.2}_{-0.2}$		254, 259, 292
050416A	<i>Swift</i>	15–150	0.6535	3.7 ± 0.4	$50.61^{+0.04}_{-0.05}$	$5.5^{+0.9}_{-0.8}$	253.1 ± 36.7	$2.24^{+0.30}_{-0.11}$	254, 268, 293, 294
050416B	<i>Swift</i>	15–150		10.8 ± 1.0		<7.8			254, 295
050418	<i>Swift</i>	15–150		52.1 ± 1.8		<943.4			254, 296
050421	<i>Swift</i>	15–150		1.5 ± 0.4		<23.3	$3.4^{+8.5}_{-2.5}$		254, 259, 297

Continued on Next Page...

Table 2 – Continued

GRB	Satellite	Channel	z	Fluence [10^{-7} erg cm $^{-2}$]	Log $E_{\gamma, ISO}$ [erg]	11 hr R -band [μ Jy]	11 hr keV [10^{-14} erg cm $^{-2}$ s $^{-1}$]	Log $F_R /$ F_X	Ref.
050422	<i>Swift</i>	15–150		6.1±0.7		<1955.2	53.5±25.7		254, 268, 298
050502A	<i>INTEGRAL</i>	20–200	3.793	14.0	$52.59^{+0.24}_{-0.61}$	$3.6^{+0.8}_{-0.7}$	<5.8 ^d	>3.87	299, 300, 301, 302
050504	<i>INTEGRAL</i>	20–200		15.0		<9.0	21.8±4.7		259, 303, 304
050505	<i>Swift</i>	15–150	4.275	24.9±1.8	52.95 ± 0.03	$8.0^{+1.7}_{-1.4}$	757.3 ± 90.6	$2.08^{+0.27}_{-0.41}$	254, 268, 305, 306
050509A	<i>Swift</i>	15–150		3.4±0.3		<2.7	325.9 ± 118.4		254, 268, 307
050509C	<i>HETE</i>	30–400		3.0		$18.8^{+8.8}_{-6.6}$	<258.5		308, 309, 310
050520	<i>INTEGRAL</i>	20–200		24.0		<6.5	22.7±10.5		268, 311, 312
050522	<i>INTEGRAL</i>	20–200		0.9		<13.5			313, 314
050525A	<i>Swift</i>	15–150	0.606	153.0 ± 2.2	52.16 ± 0.01	$151.9^{+43.3}_{-33.9}$	515.0 ± 119.4	$3.36^{+0.28}_{-0.20}$	254, 268, 315, 316
050528	<i>Swift</i>	15–150		4.5±0.7		<9.6			254, 317
050603	<i>Swift</i>	15–150	2.821	63.6 ± 2.3	53.06 ± 0.02	$87.6^{+19.3}_{-16.0}$	330.1 ± 44.4	$3.44^{+0.29}_{-0.28}$	254, 268, 318, 319
050607	<i>Swift</i>	15–150		5.9±0.6		$0.7^{+0.6}_{-0.3}$	51.1 ± 18.2		254, 268, 320
050626	<i>INTEGRAL</i>	20–200		8.7			<219.8 ^d		321, 322, 323
050701	<i>Swift</i>	15–150		13.6±0.7			204.4 ± 65.2		254, 268, 324
050712	<i>Swift</i>	15–150		10.8±1.2		$18.2^{+41.3}_{-14.0}$	177.0 ± 52.6		254, 268, 325
050713A	<i>Swift</i>	15–150		51.1±2.1		$2.1^{+11.8}_{-1.9}$	465.4 ± 65.1		254, 268, 326
050713B	<i>Swift</i>	15–150		31.8±3.2		<24.9	1180.0 ± 236.8		254, 268, 327
050714A	<i>INTEGRAL</i>	20–200		6.2		<462.3	265.7 ± 72.2		259, 328, 329
050714B	<i>Swift</i>	15–150		6.0±1.1		<3.3	96.6 ± 41.6		254, 268, 330
050716	<i>Swift</i>	15–150		61.7±2.4		$2.5^{+0.8}_{-0.7}$	108.7 ± 17.3		254, 268, 331
050717	<i>Swift</i>	15–150		63.1±1.8		<14.3	25.5 ± 5.9		254, 268, 332
050721	<i>Swift</i>	15–150		36.2±3.2		$23.8^{+5.7}_{-4.6}$	202.8 ± 37.4		254, 268, 333
050726	<i>Swift</i>	15–150		19.4±2.1		<9.7	126.0 ± 22.5		254, 268, 334
050730	<i>Swift</i>	15–150	3.969	23.8±1.5	52.88 ± 0.03	$15.2^{+3.7}_{-3.1}$	766.9 ± 41.1	$2.34^{+0.31}_{-0.26}$	254, 268, 335, 336
050801	<i>Swift</i>	15–150	1.56	3.1±0.5	$51.29^{+0.06}_{-0.07}$	$18.4^{+12.3}_{-7.7}$	38.9 ± 8.1	$3.63^{+0.21}_{-0.41}$	254, 268, 337, 338
050802	<i>Swift</i>	15–150	1.71	20.0±1.6	$52.17^{+0.03}_{-0.04}$	$14.4^{+9.6}_{-6.5}$	323.8 ± 38.6	$2.61^{+0.22}_{-0.44}$	254, 268, 339, 340

Continued on Next Page...

Table 2 – Continued

GRB	Satellite	Channel	z	Fluence [10^{-7} erg cm $^{-2}$]	Log $E_{\gamma, ISO}$ [erg]	11 hr R -band [μ Jy]	11 hr keV [10^{-14} erg cm $^{-2}$ s $^{-1}$]	Log $F_R /$ F_X	Ref.
050803	<i>Swift</i>	15–150		21.5 ± 1.4		<8.2	464.1 ± 74.1		254, 268, 341
050807	<i>HETE</i>	30–400		22.0		<25.0			342, 343
050814	<i>Swift</i>	15–150	5.3	20.1 ± 2.2	53.00 ± 0.05	$2.1^{+0.8}_{-0.6}$	138.3 ± 30.6	$2.26^{+0.32}_{-0.42}$	254, 268, 344, 345
050815	<i>Swift</i>	15–150		0.8 ± 0.2			8.7 ± 3.0		254, 268
050819	<i>Swift</i>	15–150		3.5 ± 0.6		<4.2	62.1 ± 31.1		254, 268, 346
050820A	<i>Swift</i>	15–150	2.612	34.4 ± 2.4	52.74 ± 0.03	$103.2^{+31.1}_{-24.9}$	2212.0 ± 134.8	$2.67^{+0.25}_{-0.36}$	254, 268, 347, 348
050820B	<i>Swift</i>	15–150		20.6 ± 0.6			$15.4^{+9.3}_{-6.8}$		254, 259
050822	<i>Swift</i>	15–150		24.6 ± 1.7		<8.6	352.5 ± 45.2		254, 268, 349
050824	<i>Swift</i>	15–150	0.83	2.7 ± 0.5	$50.68^{+0.08}_{-0.09}$	$19.9^{+1.5}_{-1.4}$	136.6 ± 69.5	$3.08^{+0.32}_{-0.35}$	254, 268, 350, 351
050826	<i>Swift</i>	15–150	0.296	4.1 ± 0.7	$49.95^{+0.07}_{-0.08}$	$36.4^{+12.7}_{-9.9}$	145.2 ± 78.9	$3.27^{+0.30}_{-0.39}$	254, 268, 352
050827	<i>Swift</i>	15–150		21.0 ± 1.2		<6.7	$201.1^{+62.2}_{-60.1}$		254, 259, 353
050904	<i>Swift</i>	15–150	6.295	48.3 ± 1.8	53.49 ± 0.20	$20.0^{+1.4}_{-1.3}$	5.0 ± 0.2	$4.70^{+0.31}_{-0.41}$	254, 268, 354, 355
050908	<i>Swift</i>	15–150	3.344	4.8 ± 0.5	$52.06^{+0.04}_{-0.05}$	$8.1^{+2.4}_{-1.9}$	14.0 ± 4.3	$3.79^{+0.32}_{-0.35}$	254, 268, 356, 357
050915A	<i>Swift</i>	15–150		8.5 ± 0.9		$1.0^{+2.5}_{-0.7}$	51.0 ± 12.3		254, 268, 358
050915B	<i>Swift</i>	15–150		33.8 ± 1.4		$5.4^{+3.3}_{-2.0}$	110.5 ± 47.7		254, 268, 359
050916	<i>Swift</i>	15–150		9.3 ± 1.3		<16739.7	92.1 ± 34.9		254, 259, 360
050922B	<i>Swift</i>	15–150		22.3 ± 3.6		<5.3	199.5 ± 102.3		254, 268, 361
050922C	<i>Swift</i>	15–150	2.198	16.2 ± 0.5	$52.28^{+0.01}_{-0.02}$	$23.9^{+6.6}_{-5.5}$	171.7 ± 30.0	$3.13^{+0.26}_{-0.33}$	254, 268, 283, 362
051001	<i>Swift</i>	15–150		17.4 ± 1.5		<2.1	26.6 ± 2.9		254, 268, 363
051006	<i>Swift</i>	15–150		13.4 ± 1.4		$11.4^{+5.1}_{-3.7}$	6.2 ± 0.9		254, 259, 364
051008	<i>Swift</i>	15–150		50.9 ± 1.5		$0.4^{+0.6}_{-0.2}$	206.0 ± 34.5		254, 268, 365
051012	<i>Swift</i>	15–150		3.0 ± 0.4		$7.0^{+3.8}_{-3.6}$			254, 366
051016A	<i>Swift</i>	15–150		8.4 ± 1.4		<9.7	30.9 ± 9.8		254, 268, 367
051016B	<i>Swift</i>	15–150	0.936	1.7 ± 0.2	$50.59^{+0.05}_{-0.06}$	$4.9^{+1.9}_{-1.5}$	155.2 ± 30.3	$2.42^{+0.24}_{-0.28}$	254, 268, 368, 369
051021A	<i>HETE</i>	30–400		60.0		$6.2^{+2.2}_{-1.6}$	137.1 ± 29.2		268, 370, 371
051021B	<i>Swift</i>	15–150		8.4 ± 0.9		<813.1	12.3 ± 4.0		254, 259, 372

Continued on Next Page...

Table 2 – Continued

GRB	Satellite	Channel	z	Fluence [10^{-7} erg cm $^{-2}$]	Log $E_{\gamma, ISO}$ [erg]	11 hr R -band [μ Jy]	11 hr keV [10^{-14} erg cm $^{-2}$ s $^{-1}$]	Log $F_R /$ F_X	Ref.
051022	<i>HETE</i>	30–400	0.8	1310.0 ± 10.0	$53.14^{+0.12}_{-0.17}$	<0.4	4265.0 ± 350.9	$<-0.15^{+0.28}_{-0.11}$	268, 373, 374
051028	<i>HETE</i>	30–400		60.0		$6.3^{+0.8}_{-0.7}$	218.8 ± 53.7		268, 375, 376
051109A	<i>Swift</i>	15–150	2.346	22.0 ± 2.7	$52.46^{+0.05}_{-0.06}$	$29.0^{+2.9}_{-2.7}$	997.0 ± 76.1	$2.46^{+0.28}_{-0.23}$	254, 268, 377, 378
051109B	<i>Swift</i>	15–150	0.08	2.6 ± 0.4	$48.56^{+0.07}_{-0.08}$	$3.1^{+17.4}_{-2.7}$	38.8 ± 11.0	$2.75^{+0.12}_{-0.85}$	254, 268, 379, 380
051111	<i>Swift</i>	15–150	1.55	40.8 ± 1.3	$52.40^{+0.01}_{-0.02}$	$41.6^{+36.5}_{-19.6}$	34.3 ± 6.5	$4.04^{+0.19}_{-0.45}$	259, 381, 382
051117A	<i>Swift</i>	15–150		46.0 ± 1.6		$6.9^{+3.3}_{-2.2}$	112.6 ± 56.5		254, 268, 383
051117B	<i>Swift</i>	15–150		1.4 ± 0.4		<12.4	2.4 ± 0.9		254, 259, 384
051211B	<i>INTEGRAL</i>	20–200		20.0			135.8 ± 34.9		268, 385
051221B	<i>Swift</i>	15–150		9.2 ± 1.0		<21.4	<11.2		254, 386, 387
060102	<i>Swift</i>	15–150		2.3 ± 0.5		<18.2	<152.2 ^d		254, 388, 389
060105	<i>Swift</i>	15–150		176.0 ± 3.0		<44.1	378.1 ± 314.1		254, 268, 390
060108	<i>Swift</i>	15–150		3.7 ± 0.4		$0.6^{+0.9}_{-0.4}$	98.3 ± 27.4		254, 268, 391
060109	<i>Swift</i>	15–150		6.6 ± 1.0		<35.4	126.9 ± 37.8		254, 268, 392
060110	<i>Swift</i>	15–150		15.7 ± 0.7		$59.4^{+69.4}_{-35.0}$	$211.7^{+168.1}_{-106.5}$		254, 259, 393
060111A	<i>Swift</i>	15–150		12.0 ± 0.6		$3.3^{+1.5}_{-1.2}$	115.5 ± 18.0		254, 268, 394
060111B	<i>Swift</i>	15–150		16.0 ± 1.4		$3.9^{+11.5}_{-3.1}$	51.5 ± 12.8		254, 268, 395
060114	<i>INTEGRAL</i>	20–200		13.0		<4.5	<38.4 ^d		396, 397, 398
060115	<i>Swift</i>	15–150	3.53	17.1 ± 1.5	52.65 ± 0.04	$5.2^{+11.6}_{-3.9}$	106.2 ± 25	$2.73^{+0.22}_{-0.92}$	254, 268, 399, 400
060116	<i>Swift</i>	15–150		24.1 ± 2.6		$6.9^{+8.6}_{-3.9}$	58.4 ± 13.2		254, 268, 401
060117	<i>Swift</i>	15–150		202.0 ± 3.7		$714.2^{+2593.9}_{-596.0}$			254, 402
060123	<i>Swift</i>	15–150		3.0 ± 1.2		<99.7	$275.8^{+81.9}_{-74.7}$		259, 403, 404
060124	<i>Swift</i>	15–150	2.296	4.6 ± 0.5	51.76 ± 0.05	$92.8^{+24.7}_{-19.6}$	2873.0 ± 370.7	$2.50^{+0.31}_{-0.19}$	254, 268, 405, 406
060130	<i>INTEGRAL</i>	20–200		3.0		<4.0			407, 408
060202	<i>Swift</i>	15–150	0.783	21.3 ± 1.7	$51.53^{+0.03}_{-0.04}$	$3.3^{+1.3}_{-1.0}$	719.2 ± 90.1	$1.57^{+0.26}_{-0.16}$	254, 268, 409, 410
060203	<i>Swift</i>	15–150		9.0 ± 1.3		$5.4^{+3.0}_{-2.1}$	72.6 ± 18.8		254, 268, 411
060204A	<i>INTEGRAL</i>	20–200		4.0		<3.9	<4.5		412, 413, 414

Continued on Next Page...

Table 2 – Continued

GRB	Satellite	Channel	z	Fluence [10^{-7} erg cm $^{-2}$]	Log $E_{\gamma, ISO}$ [erg]	11 hr R -band [μ Jy]	11 hr 0.2–10 keV [10^{-14} erg cm $^{-2}$ s $^{-1}$]	Log $F_R /$ F_X	Ref.
060204B	<i>Swift</i>	15–150		29.5±1.8		3.3 $^{+1.2}_{-0.9}$	173.6±79.1		254, 268, 415
060206	<i>Swift</i>	15–150	4.048	8.3±0.4	52.43±0.02	121.1 $^{+11.0}_{-10.2}$	208.1±20.5	3.81 $^{+0.28}_{-0.36}$	254, 268, 416, 417
060210	<i>Swift</i>	15–150	3.91	76.6±4.1	53.37±0.02	1.3 $^{+1.1}_{-0.7}$	855.9±81.5	1.23 $^{+0.25}_{-0.63}$	254, 268, 418, 419
060211A	<i>Swift</i>	15–150		15.7±1.4		<5.5	77.0±24.3		254, 268, 420
060211B	<i>Swift</i>	15–150		4.4±0.6		<2.8	24.8±15.7		254, 268, 421
060213	<i>Konus-Wind</i>	20–4000		1600.0±82.0		<68.9			422, 423
060218	<i>Swift</i>	15–150	0.033	15.7±1.5	48.57±0.04	1082.2 $^{+354.0}_{-274.8}$	487.7±161.5	4.18 $^{+0.28}_{-0.21}$	254, 268, 424
060219	<i>Swift</i>	15–150		4.3±0.8		<0.9	121.4±49.8		254, 268, 425
060223A	<i>Swift</i>	15–150	4.41	6.7±0.5	52.40±0.03	3.6 $^{+9.8}_{-2.8}$	8.2±2.5	3.70 $^{+0.25}_{-1.07}$	254, 259, 426, 427
060223B	<i>Swift</i>	15–150		16.0±0.6		<284.7			254, 428
060306	<i>Swift</i>	15–150		21.3±1.2		<1.2	260.3±41.7		254, 268, 429
060312	<i>Swift</i>	15–150		19.7±0.9		<652.4	61.5±21.0		254, 268, 430
060319	<i>Swift</i>	15–150		2.6±0.3		<1.1	184.4±31.7		254, 268, 431
060322	<i>Swift</i>	15–150		52.2±2.6		<68.6	142.2 $^{+83.4}_{-57.7}$		254, 259, 432
060323	<i>Swift</i>	15–150		6.2±0.7		2.4 $^{+0.9}_{-0.7}$	26.8±8.2		254, 268, 433
060403	<i>Swift</i>	15–150		13.5±0.7		<223.0	24.3±10.5		254, 268, 434
060413	<i>Swift</i>	15–150		35.6±1.5		<6702.5	923.9±183.1		254, 268, 435
060418	<i>Swift</i>	15–150	1.489	83.3±2.5	52.68±0.01	30.4 $^{+3.1}_{-2.8}$	93.8±20.0	3.46 $^{+0.28}_{-0.22}$	254, 268, 436, 437
060421	<i>Swift</i>	15–150		12.5±0.6		<6173.4	39.0±10.3		254, 268, 438
060424	<i>Swift</i>	15–150		6.8±0.8		6.4 $^{+8.7}_{-4.0}$			254, 439
060427	<i>Swift</i>	15–150		5.0±0.9		<1.3	51.6±10.5		254, 268, 440
060428A	<i>Swift</i>	15–150		13.9±0.8		110.0 $^{+32.8}_{-26.8}$	2506.0±402.8		254, 268, 441
060428B	<i>Swift</i>	15–150		8.2±0.8		6.3 $^{+3.0}_{-2.2}$	34.3±9.0		254, 259, 442
060501	<i>Swift</i>	15–150		12.2±1.0		<4.8	118.0±60.9		254, 259, 443
060502A	<i>Swift</i>	15–150	1.51	23.1±1.0	52.13±0.02	9.4 $^{+6.5}_{-4.2}$	380.5±67.3	2.35 $^{+0.22}_{-0.43}$	254, 268, 444, 445
060505	<i>Swift</i>	15–150	0.089	9.4±1.7	49.22 $^{+0.07}_{-0.09}$	2.2 $^{+1.5}_{-1.0}$	80.8±21.3	2.28 $^{+0.24}_{-0.30}$	254, 259, 446, 447

Continued on Next Page...

Table 2 – Continued

GRB	Satellite	Channel	z	Fluence [10^{-7} erg cm $^{-2}$]	Log $E_{\gamma, ISO}$ [erg]	11 hr R -band [μ Jy]	11 hr keV [10^{-14} erg cm $^{-2}$ s $^{-1}$]	Log $F_R /$ F_X	Ref.
060507	<i>Swift</i>	15–150		44.5±2.3		8.4 $^{+10.2}_{-4.6}$	126.0±26.7		254, 268, 448
060510A	<i>Swift</i>	15–150		80.5±3.1		20.0 $^{+51.1}_{-14.6}$	3309.0±639.1		254, 268, 449
060510B	<i>Swift</i>	15–150	4.9	40.7±1.8	53.25±0.02	0.4 $^{+1.3}_{-0.3}$	21.1±7.5	2.31 $^{+0.26}_{-1.35}$	254, 268, 450, 451
060512	<i>Swift</i>	15–150	0.443	2.3±0.4	50.06 $^{+0.07}_{-0.08}$	18.3 $^{+4.6}_{-3.9}$	22.8±6.7	3.79 $^{+0.27}_{-0.22}$	254, 268, 452, 453
060515	<i>Swift</i>	15–150		14.1±1.3		<24.0	2.6 $^{+1.4}_{-1.1}$		254, 259, 454
060522	<i>Swift</i>	15–150	5.11	11.4±1.1	52.73±0.04	3.7 $^{+3.7}_{-1.9}$	32.0±13.7	3.13 $^{+0.28}_{-0.71}$	254, 268, 455, 456
060526	<i>Swift</i>	15–150	3.221	12.6±1.7	52.45 $^{+0.05}_{-0.06}$	45.9±1.5	156.6±69.0	3.49 $^{+0.31}_{-0.42}$	254, 268, 283, 457
060602A	<i>Swift</i>	15–150		16.1±1.6		0.2 $^{+0.4}_{-0.1}$	65.9 $^{+58.7d}_{-36.6}$		254, 259, 458
060604	<i>Swift</i>	15–150	2.68	4.0±1.1	51.82 $^{+0.10}_{-0.13}$	8.6 $^{+2.7}_{-2.1}$	163.8±31.6	2.72 $^{+0.28}_{-0.34}$	254, 268, 459, 460
060605	<i>Swift</i>	15–150	3.711	7.0±0.9	52.30 $^{+0.05}_{-0.06}$	24.8±0.6	60.9±13.8	3.65 $^{+0.29}_{-0.35}$	254, 268, 461, 462
060607A	<i>Swift</i>	15–150	3.082	25.5±1.1	52.73±0.02	33.6 $^{+18.9}_{-12.6}$	254.8±29.7	3.14 $^{+0.24}_{-0.46}$	254, 268, 463, 464
060607B	<i>Swift</i>	15–150		16.4±1.2		<93.7			254, 465
060614	<i>Swift</i>	15–150	0.125	204.0±3.6	50.86±0.01	70.8 $^{+7.2}_{-6.6}$	855.7±195.7	2.76 $^{+0.30}_{-0.12}$	254, 268, 466
060707	<i>Swift</i>	15–150	3.425	16.0±1.5	52.60±0.04	8.1 $^{+6.7}_{-4.2}$	249.6±82.4	2.54 $^{+0.26}_{-0.63}$	254, 268, 283, 467
060708	<i>Swift</i>	15–150		4.9±0.4		9.1 $^{+12.2}_{-6.2}$	104.4±17.8		254, 268, 468
060712	<i>Swift</i>	15–150		12.4±2.2		<17.5	62.7±15.4		254, 268, 469
060714	<i>Swift</i>	15–150	2.711	28.3±1.7	52.68±0.03	20.9 $^{+7.7}_{-5.8}$	141.0±24.5	3.18 $^{+0.27}_{-0.36}$	254, 268, 283, 470
060717	<i>Swift</i>	15–150		0.7±0.2		<1.1	13.1 $^{+5.8}_{-5.0}$		254, 259, 471
060719	<i>Swift</i>	15–150		15.0±0.9		<0.1	214.4±42.4		254, 268, 472
060728	<i>Swift</i>	15–150		2.3±0.7		<13.9	<4.5		254, 473, 474
060729	<i>Swift</i>	15–150	0.54	26.1±2.1	51.29 $^{+0.03}_{-0.04}$	253.3 $^{+91.9}_{-68.7}$	3306.0±546.5	2.77 $^{+0.26}_{-0.17}$	254, 268, 475
060804	<i>Swift</i>	15–150		6.0±1.0		67.9 $^{+236.3}_{-53.1}$	214.7±48.7		254, 268, 476
060805A	<i>Swift</i>	15–150		0.7±0.2		<4.8	14.2±4.8		254, 268, 477
060805B	<i>RHESSI</i>	30–10000		1130.0±46.0		<119.9	234.8 $^{+109.2}_{-83.6}$		259, 478, 479, 480
060807	<i>Swift</i>	15–150		8.5±1.1			265.3±89.6		254, 268
060813	<i>Swift</i>	15–150		54.6±1.4		<98.9	947.7±86.7		254, 268, 481

Continued on Next Page...

Table 2 – Continued

GRB	Satellite	Channel	z	Fluence [10^{-7} erg cm $^{-2}$]	Log $E_{\gamma, ISO}$ [erg]	11 hr R -band [μ Jy]	11 hr keV [10^{-14} erg cm $^{-2}$ s $^{-1}$]	Log $F_R /$ F_X	Ref.
060814	<i>Swift</i>	15–150	0.84	146.0±2.4	52.43±0.01	8.9 $^{+3.5}_{-2.7}$	535.4±79.5	2.13±0.25	254, 268, 482, 483
060825	<i>Swift</i>	15–150		9.6±0.5		<1.6	35.8±10.9		254, 268, 484
060901	<i>INTEGRAL</i>	20–200		35.0		9.5 $^{+6.0}_{-3.9}$	157.9±48.8		268, 485, 486
060904A	<i>Swift</i>	15–150		77.2±1.5		<3.0	578.4±190.8		254, 268, 487
060904B	<i>Swift</i>	15–150	0.703	16.2±1.4	51.32±0.04	17.8 $^{+4.3}_{-3.7}$	99.7±20.0	3.15 $^{+0.28}_{-0.15}$	254, 268, 488, 489
060906	<i>Swift</i>	15–150	3.686	22.1±1.4	52.79±0.03	14.7 $^{+21.5}_{-9.4}$	69.0±22.9	3.37 $^{+0.24}_{-0.77}$	254, 268, 283, 490
060908	<i>Swift</i>	15–150	2.43	28.0±1.1	52.59±0.02	0.8 $^{+1.2}_{-0.5}$	59.2±12.0	2.13 $^{+0.20}_{-0.63}$	254, 268, 491, 492
060912A	<i>Swift</i>	15–150	0.937	13.5 ± 0.6	51.49±0.02	10.3 $^{+5.3}_{-3.9}$	49.4±8.9	3.24 $^{+0.23}_{-0.32}$	254, 268, 493, 494
060919	<i>Swift</i>	15–150		5.5±0.6	<29.8		13.0±5.5		254, 268, 495
060923A	<i>Swift</i>	15–150		8.7±1.3		0.3 $^{+0.2}_{-0.1}$	107.5±20.9		254, 268, 496
060923B	<i>Swift</i>	15–150		4.8±0.6		<91.2	628.4±174.2		254, 259, ¹ 497
060923C	<i>Swift</i>	15–150		15.8±2.2		0.8±0.1	36.1 $^{+15.4}_{-12.4}$		254, 259, ² 498
060926	<i>Swift</i>	15–150	3.208	2.2±0.3	51.69±0.05	3.3 $^{+4.3}_{-2.2}$	25.0±8.7	3.15 $^{+0.25}_{-0.84}$	254, 268, 499, 500
060927	<i>Swift</i>	15–150	5.6	11.3±0.7	52.78±0.03	4.1 $^{+2.2}_{-1.6}$	17.5±4.8	3.45 $^{+0.29}_{-0.59}$	254, 268, 501, 502
060928	<i>Konus-Wind</i>	20–2000		283.0±12.0			937.6 $^{+1109.8}_{-623.9}$		503, 504
060929	<i>Swift</i>	15–150		8.3±2.3		<6.7	15.8±4.3		254, 268, 505
060930	<i>INTEGRAL</i>	20–200		2.5		<4.0			506, 507
061002	<i>Swift</i>	15–150		6.8±0.8		<11.0	10.0±3.3		254, 268, 508
061004	<i>Swift</i>	15–150		5.7±0.3		<0.4	39.0±10.3		254, 268, 509
061007	<i>Swift</i>	15–150	1.261	444.0±5.6	53.27±0.01	10.9 $^{+1.3}_{-1.2}$	115.1±1.2	2.92 $^{+0.29}_{-0.13}$	254, 268, 510, 511
061019	<i>Swift</i>	15–150		25.9±4.1		146.4 $^{+67.6}_{-50.9}$	297.5±103.6		254, 268, 512
061021	<i>Swift</i>	15–150		29.6±1.0		31.9 $^{+12.3}_{-9.4}$	517.1±40.4		254, 268, 513
061025	<i>INTEGRAL</i>	20–200		8.0		2.9 $^{+1.3}_{-1.0}$	17.9±6.3		268, 514, 515
061027	<i>Swift</i>	15–150		3.0±0.9		<69.0	<1.7 ^d		254, 516, 517, 518
061028	<i>Swift</i>	15–150		9.7±1.7		<7.2	8.2 $^{+3.1}_{-2.7}$		254, 259, 519
061102	<i>Swift</i>	15–150		2.8±0.7		<11.0	5.4+2.0 $_{-1.9}$		254, 259, 520

Continued on Next Page...

Table 2 – Continued

GRB	Satellite	Channel	z	Fluence [10^{-7} erg cm $^{-2}$]	Log $E_{\gamma, ISO}$ [erg]	11 hr R -band [μ Jy]	11 hr keV [10^{-14} erg cm $^{-2}$ s $^{-1}$]	Log $F_R /$ F_X	Ref.
061110A	<i>Swift</i>	15–150	0.758	10.6 ± 0.8	51.20 ± 0.03	$2.5^{+0.9}_{-0.7}$	$11.5^{+2.9}_{-2.8}$	$3.25^{+0.28}_{-0.23}$	254, 259, 521, 522
061110B	<i>Swift</i>	15–150	3.44	13.3 ± 1.2	52.52 ± 0.04	$0.7^{+0.9}_{-0.4}$	12.2 ± 3.9	$2.77^{+0.24}_{-0.73}$	254, 259, 523, 524
061121	<i>Swift</i>	15–150	1.314	137.0 ± 2.0	52.79 ± 0.01	$23.2^{+5.7}_{-4.6}$	1151.0 ± 114.8	$2.25^{+0.31}_{-0.13}$	254, 268, 525, 526
061122	<i>INTEGRAL</i>	20–200		30.0		$6.4^{+1.2}_{-1.0}$	318.3 ± 39.4		268, 527, 528
061126	<i>Swift</i>	15–150	1.159	67.7 ± 2.2	52.38 ± 0.01	16.8 ± 0.6	443.5 ± 30.0	$2.51^{+0.27}_{-0.16}$	254, 268, 529, 530
061202	<i>Swift</i>	15–150		34.2 ± 1.3		<7.7	912.6 ± 135.0		254, 268, 531
061218	<i>Swift</i>	15–150		0.4 ± 0.2		<22.5			254, 532
061222A	<i>Swift</i>	15–150		79.9 ± 1.6		$0.3^{+0.2}_{-0.1}$	2821.0 ± 307.4		254, 268, 533
061222B	<i>Swift</i>	15–150	3.355	22.4 ± 1.8	$52.73^{+0.03}_{-0.04}$	$1.2^{+2.4}_{-0.9}$	31.0 ± 9.3	$2.62^{+0.23}_{-0.88}$	254, 268, 534, 535
070103	<i>Swift</i>	15–150		3.4 ± 0.5		<0.3	33.0 ± 7.6		254, 268, 536
070107	<i>Swift</i>	15–150		51.7 ± 2.6		<42.4	931.0 ± 98.2		254, 268, 537
070110	<i>Swift</i>	15–150	2.352	16.2 ± 1.1	52.33 ± 0.03	$18.9^{+7.5}_{-5.7}$	70.2 ± 15.0	$3.42^{+0.30}_{-0.28}$	254, 268, 538, 539
070125	<i>Konus-Wind</i>	20–10000	1.547	1740.0 ± 180.0	$53.60^{+0.10}_{-0.12}$	$207.7^{+86.4}_{-65.8}$	$378.4^{+101.0}_{-100.8}$	$3.70^{+0.28}_{-0.23}$	259, 540, 541, 542
070126	<i>Swift</i>	15–150		1.6 ± 0.6		<2.0			254, 543
070129	<i>Swift</i>	15–150		29.8 ± 2.7		$3.0^{+2.5}_{-1.5}$	280.9 ± 64.2		254, 268, 544
070208	<i>Swift</i>	15–150	1.165	4.5 ± 1.0	$51.20^{+0.09}_{-0.11}$	$3.4^{+1.6}_{-1.2}$	63.7 ± 20.1	$2.66^{+0.24}_{-0.36}$	254, 268, 545, 546
070219	<i>Swift</i>	15–150		3.2 ± 0.4		<0.1	15.6 ± 6.8		254, 268, 547
070220	<i>Swift</i>	15–150		104.0 ± 2.3		<66.1	105.9 ± 25.7		254, 268, 548
070223	<i>Swift</i>	15–150		17.0 ± 1.2		$0.6^{+0.3}_{-0.2}$	68.9 ± 20.7		254, 268, 549, 550
070224	<i>Swift</i>	15–150		3.1 ± 0.5		$3.2^{+0.7}_{-0.6}$	60.3 ± 38.9		254, 268, 551
070227	<i>Swift</i>	15–150		16.2 ± 2.5		<49.7	$157.0^{+45.9}_{-45.2}$		254, 259, 552
070306	<i>Swift</i>	15–150	1.497	53.8 ± 2.9	52.49 ± 0.02	$5.0^{+2.7}_{-1.8}$	161.2 ± 398.0	$1.45^{+0.22}_{-0.38}$	254, 259, 553, 554
070309	<i>INTEGRAL</i>	20–200		5.0		<4007.4	348.9 ± 84.7		259, 555, 556
070311	<i>INTEGRAL</i>	20–200		20.0		$8.1^{+11.4}_{-4.8}$	135.3 ± 27.6		259, 557, 558
070318	<i>Swift</i>	15–150	0.836	24.8 ± 1.1	51.66 ± 0.02	$34.0^{+5.8}_{-5.1}$	263.7 ± 34.9	$3.02^{+0.30}_{-0.11}$	254, 268, 559, 560
070328	<i>Swift</i>	15–150		90.6 ± 1.8		<9.8	626.6 ± 52.3		254, 268, 561

Continued on Next Page...

Table 2 – Continued

GRB	Satellite	Channel	z	Fluence [10^{-7} erg cm $^{-2}$]	Log $E_{\gamma, ISO}$ [erg]	11 hr R -band [μ Jy]	11 hr keV [10^{-14} erg cm $^{-2}$ s $^{-1}$]	Log $F_R /$ F_X	Ref.
070330	<i>Swift</i>	15–150		1.8±0.3		$5.2^{+16.7}_{-4.1}$	52.2 ± 20.5		254, 268, 562
070411	<i>Swift</i>	15–150	2.954	27.0 ± 1.6	$52.72^{+0.02}_{-0.03}$	$13.9^{+7.1}_{-5.2}$	162.7 ± 47.6	$2.95^{+0.26}_{-0.48}$	254, 259, 563, 564
070412	<i>Swift</i>	15–150		4.8±0.7		<0.1	65.4 ± 19.0		254, 268, 565
070419A	<i>Swift</i>	15–150	0.97	5.6 ± 0.8	$51.14^{+0.06}_{-0.07}$	$2.1^{+0.9}_{-0.7}$	3.9 ± 1.2	$3.66^{+0.26}_{-0.31}$	254, 259, 566, 567
070419B	<i>Swift</i>	15–150		73.6 ± 2.0		$10.7^{+4.2}_{-3.2}$	2310.0 ± 515.2		254, 268, 568
070420	<i>Swift</i>	15–150		140.0 ± 4.5		$48.0^{+35.0}_{-23.0}$	889.2 ± 107.9		254, 268, 569
070429A	<i>Swift</i>	15–150		9.1±1.4		<17.6	110.7 ± 27.1		254, 268, 570
070506	<i>Swift</i>	15–150	2.31	2.1±0.2	51.43 ± 0.05	$8.1^{+6.9}_{-4.0}$	227.2 ± 70.1	$2.54^{+0.23}_{-0.32}$	254, 259, 571, 572
070508	<i>Swift</i>	15–150	0.82	196.0 ± 2.7	52.54 ± 0.01	$2.8^{+1.6}_{-1.1}$	447.6 ± 25.3	$1.70^{+0.22}_{-0.32}$	254, 268, 573
070509	<i>Swift</i>	15–150		1.8±0.3		<3.5	9.7 ± 2.9		254, 259, 574
070517	<i>Swift</i>	15–150		2.2±0.4		<1.0	43.9 ± 12.0		254, 268, 575
070518	<i>Swift</i>	15–150		1.6±0.2		$3.3^{+0.7}_{-0.6}$	29.7 ± 22.1		254, 268, 576
070520A	<i>Swift</i>	15–150		2.5±0.5		<1.5	39.5 ± 19.4		254, 268, 577
070520B	<i>Swift</i>	15–150		2.5±1.1		<4.0	16.6 ± 11.4		254, 259, 578
070521	<i>Swift</i>	15–150		80.1 ± 1.8		<0.2	177.2 ± 27.9		254, 268, 579
070529	<i>Swift</i>	15–150	2.500	25.7 ± 2.5	52.58 ± 0.04	$8.2^{+15.5}_{-5.4}$	69.7 ± 14.7	$3.07^{+0.20}_{-0.68}$	254, 268, 580
070531	<i>Swift</i>	15–150		10.8 ± 1.3		<7.9	$20.7^{+43.0}_{-14.5}$		254, 259, 581
070611	<i>Swift</i>	15–150	2.04	3.9±0.6	$51.60^{+0.06}_{-0.07}$	$11.4^{+20.3}_{-7.4}$	29.3 ± 6.1	$3.57^{+0.19}_{-0.65}$	254, 259, 582, 583
070612A	<i>Swift</i>	15–150	0.617	106.0 ± 6.0	$52.02^{+0.02}_{-0.03}$	$329.8^{+179.7}_{-128.6}$			254, 584, 585
070612B	<i>Swift</i>	15–150		16.8±1.2		<47.0	10.8 ± 5.9		254, 268, 586
070616	<i>Swift</i>	15–150		192.0 ± 3.5		$49.0^{+240.0}_{-42.6}$	377.7 ± 70.4		254, 268, 587
070621	<i>Swift</i>	15–150		43.0±1.0		<1.0	215.6 ± 38.3		268, 588, 589
070628	<i>Swift</i>	15–150		35.0 ± 2.0		$139.4^{+180.1}_{-83.0}$	1728.0 ± 150.1		268, 590
070704	<i>Swift</i>	15–150		59.0 ± 3.0		<126.5	91.1 ± 21.1		268, 591, 592
070714A	<i>Swift</i>	15–150		1.5±0.2		<3.2	70.6 ± 17.1		268, 593, 594
070721A	<i>Swift</i>	15–150		0.7±0.2		$0.7^{+2.9}_{-0.6}$	40.8 ± 12.2		268, 595

Continued on Next Page...

Table 2 – Continued

GRB	Satellite	Channel	z	Fluence [10^{-7} erg cm $^{-2}$]	Log $E_{\gamma, ISO}$ [erg]	11 hr R -band [μ Jy]	11 hr keV [10^{-14} erg cm $^{-2}$ s $^{-1}$]	Log $F_R /$ F_X	Ref.
070721B	<i>Swift</i>	15–150	3.626	21.0±1.0	52.76±0.02	$1.1^{+0.5}_{-0.4}$	51.8 ± 11.6	2.38±0.32	268, 596, 597
070724B	<i>Konus-Wind</i>	20–500		$180.0^{+4.0}_{-25.0}$		<121.7	$847.7^{+268.6}_{-255.8}$		259, 598, 599, 600
070802	<i>Swift</i>	15–150	2.45	2.8±0.5	$51.60^{+0.07}_{-0.09}$	$0.6^{+0.9}_{-0.4}$	51.1 ± 18.5	$2.07^{+0.23}_{-0.70}$	268, 601, 602, 603
070805	<i>Swift</i>	15–150		7.2±0.8		<25.5			604, 605
070808	<i>Swift</i>	15–150		12.0±1.0		<2.8	92.5 ± 27.5		268, 606, 607
070810A	<i>Swift</i>	15–150	2.17	6.9±0.6	51.90±0.04	$9.1^{+6.6}_{-4.3}$	39.4 ± 13.4	$3.35^{+0.26}_{-0.52}$	268, 608, 609
070911	<i>Swift</i>	15–150		120.0±2.0		$32.5^{+22.6}_{-13.6}$	$547.1^{+150.3}_{-149.2}$		259, 610, 611
070913	<i>Swift</i>	15–150		2.5±0.3		$2.1^{+13.2}_{-1.9}$			612, 613
070917	<i>Swift</i>	15–150		20.0±1.0		$6.6^{+2.4}_{-1.8}$	$641.1^{+596.4}_{-354.5}$		259, 614, 615
070920A	<i>Swift</i>	15–150		5.1±0.7		<0.2			616, 617
070920B	<i>Swift</i>	15–150		6.6±0.5		<6.0	$26.2^{+14.1d}_{-11.3}$		259, 618, 619
070925	<i>INTEGRAL</i>	20–200		20.0		<1.0	$39.9^{+17.1}_{-15.2}$		259, 620, 621
071001	<i>Swift</i>	15–150		7.7±0.8			1999.3 ± 649.3		268, 622
071003	<i>Swift</i>	15–150	1.1	83.0±3.0	52.42±0.02	$180.1^{+78.9}_{-59.9}$	557.2 ± 115.5	$3.44^{+0.27}_{-0.20}$	268, 623, 624
071008	<i>Swift</i>	15–150		2.4±0.4		<0.3			625, 626
071010A	<i>Swift</i>	15–150	0.98	2.0±0.4	$50.70^{+0.08}_{-0.10}$	$43.0^{+15.3}_{-11.3}$	349.4 ± 86.0	$3.01^{+0.27}_{-0.23}$	259, 627, 628, 629
071010B	<i>Swift</i>	15–150	0.947	44.0±1.0	52.02±0.01	$48.3^{+6.2}_{-5.7}$	456.1 ± 98.4	$2.95^{+0.30}_{-0.16}$	268, 630, 631, 632
071011	<i>Swift</i>	15–150		0.22±0.02		$26.6^{+22.7}_{-12.9}$	459.8 ± 131.9		268, 633, 634
071013	<i>Swift</i>	15–150		3.2±0.7		<1.8			635, 636
071018	<i>Swift</i>	15–150		10.0±2.0		<7.8			637, 638
071020	<i>Swift</i>	15–150	2.145	23.0±1.0	52.41±0.02	13.1 ± 1.0	161.2 ± 9.2	$2.90^{+0.27}_{-0.23}$	268, 639, 640, 641
071021	<i>Swift</i>	15–150		13.0±2.0		$1.4^{+0.6}_{-0.4}$	85.8 ± 29.1		268, 642, 643
071025	<i>Swift</i>	15–150		65.0±2.0		$3.0^{+2.2}_{-1.4}$	144.5 ± 17.6		268, 644, 645
071028A	<i>Swift</i>	15–150		3.0±0.5		<24.6	32.5 ± 23.3		268, 646, 647
071028B	<i>Swift</i>	15–150		2.5±0.8		<10.4			648
071031	<i>Swift</i>	15–150	2.692	9.0±1.3	$52.18^{+0.06}_{-0.07}$	$16.6^{+10.6}_{-7.2}$	24.9 ± 4.9	$3.84^{+0.25}_{-0.50}$	259, 649, 650

Continued on Next Page...

Table 2 – Continued

GRB	Satellite	Channel	z	Fluence [10^{-7} erg cm $^{-2}$]	Log $E_{\gamma, ISO}$ [erg]	11 hr R -band [μ Jy]	11 hr keV [10^{-14} erg cm $^{-2}$ s $^{-1}$]	Log $F_R /$ F_X	Ref.
071101	<i>Swift</i>	15–150		0.8 ± 0.3		<415.3	$15.0^{+4.8}_{-4.7}$		259, 651, 652
071109	<i>INTEGRAL</i>	20–200		6.6		<140.7	40.9		653, 654
071112C	<i>Swift</i>	15–150	0.823	30.0 ± 4.0	$51.73^{+0.05}_{-0.06}$	$5.6^{+1.7}_{-1.4}$	37.0 ± 1.6	$3.09^{+0.27}_{-0.11}$	268, 655, 656
071117	<i>Swift</i>	15–150	1.331	24.0 ± 1.0	52.04 ± 0.02		144.3 ± 25.4		268, 657, 658
071118	<i>Swift</i>	15–150		5.0 ± 1.0		$5.0^{+7.1}_{-3.2}$	250.9 ± 75.3		268, 659, 660
071122	<i>Swift</i>	15–150	1.14	5.8 ± 1.1	$51.30^{+0.08}_{-0.09}$	$3.7^{+4.6}_{-2.2}$	$5.1^{+9.3}_{-3.4}$	$3.80^{+0.57}_{-0.79}$	259, 661, 662

^a: 1.6–10.0 keV, ^b: 2–10 keV, ^c: 0.5–6.0 keV, ^d: Uses estimated N_H , 1. de Pasquale et al. (2006a) 2. Castro-Tirado et al. (1997) 3. Galama et al. (1997), 4. Djorgovski et al. (1999), 5. Groot et al. (1997a), 6. Djorgovski et al. (1997), 7. Metzger et al. (1997), 8. Paciesas et al. (1999), 9. Connaughton et al. (1997), 10. Gorosabel et al. (1999), 11. Mirabal et al. (2005), 12. Soderberg et al. (2004a), 13. Groot et al. (1998a), 14. Murakami et al. (1997), 15. Djorgovski et al. (2001), 16. Diercks et al. (1998), 17. Antonelli et al. (1999), 18. Groot et al. (1997b), 19. Marshall et al. (1998), 20. Groot et al. (1998b), 21. Reichart et al. (1999), 22. Tinney et al. (1998), 23. Galama et al. (1998), 24. Vrba et al. (2000), 25. Djorgovski et al. (2003), 26. Hjorth et al. (2002), 27. Djorgovski et al. (1998), 28. Vreeswijk et al. (1999a), 29. Frontera et al. (1998), 30. Pedersen et al. (1999a), 31. Castro-Tirado et al. (1998), 32. Kulkarni et al. (1999), 33. Palazzi et al. (1999a), 34. Schaefer et al. (1999), 35. Bloom et al. (2003), 36. Masetti et al. (1999), 37. Vreeswijk et al. (1999b), 38. Harrison et al. (1999), 39. Kippen et al. (1999), 40. Castro-Tirado et al. (1999), 41. Hurley & Cline (1999), 42. Pedersen et al. (1999b), 43. Jensen et al. (1999), 44. Le Floch et al. (2002), 45. Masetti et al. (2000a), 46. Galama et al. (1999), 47. Sahu et al. (2000), 48. Greiner et al. (1999), 49. Thorstensen et al. (1999), 50. Palazzi et al. (1999b), 51. Hurley et al. (2000e), 52. Dodonov et al. (1999), 53. Castro-Tirado et al. (2001), 54. Gendre et al. (2006), 55. Vreeswijk et al. (1999c), 56. Halpern et al. (2000), 57. Gorosabel et al. (2000a), 58. Hurley et al. (2000a), 59. Kjernsmo et al. (2000), 60. Hurley et al. (2000d), 61. Andersen et al. (2000), 62. Piro et al. (2002), 63. Rhoads et al. (2000), 64. Jensen et al. (2001), 65. Castro et al. (2000), 66. Rhoads & Fruchter (2001), 67. Hurley et al. (2000f), 68. Pedersen et al. (2000), 69. Hurley et al. (2000g), 70. Henden et al. (2000a), 71. Hurley et al. (2000h), 72. Park et al. (2000), 73. Kippen & Woods (2000), 74. Price et al. (2000a), 75. Hurley et al. (2000i), 76. Klose et al. (2000), 77. Uglesich et al. (2000), 78. Henden (2000), 79. Jensen et al. (2000a), 80. Jensen et al. (2000b), 81. Palazzi et al. (2000a), 82. Hurley et al. (2000j), 83. Diercks & Cotoros (2000), 84. Stanek et al. (2000), 85. Hurley et al. (2000k), 86. Bartolini et al. (2000), 87. Hurley et al. (2000l), 88. Gorosabel et al. (2000b), 89. Hurley et al. (2000n), 90. Fynbo et al. (2001a), 91. Hurley et al. (2000m), 92. Palazzi et al. (2000b), 93. Hurley et al. (2000o), 94. Masetti et al. (2000b), 95. Hurley et al. (2000p), 96. Price et al. (2000b), 97. Hurley et al. (2000q), 98. Price et al. (2002f), 99. Hurley et al. (2000r), 100. Fynbo et al. (2001b), 101. Hurley et al. (2000s), 102. Castro Cerón et al. (2002a), 103. Hurley et al. (2000t), 104. Henden et al. (2000b), 105. Hurley et al. (2000u), 106. Pedersen et al. (2006), 107. Vreeswijk et al. (2000),

108. Hurley et al. (2000v), 109. Price et al. (2000c), 110. Hurley et al. (2000w), 111. Zhu (2000), 112. Barraud et al. (2003), 113. Masetti et al. (2001), 114. Sakamoto et al. (2005b), 115. Zhu (2001), 116. Rol et al. (2001), 117. Jha et al. (2001), 118. Galama et al. (2003), 119. Hurley et al. (2001b), 120. Oksanen et al. (2001), 121. Price et al. (2001c), 122. Hurley et al. (2001c), 123. Price et al. (2001d), 124. Andersen et al. (2001), 125. Price et al. (2002e), 126. Akerlof et al. (2001), 127. Heise et al. (2001), 128. Mohan et al. (2001), 129. Infante et al. (2001), 130. Greiner et al. (2003a), 131. Lee et al. (2001), 132. Vreeswijk et al. (2006), 133. Holland et al. (2002), 134. Saracco et al. (2001), 135. Hjorth et al. (2003), 136. Berger et al. (2002), 137. Berger et al. (2007a), 138. Castro Cerón et al. (2002b), 139. Lee et al. (2002), 140. Pavlenko & Rumyantsev (2002), 141. Price et al. (2002a), 142. Monnelly et al. (2002), 143. Hurley et al. (2002b), 144. Masetti et al. (2003), 145. Levan et al. (2005), 146. Castro-Tirado et al. (2002a), 147. Hurley et al. (2002c), 148. Price et al. (2002b), 149. Amati et al. (2004), 150. Hurley et al. (2002d), 151. Henden & Nelson (2002), 152. Hurley et al. (2002e), 153. Gorosabel et al. (2002a), 154. Hurley et al. (2002g), 155. Gorosabel et al. (2002b), 156. Hurley et al. (2002f), 157. Gorosabel et al. (2002c), 158. Kilmartin & Gilmore (2002), 159. Piccioni et al. (2002), 160. Price et al. (2002g), 161. Laursen & Stanek (2003), 162. Jakobsson et al. (2005), 163. Levan et al. (2002), 164. Price et al. (2002d), 165. Soderberg et al. (2007), 166. Salamanca et al. (2002), 167. Holland et al. (2003), 168. Hurley et al. (2002h), 169. Castro-Tirado et al. (2002b), 170. Schaefer et al. (2002a), 171. Hurley et al. (2002i), 172. Bloom & Falco (2002), 173. Fox & Price (2002), 174. Schaefer et al. (2002b), 175. Yoshida et al. (2002), 176. Nysewander et al. (2002b), 177. Vreeswijk et al. (2003), 178. Nysewander et al. (2006), 179. Mereghetti et al. (2003a), 180. Castro-Tirado et al. (2002c), 181. Levan et al. (2006a), 182. Götz et al. (2003), 183. Fox et al. (2003a), 184. Hurley et al. (2003a), 185. Nysewander et al. (2003), 186. Klose et al. (2004), 187. Mereghetti et al. (2003b), 188. Castro-Tirado et al. (2003), 189. Vreeswijk et al. (2004), 190. Gilmore et al. (2003), 191. Lamb et al. (2003), 192. Hurley et al. (2003b), 193. Buffington et al. (2006), 194. Martini et al. (2003), 195. Maiorano et al. (2006), 196. Tiengo et al. (2003), 197. Greiner et al. (2003b), 198. Resmi et al. (2005), 199. Hurley et al. (2003c), 200. Schaefer et al. (2003), 201. Hurley et al. (2003d), 202. Lipunov et al. (2003), 203. Henden et al. (2003), 204. Rykoff et al. (2004a), 205. Jakobsson et al. (2004), 206. Butler et al. (2004a), 207. Rau et al. (2005), 208. Rau et al. (2004), 209. Butler et al. (2005), 210. Bond (2003), 211. Pugliese et al. (2005), 212. Fox & Hunt (2003), 213. Ibrahimov et al. (2003), 214. Guziy et al. (2003), 215. Butler et al. (2003), 216. Chen et al. (2003), 217. Hurley et al. (2003e), 218. Silvey et al. (2003), 219. Ghisellini et al. (2006), 220. Prochaska et al. (2003), 221. Cobb et al. (2004), 222. Melandri et al. (2006a), 223. Fox et al. (2003b), 224. Moran et al. (2005), 225. Masetti et al. (2004), 226. Filliatre et al. (2006), 227. Mereghetti et al. (2005a), 228. de Ugarte et al. (2004a), 229. Filliatre et al. (2005), 230. Dulligan et al. (2004), 231. Gorosabel et al. (2004a), 232. Fugazza et al. (2004), 233. Barraud et al. (2004), 234. de Ugarte Postigo et al. (2004b), 235. <http://space.mit.edu/HETE/Bursts/GRB040810/>, 236. Price et al. (2004), 237. Urata et al. (2004), 238. Gorosabel et al. (2004b), 239. Butler et al. (2004b), 240. Stratta et al. (2007a), 241. Butler et al. (2004c), 242. Arimoto et al. (2007), 243. Kosugi et al. (2004), 244. Fenimore et al. (2004), 245. Wiersema et al. (2004), 246. Huang et al. (2005), 247. Galassi et al. (2004), 248. Butler et al. (2004d), 249. Stanek et al. (2005), 250. <http://space.mit.edu/HETE/Bursts/GRB041016/>, 251. Kuroda et al. (2004), 252. Dezalay et al.

- (2004), 253. Cenko et al. (2004), 254. Sakamoto et al. (2008), 255. Bayliss et al. (2004), 256. McBreen et al. (2006), 257. Hearty et al. (2004), 258. Nysewander et al. (2004), 259. Evans et al. (2007), 260. Berger et al. (2005c), 261. Rykoff et al. (2004b), 262. Rykoff (2004a), 263. Rykoff (2004b), 264. Hill et al. (2006), 265. de Ugarte Postigo et al. (2005), 266. Hurley et al. (2005a), 267. Li et al. (2005), 268. Gehrels et al. (2009), 269. Berger et al. (2005d), 270. Monfardini et al. (2005a), 271. Lamb et al. (2005), 272. Cenko & Fox (2005a), 273. Smith et al. (2005), 274. Levan et al. (2006c), 275. Berger & Gonzalez (2005), 276. D’Avanzo et al. (2005a), 277. Pellizza et al. (2006), 278. Nysewander et al. (2005), 279. D’Avanzo et al. (2005b), 280. Kelson & Berger (2005). 281. Berger & Mulchaey (2005), 282. Still et al. (2005), 283. Jakobsson et al. (2006a), 284. Huang et al. (2007), 285. Tristram et al. (2005a), 286. de Pasquale et al. (2006b), 287. Berger et al. (2005e), 288. Sakamoto et al. (2005a), 289. Berger et al. (2005f), 290. de Ugarte Postigo et al. (2007a), 291. Cenko & Fox (2005b), 292. Kosugi et al. (2005), 293. Cenko et al. (2005), 294. Holland et al. (2007b), 295. Berger et al. (2005b), 296. Monard & Price (2005), 297. Cenko & Fox (2005c), 298. McGowan et al. (2005), 299. Götz & Mereghetti (2005), 300. Hurkett et al. (2005), 301. Prochaska et al. (2005a), 302. Yost et al. (2006), 303. Mereghetti et al. (2005b), 304. Cenko & Fox (2005d), 305. Berger et al. (2006a), 306. Hurkett et al. (2006), 307. Fynbo et al. (2005a), 308. Prigozhin et al. (2005), 309. Campana et al. (2005), 310. Gorosabel et al. (2005a), 311. Götz et al. (2005a), 312. Guidorzi et al. (2005b), 313. Götz et al. (2005b), 314. Chiang et al. (2005), 315. Foley et al. (2005a), 316. Blustin et al. (2006a), 317. Monfardini et al. (2005b), 318. Berger & Becker (2005), 319. Grupe et al. (2006), 320. Halpern et al. (2005b), 321. Götz et al. (2005c), 322. Mangano et al. (2005), 323. Gorosabel et al. (2005b), 324. de Pasquale et al. (2005), 325. de Pasquale et al. (2006c), 326. Monfardini et al. (2005c), 327. Bikmaev et al. (2005b), 328. Götz et al. (2005d), 329. Klose et al. (2005), 330. Covino et al. (2005), 331. Rol et al. (2007a), 332. MacLeod et al. (2005), 333. Antonelli et al. (2006), 334. Haislip & Reichart (2005a), 335. Chen et al. (2005), 336. Pandey et al. (2006a), 337. de Pasquale et al. (2007a), 338. Rykoff et al. (2006), 339. Fynbo et al. (2005b), 340. Oates et al. (2007), 341. Haislip & Reichart (2005b), 342. Maetou et al. (2005), 343. Rykoff et al. (2005), 344. Jakobsson et al. (2006b), 345. Jensen et al. (2005), 346. Bikmaev et al. (2005c), 347. Prochaska et al. (2005b), 348. Cenko et al. (2006g), 349. Page et al. (2005), 350. Fynbo et al. (2005c), 351. Sollerman et al. (2007), 352. Mirabal et al. (2007a), 353. Halpern (2005). 354. Kawai et al. (2006), 355. Haislip et al. (2006), 356. Foley et al. (2005b), 357. Sharapov et al. (2005a), 358. Bloom (2005), 359. Malesani et al. (2006), 360. Brown et al. (2005a), 361. Guziy et al. (2005), 362. Durig & Price (2005), 363. Tristram et al. (2005b), 364. Rumyantsev et al. (2005a), 365. Rumyantsev et al. (2005b), 366. Beardmore et al. (2005), 367. Berger et al. (2005g), 368. Soderberg et al. (2005), 369. Sharapov et al. (2005b), 370. Olive et al. (2005), 371. Burenin et al. (2005), 372. Brown et al. (2005b), 373. Nakagawa et al. (2006), 374. Rol et al. (2007b), 375. Hurley et al. (2005b), 376. Castro-Tirado et al. (2006a), 377. Misra et al. (2005), 378. Quimby et al. (2005), 379. Perley et al. (2006), 380. Tagliaferri et al. (2005), 381. Penprase et al. (2006), 382. Guidorzi et al. (2007b), 383. Goad et al. (2007), 384. Thoene et al. (2005), 385. Mereghetti et al. (2005c), 386. Page et al. (2006a), 387. Halpern (2006), 388. Retter et al. (2006), 389. Armstrong et al. (2006), 390. Zimmerman & Tyagi (2006), 391. Oates et al. (2006), 392. Blustin et al. (2006b), 393. Swan et al. (2006), 394. Khamitov et al. (2006a), 395. Yanagisawa et al. (2006a), 396. Mereghetti et al. (2006a), 397. Perri et al. (2006), 398. Guidorzi et al.

- (2006a), 399. Piranomonte et al. (2006b), 400. Yanagisawa et al. (2006b), 401. Kocevski et al. (2006), 402. Jelínek et al. (2006a), 403. Cummings et al. (2006), 404. Palmer et al. (2006), 405. Prochaska et al. (2006), 406. Misra et al. (2007), 407. Götz & Mereghetti (2006), 408. Nielsen et al. (2006), 409. Butler (2007), 410. Cenko et al. (2006c), 411. Cenko et al. (2006b), 412. Mereghetti & Götz (2006a), 413. Kong (2006), 414. Khamitov et al. (2006b), 415. Fynbo et al. (2006a), 416. Hao et al. (2007), 417. Stanek et al. (2007), 418. Curran et al. (2007), 419. Cucchiara et al. (2006b), 420. Sharapov et al. (2006a), 421. Sharapov et al. (2006b), 422. Golenetskii et al. (2006a), 423. Guziy et al. (2006), 424. Mirabal et al. (2006), 425. Rol et al. (2006a), 426. Berger et al. (2006b), 427. Blustin & Cummings (2006), 428. Andreev & Pozanenko (2006), 429. Lamb et al. (2006), 430. Hunsberger et al. (2006), 431. D'Avanzo et al. (2006a), 432. Jelínek et al. (2006b), 433. Covino et al. (2006b), 434. Sharapov et al. (2006c), 435. Blustin et al. (2006c), 436. Vreeswijk & Jaunsen (2006), 437. Chen et al. (2006), 438. MacLeod et al. (2006), 439. Thoene et al. (2006a), 440. Lopez-Sanchez et al. (2006), 441. Cobb (2006a), 442. Halpern & Mirabal (2006), 443. Fox & Cenko (2006), 444. Cucchiara et al. (2006c), 445. Hicken & Garnavich (2006), 446. Ofek et al. (2007), 447. Fynbo et al. (2006b), 448. Thoene et al. (2006b), 449. Holland (2006), 450. Price (2006), 451. Melandri et al. (2006b), 452. Bloom et al. (2006b), 453. Milne (2006), 454. Klotz et al. (2006a), 455. Cenko et al. (2006d), 456. D'Avanzo et al. (2006b), 457. Dai et al. (2007), 458. Jensen et al. (2006), 459. Castro-Tirado et al. (2006b), 460. Tanvir et al. (2006), 461. Ferrero et al. (2006), 462. Sharapov et al. (2006d), 463. Ledoux et al. (2006), 464. Nysewander et al. (2007), 465. French et al. (2006), 466. Valle et al. (2006), 467. Stefanescu et al. (2006a), 468. Schady & Moretti (2006), 469. Cenko & Ofek (2006), 470. Jakobsson et al. (2006c), 471. Jakobsson et al. (2006d), 472. Fugazza et al. (2006a), 473. Pagani et al. (2006), 474. Morgan et al. (2006), 475. Thoene et al. (2006c), 476. Pandey et al. (2006b), 477. Rol & Page (2006), 478. Bellm et al. (2006), 479. Hurley et al. (2006), 480. Schady (2006), 481. Cucchiara et al. (2006d), 482. Thoene et al. (2007a), 483. Levan et al. (2006d), 484. D'Avanzo et al. (2006c), 485. Mereghetti & Gotz (2006b), 486. Wiersema et al. (2007), 487. Cenko & Rau (2006), 488. Fugazza et al. (2006b), 489. Soyano et al. (2006), 490. Cenko et al. (2006e), 491. Rol et al. (2006b), 492. Wiersema et al. (2006), 493. Levan et al. (2007b), 494. Hafizov et al. (2006), 495. Melandri et al. (2006c), 496. Fox et al. (2006), 497. Holland & Cucchiara (2006), 4989. Covino et al. (2006c), 499. D'Elia et al. (2006), 500. Stefanescu et al. (2006b), 501. Fynbo et al. (2006c), 502. Antoniuk et al. (2006), 503. Golenetskii et al. (2006b), 504. Page et al. (2006b), 505. Terra et al. (2006), 506. Götz et al. (2006), 507. Guidorzi et al. (2006b), 508. Cannizzo et al. (2006), 509. Jakobsson et al. (2006e), 510. Osip et al. (2006), 511. Mundell et al. (2007), 512. Updike et al. (2006), 513. Holland & Moretti (2006), 514. Mereghetti et al. (2006b), 515. Berger (2006b), 516. Stamatikos et al. (2006), 517. Parsons et al. (2006), 518. Klotz et al. (2006b), 519. Cenko et al. (2006f), 520. Holland et al. (2006), 521. Thoene et al. (2006d), 522. Fynbo (2006), 523. Fynbo et al. (2006d), 524. Thoene et al. (2006e), 525. Bloom et al. (2006c), 526. Halpern et al. (2006), 527. Mereghetti et al. (2006c), 528. Halpern & Armstrong (2006), 529. Perley et al. (2008), 530. Pozanenko et al. (2006), 531. Sakamoto et al. (2006), 532. Klotz et al. (2006c), 533. Cenko & Fox (2006), 534. Berger (2006c), 535. Cobb (2006b), 536. Chen et al. (2007a), 537. Boyd & Marshall (2007), 538. Jaunsen et al. (2007a), 539. Malesani et al. (2007b), 540. Fox et al. (2007a), 541. Cenko & Fox (2007), 542. Bellm et al. (2008), 543. Vetere et al. (2007a), 544. Malesani et al. (2007c), 545. Cucchiara et al.

- (2007b), 546. Halpern & Mirabal (2007), 547. D'Avanzo et al. (2007), 548. Yoshida et al. (2007a), 549. Mirabal et al. (2007b), 550. Rol et al. (2007c), 551. Thoene et al. (2007b), 552. Klotz et al. (2007a), 553. Jaunsen et al. (2007b), 554. Rol et al. (2007d), 555. Vergani et al. (2007), 556. Paizis et al. (2007), 557. Mereghetti et al. (2007a), 558. Halpern & Armstrong (2007), 559. Jaunsen et al. (2007c), 560. Cobb (2007a), 561. Markwardt et al. (2007e), 562. Grupe et al. (2007a), 563. Jakobsson et al. (2007a), 564. Berger et al. (2007d), 565. Prieto et al. (2007), 566. Cenko et al. (2007b), 567. Pozanenko et al. (2007), 568. de Ugarte Postigo et al. (2007b), 569. Guidorzi et al. (2007c), 570. Cannizzo et al. (2007), 571. Thoene et al. (2007c), 572. Pagani et al. (2007a), 573. Jakobsson et al. (2007b), 574. Vetere et al. (2007b), 575. Fox et al. (2007b), 576. Terra et al. (2007), 577. Hattori et al. (2007), 578. Shakhovskoy et al. (2007), 579. Cenko et al. (2007c), 580. Swan et al. (2007), 581. de Ugarte Postigo et al. (2007c), 582. Thoene et al. (2007d), 583. Rykoff et al. (2007), 584. Updike et al. (2007), 585. Cenko et al. (2007d), 586. Grupe et al. (2007b), 587. Starling et al. (2007b), 588. Sbarufatti et al. (2007), 589. Malesani et al. (2007d), 590. Holland et al. (2007c), 591. Markwardt et al. (2007a), 592. Melandri et al. (2007), 593. Barthelmy et al. (2007), 594. Grupe et al. (2007c), 595. Ziaeepour et al. (2007b), 596. Palmer et al. (2007a), 597. Malesani et al. (2007e), 598. Golenetskii et al. (2007a), 599. Feroci et al. (2007), 600. Cenko & Rau (2007), 601. Cummings et al. (2007a), 602. Prochaska et al. (2007a), 603. Berger & Murphy (2007), 604. Stamatikos et al. (2007a), 605. Schady & Parsons (2007), 606. Fenimore et al. (2007), 607. Stefanescu et al. (2007), 608. Thoene et al. (2007e), 609. Markwardt et al. (2007b), 610. Krimm & Stratta (2007), 611. Cobb (2007b), 612. Markwardt et al. (2007c), 613. Klotz et al. (2007b), 614. Cummings et al. (2007b), 615. Fynbo et al. (2007), 616. Grupe et al. (2007d), 617. Jaunsen et al. (2007d), 618. Racusin & Barthelmy (2007), 619. Cobb (2007c), 620. Mereghetti et al. (2007b), 621. Bloom et al. (2007b), 622. de Pasquale et al. (2007b), 623. Schady et al. (2007), 624. Perley et al. (2007b), 625. Moretti et al. (2007), 626. Rumyantsev & Pozanenko (2007), 627. Guidorzi et al. (2007d). 628. Roy et al. (2007e), 629. Prochaska et al. (2007b), 630. Markwardt et al. (2007d), 631. Stern et al. (2007), 632. Im et al. (2007), 633. Marshall et al. (2007c), 634. Iizuka & Maeno (2007), 635. Palmer et al. (2007b), 636. Kann et al. (2007), 637. Krimm et al. (2007), 638. Xin et al. (2007b), 639. Holland et al. (2007d), 640. Jakobsson et al. (2007c), 641. Xin et al. (2007c), 642. Sakamoto et al. (2007), 643. Terada et al. (2007), 644. Pagani et al. (2007b), 645. Minezaki et al. (2007), 646. Racusin et al. (2007), 647. Xin et al. (2007d), 648. Grupe et al. (2007e), 649. Stroh et al. (2007), 650. Ledoux et al. (2007), 651. Lee et al. (2007), 652. McBreen et al. (2007b), 653. Perri et al. (2007b), 654. Milne (2007), 655. Stratta et al. (2007c), 656. Chen et al. (2007b), 657. Ukwatta et al. (2007), 658. Bloom (2007), 659. Cummings et al. (2007c), 660. Yoshida et al. (2007b), 661. Stamatikos et al. (2007b), 662. Cenko et al. (2007e)

REFERENCES

- Akerlof, C., McKay, T., Rykoff, E., & Smith, D., 2001, GRB Coordinates Network, 1115, 1
- Amati, L., et al. 2004, A&A, 426, 415
- Andersen, M. I., et al. 2000, A&A, 364, L54
- Andersen, M. I., Jensen, B. L., Hjorth, J., Pedersen, H., Kjeldsen, H., Gorosabel, J., & Fynbo, J. U. 2001, GRB Coordinates Network, 1080, 1
- Andreev, M., & Pozanenko, A. 2006, GRB Coordinates Network, 4844, 1
- Antonelli, L. A., et al. 1999, A&AS, 138, 435
- Antonelli, L. A., et al. 2006, A&A, 456, 509
- Antoniuk, K., Rumyantsev, V., & Pozanenko, A. 2006, GRB Coordinates Network, 5647, 1
- Arimoto, M., et al. 2007, PASJ, 59, 695
- Armstrong, E., Halpern, J. P., Tyagi, S., & Zimmerman, N. 2006, GRB Coordinates Network, 4427, 1
- Barbier, L., et al. 2007, GRB Coordinates Network, 6623, 1
- Barraud, C., et al. 2003, A&A, 400, 1021
- Barraud, C., et al. 2004, GRB Coordinates Network, 2620, 1
- Barthelmy, S. D., et al. 2007, GRB Coordinates Network, 6622, 1
- Bartolini, C., Gualandi, R., Guarneri, A., Piccioni, A., Palazzi, E., Pian, E., & Masetti, N. 2000, GRB Coordinates Network, 714, 1
- Bayliss, M., Nysewander, M., Foster, A., Reichart, D., & Moran, J. 2004, GRB Coordinates Network, 2864, 1
- Beardmore, A. P., et al. 2005, GRB Coordinates Network, 4162, 1
- Bellm, E., et al. 2006, GRB Coordinates Network, 5418, 1
- Bellm, E. C., et al. 2008, ApJ, 688, 491
- Berger, E., et al. 2002, ApJ, 581, 981

- Berger, E. 2005, GRB Coordinates Network, 3801, 1
- Berger, E., & Becker, G. 2005, GRB Coordinates Network, 3520, 1
- Berger, E., & Boss, A. 2005, GRB Coordinates Network, 4323, 1
- Berger, E., & Fox, D. 2005, GRB Coordinates Network, 4316, 1
- Berger, E., & Gonzalez, S. 2005, GRB Coordinates Network, 3048, 1
- Berger, E., & Mulchaey, J. 2005, GRB Coordinates Network, 3122, 1
- Berger, E., et al. 2005a, Nature, 438, 988
- Berger, E., Mulchaey, J., Morrell, N., & Krzeminski, W. 2005b, GRB Coordinates Network, 3282, 1
- Berger, E., et al. 2005c, ApJ, 629, 328
- Berger, E., Cenko, S. B., & Kulkarni, S. R. 2005d, GRB Coordinates Network, 3088, 1
- Berger, E., Oemler, G., & Gladders, M. 2005e, GRB Coordinates Network, 3185, 1
- Berger, E., Gladders, M., & Oemler, G. 2005f, GRB Coordinates Network, 3201, 1
- Berger, E., Roth, M., & Gonzalez, S. 2005g, GRB Coordinates Network, 4098, 1
- Berger, E. 2006a, GRB Coordinates Network, 5965, 1
- Berger, E. 2006b, GRB Coordinates Network, 5754, 1
- Berger, E. 2006c, GRB Coordinates Network, 5962, 1
- Berger, E., Penprase, B. E., Cenko, S. B., Kulkarni, S. R., Fox, D. B., Steidel, C. C., & Reddy, N. A. 2006a, ApJ, 642, 979
- Berger, E., Kulkarni, S. R., Rau, A., & Fox, D. B. 2006b, GRB Coordinates Network, 4815, 1
- Berger, E. 2007, GRB Coordinates Network, 5995, 1
- Berger, E., & Murphy, D. 2007, GRB Coordinates Network, 6695, 1
- Berger, E., & Kaplan, D. L. 2007, GRB Coordinates Network, 6680, 1

- Berger, E., Fox, D. B., Kulkarni, S. R., Frail, D. A., & Djorgovski, S. G. 2007a, ApJ, 660, 504
- Berger, E., Morrell, N., & Roth, M. 2007b, GRB Coordinates Network, 7154, 1
- Berger, E., et al. 2007c, ApJ, 664, 1000
- Berger, E., Modjaz, M., Garg, A., Kirshner, R., Challis, P., & Rest, A. 2007d, GRB Coordinates Network, 6278, 1
- Berger, E., Fox, D. B., & Cucchiara, A. 2007e, GRB Coordinates Network, 6470, 1
- Bikmaev, I., et al. 2005a, GRB Coordinates Network, 3797, 1
- Bikmaev, I., et al. 2005b, GRB Coordinates Network, 3617, 1
- Bikmaev, I., et al. 2005c, GRB Coordinates Network, 3831, 1
- Bloom, J. S., Djorgovski, S. G., Kulkarni, S. R., & Frail, D. A. 1998, ApJ, 507, L25
- Bloom, J. S., & Falco, E. 2002, GRB Coordinates Network, 1659, 1
- Bloom, J. S., Berger, E., Kulkarni, S. R., Djorgovski, S. G., & Frail, D. A. 2003, AJ, 125, 999
- Bloom, J. S. 2005, GRB Coordinates Network, 3990, 1
- Bloom, J. S., et al. 2006, ApJ, 638, 354
- Bloom, J. S., Foley, R. J., Kocevki, D., & Perley, D. 2006b, GRB Coordinates Network, 5217, 1
- Bloom, J. S., Perley, D. A., & Chen, H. W. 2006c, GRB Coordinates Network, 5826, 1
- Bloom, J. S. 2007, GRB Coordinates Network, 7105, 1
- Bloom, J. S., et al. 2007a, ApJ, 654, 878
- Bloom, J. S., Perley, D. A., Chen, H.-W., & Prochaska, J. X. 2007b, GRB Coordinates Network, 6827, 1
- Blustin, A. J., et al. 2006a, ApJ, 637, 901
- Blustin, A. J., de Pasquale, M., Rosen, S. R., Cominsky, L., Norris, J., & Gehrels, N. 2006b, GRB Coordinates Network, 4461, 1

- Blustin, A. J., Pagani, C., & Kennea, J. 2006c, GRB Coordinates Network, 4964, 1
- Blustin, A. J., & Cummings, J. R. 2006, GRB Coordinates Network, 4824, 1
- Bond, H. E. 2003, GRB Coordinates Network, 2329, 1
- Boyd, P. T., & Marshall, F. E. 2007, GRB Coordinates Network, 6006, 1
- Brown, P. J., Morris, D., Huckle, H., Hancock, B., & Gehrels, N. 2005a, GRB Coordinates Network, 4004, 1
- Brown, P. J., Retter, A., Marshall, F., Smale, A., & Gehrels, N. 2005b, GRB Coordinates Network, 4167, 1
- Buffington, A., Band, D. L., Jackson, B. V., Hick, P. P., & Smith, A. C. 2006, ApJ, 637, 880
- Burenin, R., et al. 2005, GRB Coordinates Network, 4180, 1
- Butler, N., et al. 2003, GRB Coordinates Network, 2429, 1
- Butler, N., Dullaghan, A., Ford, P., Ricker, G., Vanderspek, R., Hurley, K., Jernigan, J., & Lamb, D. 2004a, Gamma-Ray Bursts: 30 Years of Discovery, 727, 435
- Butler, N., et al. 2004b, GRB Coordinates Network, 2701, 1
- Butler, N., et al. 2004c, GRB Coordinates Network, 2728, 1
- Butler, N., Vanderspek, R., Marshall, H. L., Ford, P. G., Ricker, G. R., Lamb, D. Q., & Garmire, G. P. 2004d, GRB Coordinates Network, 2808, 1
- Butler, N. R., et al. 2005, ApJ, 621, 884
- Butler, N. R. 2007, ApJ, 656, 1001
- Campana, S., Pagani, C., Burrows, D. N., & Gehrels, N. 2005, GRB Coordinates Network, 3441, 1
- Cannizzo, J. K., Barthelmy, S. D., Cummings, J., Page, K., Breeveld, A., Burrows, D., Roming, P., & Gehrels, N. 2006, GCNR, 5, 1 (2006), 5, 1
- Cannizzo, J. K., et al. 2007, GCNR, 52, 1 (2007), 52, 1
- Castro, S. M., Diercks, A., Djorgovski, S. G., Kulkarni, S. R., Galama, T. J., Bloom, J. S., Harrison, F. A., & Frail, D. A. 2000, GRB Coordinates Network, 605, 1

- Castro Cerón, J. M., et al. 2002a, A&A, 393, 445
- Castro Cerón, J. M., Gorosabel, J., Greiner, J., Klose, S., Snigula, J., & Castro-Tirado, A. J. 2002b, GRB Coordinates Network, 1234, 1
- Castro-Tirado, A. J., et al. 1997, IAU Circ., 6598, 2
- Castro-Tirado, A. J., et al. 1998, GRB Coordinates Network, 173, 1
- Castro-Tirado, A. J., Greiner, J., Phelps, S., Pian, E., & Costa, E. 1999, GRB Coordinates Network, 336, 1
- Castro-Tirado, A., Alises, M., & Greiner, J. 2000, GRB Coordinates Network, 870, 1
- Castro-Tirado, A. J., et al. 2001, A&A, 370, 398
- Castro-Tirado, A. J., Gorosabel, J., Castro Cerón, J. M., Nelson, B., & Tristram, P. 2002a, GRB Coordinates Network, 1355, 1
- Castro-Tirado, A. J., Klose, S., Wisotzki, L., Huferath, S., Greiner, J., Castro Cerón, J. M., & Gorosabel, J. 2002b, GRB Coordinates Network, 1642, 1
- Castro-Tirado, A. J., Gorosabel, J., Amado, P., & Castro Cerón, J. M. 2002c, GRB Coordinates Network, 1775, 1
- Castro-Tirado, A. J., et al. 2003, A&A, 411, L315
- Castro-Tirado, A. J., Bond, I., Kilmartin, P., de Ugarte Postigo, A., Gorosabel, J., Jelinek, M., & Yock, P. 2005, GRB Coordinates Network, 3018, 1
- Castro-Tirado, A. J., et al. 2006a, A&A, 459, 763
- Castro-Tirado, A. J., Amado, P., Negueruela, I., Gorosabel, J., Jelinek, M., & de Ugarte Postigo, A. 2006b, GRB Coordinates Network, 5218, 1
- Cenko, S. B., Fox, D. B., & Gal-Yam, A. 2004, GRB Coordinates Network, 2848, 1
- Cenko, S. B., & Fox, D. B. 2005a, GRB Coordinates Network, 3014, 1
- Cenko, S. B., & Fox, D. B. 2005b, GRB Coordinates Network, 3231, 1
- Cenko, S. B., & Fox, D. B. 2005c, GRB Coordinates Network, 3299, 1
- Cenko, S. B., & Fox, D. B. 2005d, GRB Coordinates Network, 3349, 1

- Cenko, S. B., Kulkarni, S. R., Gal-Yam, A., & Berger, E. 2005, GRB Coordinates Network, 3542, 1
- Cenko, S. B., & Fox, D. B. 2006, GRB Coordinates Network, 5978, 1
- Cenko, S. B., & Ofek, E. O. 2006, GRB Coordinates Network, 5309, 1
- Cenko, S. B., & Rau, A. 2006, GRB Coordinates Network, 5512, 1
- Cenko, S. B., Fox, D. B., & Price, P. A. 2006a, GRB Coordinates Network, 5912, 1
- Cenko, S. B., Ofek, E., Soderberg, A. M., Cucchiara, N., & Fox, D. B. 2006b, GRB Coordinates Network, 4646, 1
- Cenko, S. B., Moon, D.-S., & Schmidt, B. P. 2006c, GRB Coordinates Network, 4636, 1
- Cenko, S. B., Berger, E., Djorgovski, S. G., Mahabal, A. A., & Fox, D. B. 2006d, GRB Coordinates Network, 5155, 1
- Cenko, S. B., Ofek, E. O., & Fox, D. B. 2006e, GRB Coordinates Network, 5529, 1
- Cenko, S. B., Ofek, E. O., & Kasliwal, M. 2006f, GRB Coordinates Network, 5770, 1
- Cenko, S. B., et al. 2006, ApJ, 652, 490
- Cenko, S. B., & Fox, D. B. 2007, GRB Coordinates Network, 6028, 1
- Cenko, S. B., & Rau, A. 2007, GRB Coordinates Network, 6679, 1
- Cenko, S. B., Rau, A., Berger, E., Price, P. A., & Cucchiara, A. 2007a, GRB Coordinates Network, 6664, 1
- Cenko, S. B., Gezari, S., Small, T., Fox, D. B., & Chornock, R. 2007b, GRB Coordinates Network, 6322, 1
- Cenko, S. B., Price, P. A., & Berger, E. 2007c, GRB Coordinates Network, 6450, 1
- Cenko, S. B., Fox, D. B., Cucchiara, A., Schmidt, B. P., Berger, E., Price, P. A., & Roth, K. C. 2007d, GRB Coordinates Network, 6556, 1
- Cenko, S. B., Fox, D. B., & Ofek, E. 2007e, GRB Coordinates Network, 7123, 1
- Chen, A. C., Ting, H. C., Lin, H. C., Huang, K. Y., Kinoshita, D., Ip, W. H., Urata, Y., & Tamagawa, T. 2003, GRB Coordinates Network, 2436, 1

- Chen, H.-W., Prochaska, J. X., Bloom, J. S., & Thompson, I. B. 2005, ApJ, 634, L25
- Chen, B. A., Lin, C. S., Huang, K. Y., Ip, W. H., & Urata, Y. 2006, GRB Coordinates Network, 4982, 1
- Chen, H.-W., Dembicky, J., York, D., Lamb, D., McMillan, R., Ketzeback, B., & Saurage, G. 2007a, GRB Coordinates Network, 5996, 1
- Chen, I. C., Huang, K. Y., & Urata, Y. 2007b, GRB Coordinates Network, 7083, 1
- Chiang, P. S., Huang, K. Y., Ip, W. H., Urata, Y., Qiu, Y., & Lou, Y. Q. 2005, GRB Coordinates Network, 3450, 1
- Cobb, B. E., Bailyn, C. D., van Dokkum, P. G., Buxton, M. M., & Bloom, J. S. 2004, ApJ, 608, L93
- Cobb, B. E. 2006, GRB Coordinates Network, 5935, 1
- Cobb, B. E. 2006a, GRB Coordinates Network, 5111, 1
- Cobb, B. E. 2006b, GRB Coordinates Network, 5961, 1
- Cobb, B. E. 2007a, GRB Coordinates Network, 6296, 1
- Cobb, B. E. 2007b, GRB Coordinates Network, 6829, 1
- Cobb, B. E. 2007c, GRB Coordinates Network, 6814, 1
- Connaughton, V., et al. 1997, IAU Circ., 6683, 1
- Covino, S., D'Avanzo, P., Malesani, D., Israel, G. L., Piranomonte, S., Tagliaferri, G., Chincarini, G., & Stella, L. 2005, GRB Coordinates Network, 3616, 1
- Covino, S., et al. 2006a, A&A, 447, L5
- Covino, S., Malesani, D., Antonelli, L. A., & Fugazza, D. 2006b, GRB Coordinates Network, 4911, 1
- Covino, S., Malesani, D., & Tagliaferri, G. 2006c, GRB Coordinates Network, 5604, 1
- Cucchiara, A., Fox, D. B., Berger, E., & Price, P. A. 2006a, GRB Coordinates Network, 5470, 1
- Cucchiara, A., Fox, D. B., & Berger, E. 2006b, GRB Coordinates Network, 4729, 1

- Cucchiara, A., Price, P. A., Fox, D. B., Cenko, S. B., & Schmidt, B. P. 2006c, GRB Coordinates Network, 5052, 1
- Cucchiara, A., Brown, P., & Moretti, A. 2006d, GRB Coordinates Network, 5445, 1
- Cucchiara, A., Fox, D. B., Cenko, S. B., Berger, E., Price, P. A., & Radomska, J. 2007a, GRB Coordinates Network, 6665, 1
- Cucchiara, A., Fox, D. B., Cenko, S. B., & Price, P. A. 2007b, GRB Coordinates Network, 6083, 1
- Cummings, J., et al. 2006, GRB Coordinates Network, 4608, 1
- Cummings, J., et al. 2007a, GRB Coordinates Network, 6699, 1
- Cummings, J. R., Barthelmy, S. D., Evans, P., & Page, K. 2007b, GCNR, 85, 1 (2007b), 85, 1
- Cummings, J. R., Moretti, A., & de Pasquale, M. 2007c, GCNR, 109, 1 (2007c), 109, 1
- Curran, P. A., et al. 2007, A&A, 467, 1049
- Cusumano, G., Burrows, D. N., Hunsberger, S., Pagani, C., La Parola, V., & Mangano, V. 2005, GRB Coordinates Network, 4326, 1
- Dai, X., Halpern, J. P., Morgan, N. D., Armstrong, E., Mirabal, N., Haislip, J. B., Reichart, D. E., & Stanek, K. Z. 2007, ApJ, 658, 509
- D'Avanzo, P., et al. 2005a, GRB Coordinates Network, 3064, 1
- D'Avanzo, P., et al. 2005b, GRB Coordinates Network, 3089, 1
- D'Avanzo, P., Israel, G. L., & Cosentino, R. 2006a, GRB Coordinates Network, 4890, 1
- D'Avanzo, P., Piranomonte, S., & Magazzu, G. 2006b, GCN Coordinates Network, 5151, 1
- D'Avanzo, P., Covino, S., & Antonelli, L. A. 2006c, GRB Coordinates Network, 5475, 1
- D'Avanzo, P., Magazzu, A., de Gurtubai, A. G., Antonelli, L. A., & Sakamoto, T. 2007, GRB Coordinates Network, 6108, 1
- D'Avanzo, P., et al. 2008, in preparation
- D'Elia, V., et al. 2006, GRB Coordinates Network, 5637, 1

- de Pasquale, M., Boyd, P., Blustin, A., Nousek, J., & Voges, W. 2005, GRB Coordinates Network, 3559, 1
- de Pasquale, M., et al. 2006a, A&A, 455, 813
- de Pasquale, M., et al. 2006b, MNRAS, 365, 1031
- de Pasquale, M., et al. 2006c, MNRAS, 370, 1859
- de Pasquale, M., et al. 2007a, MNRAS, 377, 1638
- de Pasquale, M., Stamatikos, M., & Page, K. 2007b, GCNR, 86, 1 (2007b), 86, 1
- de Ugarte, A., Sota, A., Gorosabel, J., Castro-Tirado, A. J., & Castro Cerón, J. M. 2004a, GRB Coordinates Network, 2571, 1
- de Ugarte Postigo, A., Tristram, P., Gorosabel, J., Yock, P., & Castro-Tirado, A. J. 2004b, GRB Coordinates Network, 2621, 1
- de Ugarte Postigo, A., Sota, A., Jelinek, M., Gorosabel, J., Castro-Tirado, A. J., & Castro Cerón, J. M. 2005, GRB Coordinates Network, 2957, 1
- de Ugarte Postigo, A., et al. 2007a, A&A, 462, L57
- de Ugarte Postigo, A., Jelinek, M., Tristram, P., Bond, I., Yock, P., Hearnshaw, J., & Castro-Tirado, A. J. 2007b, GRB Coordinates Network, 6321, 1
- de Ugarte Postigo, A., Castro-Tirado, A. J., Gonzalez, C., & Cabrera, A. 2007c, GRB Coordinates Network, 6480, 1
- Dezalay, J. P. et al. 2004, GRB Coordinates Network, 2839, 1
- Diercks, A. H., et al. 1998, ApJ, 503, L105
- Diercks, A., & Cotoros, I. 2000, GRB Coordinates Network, 692, 1
- Djorgovski, S. G., et al. 1997, Nature, 387, 876
- Djorgovski, S. G., Kulkarni, S. R., Goodrich, R., Frail, D. A., & Bloom, J. S. 1998, GRB Coordinates Network, 137, 1
- Djorgovski, S. G., Kulkarni, S. R., Bloom, J. S., & Frail, D. A. 1999, GRB Coordinates Network, 289, 1

- Djorgovski, S. G., Frail, D. A., Kulkarni, S. R., Bloom, J. S., Odewahn, S. C., & Diercks, A. 2001, ApJ, 562, 654
- Djorgovski, S. G., Bloom, J. S., & Kulkarni, S. R. 2003, ApJ, 591, L13
- Dodonov, S. N., Afanasiev, V. L., Sokolov, V. V., Moiseev, A. V., & Castro-Tirado, A. J. 1999, GRB Coordinates Network, 475, 1
- Donaghy, T. Q., et al. 2006, ArXiv Astrophysics e-prints, arXiv:astro-ph/0605570
- Dulligan, A., et al. 2004, GRB Coordinates Network, 2588, 1
- Durig, D. T., & Price, A. 2005, GRB Coordinates Network, 4023, 1
- Eldridge, J. J. 2007, MNRAS, 377, L29
- Evans, P. A., et al. 2007, A&A, 469, 379
- Fenimore, E. E., et al. 2004, GRB Coordinates Network, 2735, 1
- Fenimore, E., et al. 2007, GRB Coordinates Network, 6724, 1
- Feroci, M., et al. 2007, GRB Coordinates Network, 6668, 1
- Ferrero, P., et al. 2006, GRB Coordinates Network, 5489, 1
- Filliatre, P., et al. 2005, A&A, 438, 793
- Filliatre, P., et al. 2006, A&A, 448, 971
- Foley, R. J., Chen, H.-W., Bloom, J., & Prochaska, J. X. 2005a, GRB Coordinates Network, 3483, 1
- Foley, R. J., Chen, H.-W., Bloom, J. S., & Prochaska, J. X. 2005b, GRB Coordinates Network, 3949, 1
- Fox, D. W., & Price, P. A. 2002, GRB Coordinates Network, 1671, 1
- Fox, D. B., & Hunt, M. P. 2003, GRB Coordinates Network, 2365, 1
- Fox, D. W., Price, P. A., Herter, T., Appleton, P., & Cotter, G. 2003a, GRB Coordinates Network, 1857, 1
- Fox, D. B., Soderberg, A. M., & Berger, E. 2003b, GRB Coordinates Network, 2499, 1
- Fox, D. B., et al. 2005, Nature, 437, 845

- Fox, D. B., & Cenko, S. B. 2006, GRB Coordinates Network, 5044, 1
- Fox, D. B., Rau, A., & Ofek, E. O. 2006, GRB Coordinates Network, 5597, 1
- Fox, D. B., Berger, E., Price, P. A., & Cenko, S. B. 2007a, GRB Coordinates Network, 6071, 1
- Fox, D. B., Price, P. A., & Berger, E. 2007b, GRB Coordinates Network, 6420, 1
- French, J., Melady, G., Jelinek, M., de Ugarte Postigo, A., & Kubanek, P. 2006, GRB Coordinates Network, 5247, 1
- Frontera, F., Amati, L., Feroci, M., & Costa, E. 1998, GRB Coordinates Network, 167, 1
- Fugazza, D., et al. 2004, GRB Coordinates Network, 2617, 1
- Fugazza, D., Malesani, D., & Covino, S. 2006a, GRB Coordinates Network, 5347, 1
- Fugazza, D., et al. 2006b, GRB Coordinates Network, 5513, 1
- Fynbo, J. U., et al. 2001a, A&A, 369, 373
- Fynbo, J. U., et al. 2001b, A&A, 373, 796
- Fynbo, J. P. U., et al. 2005a, GRB Coordinates Network, 3460, 1
- Fynbo, J. P. U., et al. 2005b, GRB Coordinates Network, 3749, 1
- Fynbo, J. P. U., et al. 2005c, GRB Coordinates Network, 3874, 1
- Fynbo, J. P. U. 2006, GRB Coordinates Network, 5818, 1
- Fynbo, J. P. U., Gorosabel, J., Jensen, B. L., & Naeraenen, J. 2006a, GRB Coordinates Network, 4677, 1
- Fynbo, J. P. U., et al. 2006b, Nature, 444, 1047
- Fynbo, J. P. U., et al. 2006c, GRB Coordinates Network, 5651, 1
- Fynbo, J. P. U., Malesani, D., Thoene, C. C., Vreeswijk, P. M., Hjorth, J., & Henriksen, C. 2006d, GRB Coordinates Network, 5809, 1
- Fynbo, J. P. U., et al. 2007, GRB Coordinates Network, 6803, 1
- Galama, T., et al. 1997, Nature, 387, 479

- Galama, T., et al., 1998, GRB Coordinates Network, 62, 1
- Galama, T. J., et al. 1999, GRB Coordinates Network, 388, 1
- Galama, T. J., et al. 2003, ApJ, 587, 135
- Galassi, M., et al. 2004, GRB Coordinates Network, 2770, 1
- Gehrels, N., et al. 2005, Nature, 437, 851
- Gehrels, N., et al. 2009, in preparation
- Gendre, B., Corsi, A., & Piro, L. 2006, A&A, 455, 803
- Ghisellini, G., Ghirlanda, G., Mereghetti, S., Bosnjak, Z., Tavecchio, F., & Firmani, C. 2006, MNRAS, 372, 1699
- Gilmore, A., Kilmartin, P., & Henden, A. 2003, GRB Coordinates Network, 1949, 1
- Goad, M. R., et al. 2007, A&A, 468, 103
- Golenetskii, S., Aptekar, R., Mazets, E., Pal'Shin, V., Frederiks, D., & Cline, T. 2006a, GRB Coordinates Network, 4763, 1
- Golenetskii, S., Aptekar, R., Mazets, E., Pal'Shin, V., Frederiks, D., & Cline, T. 2006b, GRB Coordinates Network, 5689, 1
- Golenetskii, S., Aptekar, R., Mazets, E., Pal'Shin, V., Frederiks, D., & Cline, T. 2007a, GRB Coordinates Network, 6615, 1
- Golenetskii, S., Aptekar, R., Mazets, E., Pal'Shin, V., Frederiks, D., & Cline, T. 2007b, GRB Coordinates Network, 6671, 1
- Gorosabel, J., et al. 1999, A&AS, 138, 455
- Gorosabel, J., et al. 2000a, GRB Coordinates Network, 563, 1
- Gorosabel, J., Pascual, S., Gallego, J., Zamorano, J., Castro-Tirado, A. J., Castro Cerón, J. M., Klose, S., & Greiner, J. 2000b, GRB Coordinates Network, 735, 1
- Gorosabel, J., Hjorth, J., Jensen, B. L., Pedersen, H., Jakobsson, P., Fynbo, J., & Andersen, M. I. 2002a, GRB Coordinates Network, 1429, 1
- Gorosabel, J., Castro Cerón, J. M., Castro-Tirado, A. J., Guijarro, A., Hoyo, F., Pedraz, S., & Wolf, C. 2002b, GRB Coordinates Network, 1466, 1

- Gorosabel, J., Castro Cerón, J. M., Castro Tirado, A. J., Guijarro, A., Hoyo, F., Pedraz, S., & Wolf, C. 2002c, GRB Coordinates Network, 1467, 1
- Gorosabel, J., Jelinek, M., Mendez, J., Ruiz-Lapuente, P., Castro Cerón, J. M., Ugarte, P., & Castro-Tirado, A. J. 2004a, GRB Coordinates Network, 2592, 1
- Gorosabel, J., de Ugarte Postigo, A., Miranda, L. F., Castro-Tirado, A. J., Jelinek, M., Pereira, C. B., Castro Cerón, J. M., & Aceituno, J. 2004b, GRB Coordinates Network, 2675, 1
- Gorosabel, J., et al. 2005a, GRB Coordinates Network, 3425, 1
- Gorosabel, J., et al. 2005b, GRB Coordinates Network, 3565, 1
- Götz, D., et al. 2003, A&A, 409, 831
- Götz, D., & Mereghetti, S. 2005, GRB Coordinates Network, 3329, 1
- Götz, D., Mereghetti, S., Mowlavi, N., Shaw, S., Beck, M., & Borkowski, J. 2005a, GRB Coordinates Network, 3430, 1
- Götz, D., Mereghetti, S., Milano, I., Mowlavi, N., Shaw, S., Beck, M., & Borkowski, J. 2005b, GRB Coordinates Network, 3446, 1
- Götz, D., Mereghetti, S., Mowlavi, N., Shaw, S., Beck, M., Neronov, A., & Borkowski, J. 2005c, GRB Coordinates Network, 3552, 1
- Götz, D., Mereghetti, S., Shaw, S., Mowlavi, N., Beck, M., Soldi, S., & Borkowski, J. 2005d, GRB Coordinates Network, 3607, 1
- Götz, D., & Mereghetti, S. 2006, GRB Coordinates Network, 4616, 1
- Götz, D., Mereghetti, S., Paizis, A., Lazos, M., Mowlavi, N., Beck, M., & Borkowski, J. 2006, GRB Coordinates Network, 5665, 1
- Graham, J. F., Fruchter, A. S., Levan, A. J., Nysewander, M., Tanvir, N. R., Dahlen, T., Bersier, D., & Pe'Er, A. 2007, GRB Coordinates Network, 6836, 1
- Greiner, J., Pompei, E., Els, S., Pinfield, D., Brillant, S., Sterzik, M., Wolf, C., & Antonelli, A. 1999, GRB Coordinates Network, 396, 1
- Greiner, J., et al. 2003a, ApJ, 599, 1223
- Greiner, J., Peimbert, M., Estaban, C., Kaufer, A., Jaunsen, A., Smoke, J., Klose, S., & Reimer, O. 2003b, GRB Coordinates Network, 2020, 1

- Groot, P. J., et al. 1997a, IAU Circ., 6616, 2
- Groot, P. J. et al. 1997b, GRB Coordinates Network, 17, 1
- Groot, P. J., et al. 1998a, ApJ, 493, L27
- Groot, P. J., et al. 1998b, ApJ, 502, L123
- Grupe, D., et al. 2006, ApJ, 645, 464
- Grupe, D., et al. 2007a, GCNR, 43, 2 (2007), 43, 2
- Grupe, D., et al. 2007b, GCNR, 65, 1 (2007), 65, 1
- Grupe, D., et al. 2007c, GCNR, 71, 1 (2007), 71, 1
- Grupe, D., Barthelmy, S. D., Palmer, D. M., Burrows, D. N., & Gehrels, N. 2007d, GCNR, 83, 1 (2007), 83, 1
- Grupe, D., Cummings, J. R., Schady, P., Barthelmy, S. D., Burrows, D. N., Roming, P., & Gehrels, N. 2007e, GCNR, 107, 1 (2007), 107, 1
- Guidorzi, C., et al. 2005a, GRB Coordinates Network, 4356, 1
- Guidorzi, C., et al. 2005b, GRB Coordinates Network, 3437, 1
- Guidorzi, C., et al. 2006a, GRB Coordinates Network, 4504, 1
- Guidorzi, C., et al. 2006b, GRB Coordinates Network, 5670, 1
- Guidorzi, C., et al. 2007a, GCNR, 77, 1 (2007), 77, 1
- Guidorzi, C., et al. 2007b, A&A, 463, 539
- Guidorzi, C., et al. 2007c, GRB Coordinates Network, 6334, 1
- Guidorzi, C., Romano, P., Moretti, A., Krimm, H., Barthelmy, S. D., Burrows, D. N., Roming, P., & Gehrels, N. 2007d, GCNR, 89, 2 (2007), 89, 2
- Guziy, S., et al. 2003, GRB Coordinates Network, 2391, 1
- Guziy, S., Jelinek, M., Gorosabel, J., Castro-Tirado, A. J., de Ugarte Postigo, A., Flores, E. R., & Vlijanen, K. 2005, GRB Coordinates Network, 4025, 1
- Guziy, S., et al. 2006, GRB Coordinates Network, 4771, 1

- Hafizov, B., Ibrahimov, M., & Pozanenko, A. 2006, GRB Coordinates Network, 5567, 1
- Haislip, J., & Reichart, D. 2005a, GRB Coordinates Network, 3719, 1
- Haislip, J., & Reichart, D. 2005b, GRB Coordinates Network, 3780, 1
- Haislip, J. B., et al. 2006, Nature, 440, 181
- Halpern, J. P., et al. 2000, ApJ, 543, 697
- Halpern, J. P. 2005, GRB Coordinates Network, 3900, 1
- Halpern, J. P., Tonnesen, S., Tuttle, S., & Mirabal, N. 2005a, GRB Coordinates Network, 4202, 1
- Halpern, J. P., Kemp, J., & Mirabal, N. 2005b, GRB Coordinates Network, 3530, 1
- Halpern, J. 2006, GRB Coordinates Network, 4614, 1
- Halpern, J. P., & Armstrong, E. 2006, GRB Coordinates Network, 5849, 1
- Halpern, J. P., & Mirabal, N. 2006, GRB Coordinates Network, 5034, 1
- Halpern, J. P., Mirabal, N., & Armstrong, E. 2006, GRB Coordinates Network, 5840, 1
- Halpern, J. P., & Mirabal, N. 2007, GRB Coordinates Network, 6082, 1
- Halpern, J. P., & Armstrong, E. 2007, GRB Coordinates Network, 6195, 1
- Hammer, F., Flores, H., Schaerer, D., Dessauges-Zavadsky, M., Le Floc'h, E., & Puech, M. 2006, A&A, 454, 103
- Hao, H., et al. 2007, ApJ, 659, L99
- Harrison, F. A., et al. 1999, ApJ, 523, L121
- Hattori, T., Aoki, K., & Kawai, N. 2007, GRB Coordinates Network, 6441, 1
- Hearty, F., et al. 2004, GRB Coordinates Network, 2916, 1
- Heise, J., in't Zand, J. J. M., Kulkarni, S. R., & Costa, E. 2001, GRB Coordinates Network, 1138, 1
- Henden, A. 2000, GRB Coordinates Network, 658, 1

- Henden, A., Castro-Tirado, A. J., & Castro Cerón, J. M. 2000a, GRB Coordinates Network, 621, 1
- Henden, A., Kaiser, D., Hohman, D., Pason, R., & Aquino, B. 2000b, GRB Coordinates Network, 858, 1
- Henden, A., & Nelson, P. 2002, GRB Coordinates Network, 1397, 1
- Henden, A., Silvay, J., Moran, J., Soule, R., Reichart, D., Schaefer, J., Canterna, R., & Scoggins, B. 2003, GRB Coordinates Network, 2250, 1
- Hicken, M., & Garnavich, P. 2006, GRB Coordinates Network, 5070, 1
- Hill, J. E., et al. 2006, ApJ, 639, 303
- Hjorth, J., et al. 2002, ApJ, 576, 113
- Hjorth, J., et al. 2003, ApJ, 597, 699
- Holland, S. T., et al. 2002, AJ, 124, 639
- Holland, S. T., et al. 2003, AJ, 125, 2291
- Holland, S. T. 2006, GRB Coordinates Network, 5116, 1
- Holland, S., & Cucchiara, A. 2006, GRB Coordinates Network, 5603, 1
- Holland, S. T., & Moretti, A. 2006, GRB Coordinates Network, 5745, 1
- Holland, S. T., Tueller, J., Starling, R. L. C., Page, K., Burrows, D. N., Nosek, J., Barthelmy, S., & Gehrels, N. 2006, GCNR, 12, 2 (2006), 12, 2
- Holland, S. T., de Pasquale, M., & Markwardt, C. B. 2007a, GRB Coordinates Network, 7145, 1
- Holland, S. T., et al. 2007b, AJ, 133, 122
- Holland, S. T., et al. 2007c, GCNR, 68, 1 (2007), 68, 1
- Holland, S. T., et al. 2007d, GCNR, 94, 2 (2007), 94, 2
- Huang, K. Y., et al. 2005, ApJ, 628, L93
- Huang, K. Y., et al. 2007, ApJ, 654, L25
- Hunsberger, S. D., Grupe, D., & Marshall, F. 2006, GRB Coordinates Network, 4865, 1

- Hurkett, C., Page, K., Osborne, J. P., Zhang, B., Kennea, J., Burrows, D. N., & Gehrels, N. 2005, GRB Coordinates Network, 3374, 1
- Hurkett, C. P., et al. 2006, MNRAS, 368, 1101
- Hurley, K., & Cline, T. 1999, GRB Coordinates Network, 347, 1
- Hurley, K., Cline, T., & Mazets, E. 2000a, GRB Coordinates Network, 525, 1
- Hurley, K., Cline, T., Frontera, F., Guidorzi, C., Montanari, E., Mazets, E., & Golenetskii, S. 2000b, GRB Coordinates Network, 895, 1
- Hurley, K., Cline, T., Mazets, E., & Golenetskii, S. 2000c, GRB Coordinates Network, 865, 1
- Hurley, K., Cline, T., & Mazets, E. 2000d, GRB Coordinates Network, 529, 1
- Hurley, K., et al. 2000e, ApJ, 534, L23
- Hurley, K., Cline, T., Kouveliotou, C., Kippen, R. M., Mazets, E., & Golenetskii, S. 2000f, GRB Coordinates Network, 601, 1
- Hurley, K., Kippen, R. M., Barthelmy, S., & Cline, T. 2000g, GRB Coordinates Network, 616, 1
- Hurley, K., Barthelmy, S., Kippen, R. M., & Cline, T. 2000h, GRB Coordinates Network, 626, 1
- Hurley, K., Cline, T., & Mazets, E. 2000i, GRB Coordinates Network, 642, 1
- Hurley, K., Cline, T., Mazets, E., & Golenetskii, S. 2000j, GRB Coordinates Network, 687, 1
- Hurley, K., Cline, T., Mazets, E., & Golenetskii, S. 2000k, GRB Coordinates Network, 711, 1
- Hurley, K., Cline, T., Mazets, E., & Golenetskii, S. 2000l, GRB Coordinates Network, 730, 1
- Hurley, K., Golenetskii, S., Mazets, E., & Cline, T. 2000m, GRB Coordinates Network, 761, 1
- Hurley, K., Cline, T., Mazets, E., Golenetskii, S., Frontera, F., Montanari, E., & Guidorzi, C. 2000n, GRB Coordinates Network, 736, 1

Hurley, K., Cline, T., Mazets, E., & Golenetskii, S. 2000o, GRB Coordinates Network, 770, 1

Hurley, K., Cline, T., Mazets, E., & Golenetskii, S. 2000p, GRB Coordinates Network, 779, 1

Hurley, K., Cline, T., Mazets, E., & Golenetskii, S. 2000q, GRB Coordinates Network, 791, 1

Hurley, K., Mazets, E., Golenetskii, S., & Cline, T. 2000r, GRB Coordinates Network, 801, 1

Hurley, K., Cline, T., Mazets, E., & Golenetskii, S. 2000s, GRB Coordinates Network, 841, 1

Hurley, K., Cline, T., Mazets, E., & Golenetskii, S. 2000t, GRB Coordinates Network, 855, 1

Hurley, K., Cline, T., & Smith, D. 2000u, GRB Coordinates Network, 863, 1

Hurley, K., Cline, T., Mazets, E., & Golenetskii, S. 2000v, GRB Coordinates Network, 888, 1

Hurley, K., Cline, T., Montanari, E., Guidorzi, C., Frontera, F., Mazets, E., & Golenetskii, S. 2000w, GRB Coordinates Network, 899, 1

Hurley, K., Cline, T., Mazets, E., & Golenetskii, S. 2001a, GRB Coordinates Network, 916, 1

Hurley, K., Guidorzi, C., Montanari, E., & Frontera, F. 2001b, GRB Coordinates Network, 1013, 1

Hurley, K., Guidorzi, C., Montanari, E., & Frontera, F. 2001c, GRB Coordinates Network, 1036, 1

Hurley, K., et al. 2002a, GRB Coordinates Network, 1409, 1

Hurley, K., et al. 2002b, GRB Coordinates Network, 1325, 1

Hurley, K., et al. 2002c, GRB Coordinates Network, 1376, 1

Hurley, K., et al. 2002d, GRB Coordinates Network, 1395, 1

Hurley, K., et al. 2002e, GRB Coordinates Network, 1417, 1

- Hurley, K., et al. 2002f, GRB Coordinates Network, 1454, 1
- Hurley, K., et al. 2002g, GRB Coordinates Network, 1455, 1
- Hurley, K., Mazets, E., Golenetskii, S., & Cline, T. 2002h, GRB Coordinates Network, 1617, 1
- Hurley, K., et al. 2002i, GRB Coordinates Network, 1653, 1
- Hurley, K., et al. 2002j, GRB Coordinates Network, 1719, 1
- Hurley, K., et al. 2003a, GRB Coordinates Network, 1854, 1
- Hurley, K., et al. 2003b, GRB Coordinates Network, 1962, 1
- Hurley, K., et al. 2003c, GRB Coordinates Network, 2135, 1
- Hurley, K., et al. 2003d, GRB Coordinates Network, 2138, 1
- Hurley, K., et al. 2003e, GRB Coordinates Network, 2443, 1
- Hurley, K., et al. 2005a, GRB Coordinates Network, 2966, 1
- Hurley, K., et al. 2005b, GRB Coordinates Network, 4172, 1
- Hurley, K., et al. 2006, GRB Coordinates Network, 5407, 1
- Ibrahimov, M. A., Asfandiyarov, I. M., Kahharov, B. B., Pozanenko, A., Rumyantsev, V., & Beskin, G. 2003, GRB Coordinates Network, 2368, 1
- Iizuka, R., & Maeno, S. 2007, GRB Coordinates Network, 6900, 1
- Im, M., Lee, I., & Urata, Y. 2007, GRB Coordinates Network, 6920, 1
- Infante, L., Garnavich, P. M., Stanek, K. Z., & Wyrzykowski, L. 2001, GRB Coordinates Network, 1152, 1
- Jakobsson, P., et al. 2004, A&A, 427, 785
- Jakobsson, P., et al. 2005, ApJ, 629, 45
- Jakobsson, P., et al. 2006a, A&A, 460, L13
- Jakobsson, P., et al. 2006b, Gamma-Ray Bursts in the Swift Era, 836, 552

- Jakobsson, P., Vreeswijk, P., Fynbo, J. P. U., Hjorth, J., Starling, R., Kann, D. A., & Hartmann, D. 2006c, GRB Coordinates Network, 5320, 1
- Jakobsson, P., Fynbo, J. P. U., Hjorth, J., Nielsen, T. B., & Holhjem, K. 2006d, GRB Coordinates Network, 5335, 1
- Jakobsson, P., et al. 2006e, GRB Coordinates Network, 5782, 1
- Jakobsson, P., Malesani, D., Thoene, C. C., Fynbo, J. P. U., Hjorth, J., Jaunsen, A. O., Andersen, M. I., & Vreeswijk, P. M. 2007a, GRB Coordinates Network, 6283, 1
- Jakobsson, P., et al. 2007b, GRB Coordinates Network, 6398, 1
- Jakobsson, P., Vreeswijk, P. M., Hjorth, J., Malesani, D., Fynbo, J. P. U., & Thoene, C. C. 2007c, GRB Coordinates Network, 6952, 1
- Jaunsen, A. O., Malesani, D., Fynbo, J. P. U., Sollerman, J., & Vreeswijk, P. M. 2007a, GRB Coordinates Network, 6010, 1
- Jaunsen, A. O., Thoene, C. C., Fynbo, J. P. U., Hjorth, J., & Vreeswijk, P. 2007b, GRB Coordinates Network, 6202, 1
- Jaunsen, A. O., Fynbo, J. P. U., Andersen, M. I., & Vreeswijk, P. 2007c, GRB Coordinates Network, 6216, 1
- Jaunsen, A. O., et al. 2007d, GRB Coordinates Network, 6921, 1
- Jelínek, M., et al. 2006a, A&A, 454, L119
- Jelinek, M., Guziy, S., Gonzalez-Perez, J. M., & Castro-Tirado, A. J. 2006b, GRB Coordinates Network, 4920, 1
- Jensen, B. L., et al. 1999, GRB Coordinates Network, 371, 1
- Jensen, B. L., et al. 2000a, GRB Coordinates Network, 670, 1
- Jensen, B. L., Pedersen, H., Hjorth, J., Gorosabel, J., dall, T. H., Fynbo, J. P. U., & O'Toole, S. 2000b, GRB Coordinates Network, 679, 1
- Jensen, B. L., et al. 2001, A&A, 370, 909
- Jensen, B. L., et al. 2005, GRB Coordinates Network, 3809, 1
- Jensen, B. L., Hjorth, J., Fynbo, J., & Naranen, J. 2006, GRB Coordinates Network, 5203, 1

- Jha, S., et al. 2001, ApJ, 554, L155
- Johnson, S., et al. 2007, GRB Coordinates Network, 6218, 1
- Kann, D. A., Hoegner, C., & Filgas, R. 2007, GRB Coordinates Network, 6917, 1
- Kawai, N., et al. 2006, Nature, 440, 184
- Kelson, D., & Berger, E. 2005, GRB Coordinates Network, 3101, 1
- Khamitov, I., et al. 2006a, GRB Coordinates Network, 4494, 1
- Khamitov, I., et al. 2006b, GRB Coordinates Network, 4720, 1
- Kilmartin, P., & Gilmore, A. 2002, GRB Coordinates Network, 1462, 1
- Kippen, R. M., Preece, R. D., Giblin, T., Kouveliotou, C. 2007, GRB Coordinates Network, 344, 1
- Kippen, R. M. & Woods, P. M. 2000, GRB Coordinates Network, 639, 1
- Kjernsmo, K., Jaunsen, A., Saanum, O., Jensen, B. L., Hjorth, J., Pedersen, H., & Gorosabel, J. 2000, GRB Coordinates Network, 533, 1
- Klose, S., et al. 2000, ApJ, 545, 271
- Klose, S., et al. 2004, AJ, 128, 1942
- Klose, S., Stecklum, B., Fuhrmann, B., Ludwig, F., & Greiner, J. 2005, GRB Coordinates Network, 3609, 1
- Klotz, A., Boer, M., & Atteia, J. L. 2006a, GRB Coordinates Network, 5134, 1
- Klotz, A., Boer, M., & Atteia, J. L. 2006b, GRB Coordinates Network, 5788, 1
- Klotz, A., Boer, M., & Atteia, J. L. 2006c, GRB Coordinates Network, 5980, 1
- Klotz, A., Boer, M., & Atteia, J. L. 2007a, GRB Coordinates Network, 6159, 1
- Klotz, A., Boer, M., & Atteia, J. L. 2007b, GRB Coordinates Network, 6787, 1
- Kocevski, D., Bloom, J. S., & McGrath, E. J. 2006, GRB Coordinates Network, 4528, 1
- Kocevski, D., & Bloom, J. S. 2007, GRB Coordinates Network, 7107, 1
- Kong, A. 2006, GRB Coordinates Network, 4676, 1

- Kosugi, G., Kawai, N., Tajitsu, A., & Furusawa, H. 2004, GRB Coordinates Network, 2726, 1
- Kosugi, G., Kawai, N., Aoki, K., Hattori, T., Ohta, K., & Yamada, T. 2005, GRB Coordinates Network, 3263, 1
- Krimm, H. A., & Stratta, G. 2007, GCNR, 82, 1 (2007), 82, 1
- Krimm, H. A., Beardmore, A., Cummings, J. R., Barthelmy, S. D., Burrows, D. N., Gehrels, N., & Roming, P. W. A. 2007, GCNR, 96, 2 (2007), 96, 2
- Kulkarni, S. R., et al. 1999, Nature, 398, 389
- Kuroda, D., Yanagisawa, K., & Kawai, N. 2004, GRB Coordinates Network, 2818, 1
- La Parola, V., et al. 2006, A&A, 454, 753
- Lamb, D. Q., et al. 2002, GRB Coordinates Network, 1403, 1
- Lamb, D. Q., Nysewander, M., Reichart, D., York, D. G., Barentine, J., McMillan, R., Dembicky, J., & Ketzeback, B. 2003, GRB Coordinates Network, 2139, 1
- Lamb, D., et al. 2005, GRB Coordinates Network, 3019, 1
- Lamb, D. Q., Nysewander, M., Hearty, F., Chen, H.-W., & Reichart, D. E. 2006, GRB Coordinates Network, 5079, 1
- Laursen, L. T., & Stanek, K. Z. 2003, ApJ, 597, L107
- Ledoux, C., Vreeswijk, P., Smette, A., Jaunsen, A., & Kaufer, A. 2006, GRB Coordinates Network, 5237, 1
- Ledoux, C., Jakobsson, P., Jaunsen, A. O., Thoene, C. C., Vreeswijk, P. M., Malesani, D., Fynbo, J. P. U., & Hjorth, J. 2007, GRB Coordinates Network, 7023, 1
- Lee, I., Im, M., & Urata, Y. 2007, GRB Coordinates Network, 7033, 1
- Le Floc'h, E., et al. 2002, ApJ, 581, L81
- Lee, B. C., Tucker, D. L., Lamb, D. Q., vanden Berk, D. E., & Neilsen, E. 2001, GRB Coordinates Network, 1175, 1
- Lee, B. C., et al. 2002, GRB Coordinates Network, 1275, 1

- Levan, A., Burud, I., Fruchter, A., Rhoads, J., van den Berg, M., Homan, J., Rol, E., & Tanvir, N. 2002, GRB Coordinates Network, 1517, 1
- Levan, A., et al. 2005, ApJ, 624, 880
- Levan, A., et al. 2006a, ApJ, 647, 471
- Levan, A. J., et al. 2006b, ApJ, 648, L9
- Levan, A. J., et al. 2006c, ApJ, 648, 1132
- Levan, A. J., Tanvir, N. R., Rol, E., Fruchter, A., & Adamson, A. 2006d, GRB Coordinates Network, 5455, 1
- Levan, A. J., et al. 2007a, GRB Coordinates Network, 6603, 1
- Levan, A. J., et al. 2007b, MNRAS, 378, 1439
- Levan, A. J., et al. 2008, MNRAS, 384, 541
- Li, W., Filippenko, A. V., Chornock, R., & Jha, S. 2005, GRB Coordinates Network, 2968, 1
- Lipunov, V., et al. 2003, GRB Coordinates Network, 2157, 1
- Lopez-Sanchez, A. R., Garcia-Rojas, J., Jelinek, M., & Castro-Tirado, A. J. 2006, GRB Coordinates Network, 5013, 1
- MacLeod, C., Kirschbrown, J., Haislip, J., Nysewander, M., Crain, J. A., & Reichart, D. 2005, GRB Coordinates Network, 3652, 1
- MacLeod, C., et al. 2006, GRB Coordinates Network, 4999, 1
- Maetou, M., et al. 2005, GRB Coordinates Network, 3785, 1
- Maiorano, E., et al. 2006, A&A, 455, 423
- Malesani, D., Covino, S., Piranomonte, S., Antonelli, L. A., Chincarini, G., D'Avanzo, P., Stella, L., & Tagliaferri, G. 2006, GRB Coordinates Network, 5821, 1
- Malesani, D., et al. 2007a, A&A, 473, 77
- Malesani, D., Jaunsen, A. O., & Vreeswijk, P. M. 2007b, GRB Coordinates Network, 6015, 1

- Malesani, D., Jakobsson, P., Vreeswijk, P. M., Jaunsen, A. O., & Kann, D. A. 2007c, GRB Coordinates Network, 6055, 1
- Malesani, D., Thoene, C. C., Fynbo, J. P. U., Tanvir, N. R., & Tziampzis, A. 2007d, GRB Coordinates Network, 6565, 1
- Malesani, D., Jakobsson, P., Fynbo, J. P. U., Hjorth, J., & Vreeswijk, P. M. 2007e, GRB Coordinates Network, 6651, 1
- Mangano, V., et al. 2005, GRB Coordinates Network, 3564, 1
- Markwardt, C., et al. 2007a, GRB Coordinates Network, 6596, 1
- Markwardt, C., et al. 2007b, GRB Coordinates Network, 6748, 1
- Markwart, C. B., Beardmore, A., Barthelmy, S. D., Burrows, D. N., Roming, P., & Gehrels, N. 2007c, GCNR, 88, 1 (2007), 88, 1
- Markwardt, C., Kennea, J., Mangano, V., Barthelmy, S. D., Burrows, D. N., Roming, P., & Gehrels, N. 2007d, GCNR, 92, 1 (2007), 92, 1
- Markwardt, C. B., Evans, P. A., Goad, M., & Marshall, F. E. 2007, GCNR, 42, 3 (2007), 42, 3
- Marshall, F. E., Takeshima, T. 2000, GRB Coordinates Network, 58, 1
- Marshall, F. E., Barthelmy, S. D., Burrows, D. N., Chester, M. M., Cummings, J., Evans, P. A., Roming, P., & Gehrels, N. 2007a, GCNR, 80, 1 (2007), 80, 1
- Marshall, F. E., Barthelmy, S. D., Brown, P. J., Burrows, D. N., Cummings, J., Roming, P., Starling, R., & Gehrels, N. 2007b, GCNR, 81, 1 (2007), 81, 1
- Marshall, F. E., Barthelmy, S. D., Burrows, D. N., Roming, P., Sbarufatti, B., & Gejrels, N. 2007c, GCNR, 93, 1 (2007), 93, 1
- Martini, P., Garnavich, P., & Stanek, K. Z. 2003, GRB Coordinates Network, 1980, 1
- Masetti, N., et al. 1999, GRB Coordinates Network, 327, 1
- Masetti, N., et al. 2000a, A&A, 354, 473
- Masetti, N., Palazzi, E., Pian, E., Cosentino, R., Ghinassi, F., Magazzu, A., & Benetti, S. 2000b, GRB Coordinates Network, 774, 1

- Masetti, N., Palazzi, E., Pedani, M., Magazzu, A., Ghinassi, F., & Pian, E. 2001, GRB Coordinates Network, 926, 1
- Masetti, N., et al. 2003, A&A, 404, 465
- Masetti, N., Palazzi, E., Rol, E., Pian, E., & Pompei, E. 2004, GRB Coordinates Network, 2515, 1
- McBreen, S., Hanlon, L., McGlynn, S., McBreen, B., Foley, S., Preece, R., von Kienlin, A., & Williams, O. R. 2006, A&A, 455, 433
- McBreen, S., et al. 2007a, GCNR, 46, 2 (2007), 46, 2
- McBreen, S., et al. 2007b, GCNR, 101, 1 (2007), 101, 1
- McGowan, K., et al. 2005, GRB Coordinates Network, 3317, 1
- Melandri, A., et al. 2006a, A&A, 451, 27
- Melandri, A., et al. 2006b, GRB Coordinates Network, 5103, 1
- Melandri, A., Gomboc, A., Smith, R. J., & Tanvir, N. 2006c, GRB Coordinates Network, 5579, 1
- Melandri, A., Rol, E., & Tanvir, N. 2007, GRB Coordinates Network, 6602, 1
- Mereghetti, S., Götz, D., Borkowski, J., Walter, R., & Pedersen, H. 2003a, A&A, 411, L291
- Mereghetti, S., et al. 2003b, ApJ, 590, L73
- Mereghetti, S., et al. 2005a, A&A, 433, 113
- Mereghetti, S., Götz, D., Mowlavi, N., Shaw, S., Beck, M., Turler, M., & Borkowski, J. 2005b, GRB Coordinates Network, 3348, 1
- Mereghetti, S., Götz, D., Mowlavi, N., Eckert, D., Beck, M., & Borkowski, J. 2005c, GRB Coordinates Network, 4327, 1
- Mereghetti, S., & Götz, D. 2006, GRB Coordinates Network, 4659, 1
- Mereghetti, S., & Gotz, D. 2006, GRB Coordinates Network, 5493, 1
- Mereghetti, S., Götz, D., Shaw, S., Haymoz, P., Beck, M., & Borkowski, J. 2006a, GRB Coordinates Network, 4505, 1

- Mereghetti, S., Paizis, A., Götz, D., Shaw, S., Beck, M., Kreykenbohm, I., & Borkowski, J. 2006b, GRB Coordinates Network, 5751, 1
- Mereghetti, S., Paizis, A., Götz, D., Petry, D., Mowlavi, N., Beck, M., & Borkowski, J. 2006c, GRB Coordinates Network, 5834, 1
- Mereghetti, S., Paizis, A., Götz, D., Kreykenbohm, I., Mowlavi, N., Beck, M., & Borkowski, J. 2007a, GRB Coordinates Network, 6189, 1
- Mereghetti, S., Paizis, A., Götz, D., Petry, D., Beckmann, V., Beck, M., & Borkowski, J. 2007b, GRB Coordinates Network, 6823, 1
- Metzger, M. R., Djorgovski, S. G., Kulkarni, S. R., Steidel, C. C., Adelberger, K. L., Frail, D. A., Costa, E., & Frontera, F. 1997, Nature, 387, 878
- Michałowski, M. J., Hjorth, J., Castro Cerón, J. M., & Watson, D. 2008, ApJ, 672, 817
- Milne, P. A. 2006, GRB Coordinates Network, 5127, 1
- Milne, P. A. 2007, GRB Coordinates Network, 7056, 1
- Mineo, T., Tagliaferri, G., Malesani, D., Giommi, P., Burrows, D., Fox, D., Chincarini, G., & Page, K. 2005, GRB Coordinates Network, 4195, 1
- Minezaki, T., Price, P. A., Yoshii, Y., Cowie, L., & Kakazu, Y. 2007, GRB Coordinates Network, 7018, 1
- Mirabal, N., Halpern, J. P., Gotthelf, E. V., & Mukherjee, R. 2005, ApJ, 620, 379
- Mirabal, N., Halpern, J. P., An, D., Thorstensen, J. R., & Terndrup, D. M. 2006, ApJ, 643, L99
- Mirabal, N., Halpern, J. P., & O'Brien, P. T. 2007a, ApJ, 661, L127
- Mirabal, N., Melandri, A., & Halpern, J. P. 2007b, GRB Coordinates Network, 6162, 1
- Misra, K., Kamble, A. P., Sahu, D. K., Srividya, S., Bama, P., Anupama, G. C., & Van-niarajan, M. S. 2005, GRB Coordinates Network, 4259, 1
- Misra, K., Bhattacharya, D., Sahu, D. K., Sagar, R., Anupama, G. C., Castro-Tirado, A. J., Guziy, S. S., & Bhatt, B. C. 2007, A&A, 464, 903
- Mohan, V., et al. 2001, GRB Coordinates Network, 1120, 1
- Monard, B., & Price, A. 2005, GRB Coordinates Network, 3292, 1

- Monfardini, A., et al. 2005a, GRB Coordinates Network, 3001, 1
- Monfardini, A., et al. 2005b, GRB Coordinates Network, 3503, 1
- Monfardini, A., et al. 2005c, GRB Coordinates Network, 3588, 1
- Monnelly, G., Dullighan, A., Butler, N., Vanderspek, R., & Ricker, G. 2002, GRB Coordinates Network, 1339, 1
- Moran, L., et al. 2005, A&A, 432, 467
- Moretti, A., Guidorzi, C., Romano, P., Barthelmy, S. D., Burrows, D. N., Roming, P., & Gehrels, N. 2007, GCNR, 91, 1 (2007), 91, 1
- Morgan, A. N., Chester, M. M., & Pagani, C. 2006, GRB Coordinates Network, 5364, 1
- Mundell, C. G., et al. 2007, ApJ, 660, 489
- Murakami, T., Ueda, Y., Yoshida, A., Kawai, N., Marshall, F. E., Corbet, R. H. D., & Takeshima, T. 1997, IAU Circ., 6732, 1
- Nakagawa, Y. E., et al. 2006, PASJ, 58, L35
- Nielsen, J., Jensen, B. L., Fynbo, J. P. U., Hjorth, J., & Karoff, C. 2006, GRB Coordinates Network, 4620, 1
- Nysewander, M., Moran, J., Johnson, L., Moschler, D., Reichart, D., & Henden, A. 2002a, GRB Coordinates Network, 1760, 1
- Nysewander, M., Reichart, D., & Schwartz, M. 2002b, GRB Coordinates Network, 1699, 1
- Nysewander, M., Henden, A., Lopez-Morales, M., Reichart, D., & Schwartz, M. 2003, GRB Coordinates Network, 1861, 1
- Nysewander, M., Bayliss, M., Foster, A., & Reichart, D. 2004, GRB Coordinates Network, 2900, 1
- Nysewander, M., et al. 2005, GRB Coordinates Network, 3067, 1
- Nysewander, M. C., et al. 2006, ApJ, 651, 994
- Nysewander, M., Reichart, D. E., Crain, J. A., Foster, A., Haislip, J., Ivarsen, K., LaCluyze, A., & Trotter, A. 2007, ArXiv e-prints, 708, arXiv:0708.3444
- Oates, S. R., et al. 2006, MNRAS, 372, 327

- Oates, S. R., et al. 2007, MNRAS, 380, 270
- Ofek, E. O., et al. 2007, ApJ, 662, 1129
- Oksanen, A., et al. 2001, GRB Coordinates Network, 1019, 1
- Olive, J.-F., et al. 2005, GRB Coordinates Network, 4124, 1
- Osip, D., Chen, H.-W., & Prochaska, J. X. 2006, GRB Coordinates Network, 5715, 1
- Paciesas, W. S., et al. 1999, ApJS, 122, 465
- Pagani, C., La Parola, V., & Burrows, D. N. 2005, GRB Coordinates Network, 3934, 1
- Pagani, C., Morris, D., & Burrows, D. N. 2006, GRB Coordinates Network, 5393, 1
- Pagani, C., Vetere, L., Racusin, J. L., Landsman, W., Barbier, L., & Stamatikos, M. 2007a, GCNR, 53, 1 (2007), 53, 1
- Pagani, C., Racusin, J. L., Kuin, N. P. M., Holland, S. T., Barthelmy, S. D., & Gehrels, N. 2007b, GCNR, 97, 1 (2007), 97, 1
- Page, M. J., Ziaeepour, H., Blustin, A. J., Chester, M., Fink, R., & Gehrels, N. 2005, GRB Coordinates Network, 3859, 1
- Page, K. L., Burrows, D. N., Rol, E., & Boyd, P. 2006a, GRB Coordinates Network, 4796, 1
- Page, K. L., Cummings, J., Hurley, K., Burrows, D. N., Morris, D. C., Kennea, J. A., Brown, P., & Palmer, D. M. 2006b, GRB Coordinates Network, 5686, 1
- Paizis, A., Mereghetti, S., Götz, D., Kreykenbohm, I., Mowlavi, N., Beck, M., & Borkowski, J. 2007, GRB Coordinates Network, 6182, 1
- Palazzi, E., et al. 1999a, GRB Coordinates Network, 262, 1
- Palazzi, E., et al. 1999b, GRB Coordinates Network, 449, 1
- Palazzi, E., et al. 2000a, GRB Coordinates Network, 691, 1
- Palazzi, E., et al. 2000b, GRB Coordinates Network, 767, 1
- Palmer, D., et al. 2006, GRB Coordinates Network, 4584, 1
- Palmer, D., et al. 2007a, GRB Coordinates Network, 6643, 1
- Palmer, D., et al. 2007b, GRB Coordinates Network, 6911, 1

- Pandey, S. B., et al. 2006a, A&A, 460, 415
- Pandey, S. B., de Pasquale, M., Page, M. J., & Ziaeepour, H. Z. 2006b, GRB Coordinates Network, 5397, 1
- Park, H. S., Porrata, R., Williams, G. G., Hartmann, D., Hurley, K., & Barthelmy, S. 2000, GRB Coordinates Network, 628, 1
- Parsons, A., et al. 2006, GRB Coordinates Network, 5761, 1
- Pavlenko, E., & Rumyantsev, V. 2002, GRB Coordinates Network, 1277, 1
- Pedersen, H., Lindgren, B., Hjorth, J., Andersen, M. I., Jaunsen, A. O., Sollerman, J., Smoker, J., & Mooney, C. 1999a, GRB Coordinates Network, 192, 1
- Pedersen, H., Hjorth, J., Jensen, B. L., Rasmussen, M. B., Jaunsen, A. O., & Hurley, K. 1999b, GRB Coordinates Network, 349, 1
- Pedersen, H., Jensen, B. L., Gorosabel, J., & Fynbo, J. P. U. 2000, GRB Coordinates Network, 617, 1
- Pedersen, K., et al. 2006, ApJ, 636, 381
- Pellizza, L. J., et al. 2006, A&A, 459, L5
- Penprase, B. E., et al. 2006, ApJ, 646, 358
- Perley, D. A., Foley, R. J., Bloom, J. S., & Butler, N. R. 2006, GRB Coordinates Network, 5387, 1
- Perley, D. A., Thoene, C. C., & Bloom, J. S. 2007a, GRB Coordinates Network, 6774, 1
- Perley, D. A., Chornock, R., Bloom, J. S., Fassnacht, C., & Auger, M. W. 2007b, GRB Coordinates Network, 6850, 1
- Perley, D. A., Bloom, J. S., Modjaz, M., Poznanski, D., & Thoene, C. C. 2007c, GRB Coordinates Network, 7140, 1
- Perley, D. A., et al. 2008, ApJ, 672, 449
- Perri, M., Tagliaferri, G., & Burrows, D. N. 2006, GRB Coordinates Network, 4508, 1
- Perri, M., Stratta, G., Fenimore, E., Schady, P., Barthelmy, S. D., Burrows, D. N., Roming, P., & Gehrels, N. 2007a, GCNR, 103, 1 (2007), 103, 1

- Perri, M., Stratta, G., Kuin, N. P. M., Barthelmy, S. D., Burrows, D. N., Roming, P., & Gehrels, N. 2007b, GCNR, 102, 2 (2007), 102, 2
- Piccioni, A., Bartolini, C., Bruni, I., de Blasi, A., Guarnieri, A., Giovannelli, F., & Pizzichini, G. 2002, GRB Coordinates Network, 1486, 1
- Piranomonte, S., Covino, S., Malesani, D., Tagliaferri, G., Chincarini, G., & Stella, L. 2006a, GRB Coordinates Network, 5392, 1
- Piranomonte, S., et al. 2006b, GRB Coordinates Network, 4520, 1
- Piranomonte, S., Vergani, S., D'Avanzo, P., & Tagliaferri, G. 2007, GRB Coordinates Network, 6612, 1
- Piro, L., et al. 2002, ApJ, 577, 680
- Pozanenko, A., Shulga, A., Volnova, A., Msu, S., Ibrahimov, M., & Karimov, R. 2006, GRB Coordinates Network, 5902, 1
- Pozanenko, A., Shulga, A., Volnova, A., Hafizov, B., Asfandiyarov, I., & Ibrahimov, M. 2007, GRB Coordinates Network, 6407, 1
- Price, P., Axelrod, T., & Schmidt, B. 2000a, GRB Coordinates Network, 640, 1
- Price, P., Axelrod, T., & Schmidt, B. 2000b, GRB Coordinates Network, 780, 1
- Price, P. A., Meltzer, J., Stalder, B., Djorgovski, S. G., & Galama, T. J. 2000c, GRB Coordinates Network, 893, 1
- Price, P. A., Axelrod, T. S., & Schmidt, B. P. 2000d, GRB Coordinates Network, 898, 1
- Price, P. A., Morrison, G., & Bloom, J. S. 2001a, GRB Coordinates Network, 919, 1
- Price, P. A., Axelrod, T. S., Schmidt, B. P., & Reichart, D. E. 2001b, GRB Coordinates Network, 1020, 1
- Price, P. A., Axelrod, T. S., Schmidt, B. P., Reichart, D. E., Bloom, J. S., & Fox, D. 2001c, GRB Coordinates Network, 1017, 1
- Price, P. A., Gorham, P., Yost, S. A., & Kulkarni, S. R. 2001d, GRB Coordinates Network, 1039, 1
- Price, P. A., Jones, B., & Peterson, B. A. 2002a, GRB Coordinates Network, 1289, 1
- Price, P. A., Schmidt, B. P., & Axelrod, T. S. 2002b, GRB Coordinates Network, 1379, 1

- Price, P. A., Schmidt, B. P., & Axelrod, T. S. 2002c, GRB Coordinates Network, 1410, 1
- Price, P. A., Schmidt, B. P., & Axelrod, T. S. 2002d, GRB Coordinates Network, 1533, 1
- Price, P. A., et al. 2002e, ApJ, 571, L121
- Price, P. A., et al. 2002f, ApJ, 573, 85
- Price, P. A., Bloom, J. S., Goodrich, R. W., Barth, A. J., Cohen, M. H., & Fox, D. W. 2002g, GRB Coordinates Network, 1475, 1
- Price, P. A., Hauser, M., Puhlhofer, G., & Wagner, S. J. 2004, GRB Coordinates Network, 2639, 1
- Price, P. A. 2006, GRB Coordinates Network, 5104, 1
- Price, P. A., Berger, E., Fox, D. B., Cenko, S. B., & Rau, A. 2006, GRB Coordinates Network, 5077, 1
- Prieto, J., et al. 2007, GRB Coordinates Network, 6374, 1
- Prigozhin, G., et al. 2005, GRB Coordinates Network, 3402, 1
- Prochaska, J. X., Bloom, J. S., Chen, H. W., Hurley, K., Dressler, A., & Osip, D. 2003, GRB Coordinates Network, 2482, 1
- Prochaska, J. X., Ellison, S., Foley, R. J., Bloom, J. S., & Chen, H.-W. 2005a, GRB Coordinates Network, 3332, 1
- Prochaska, J. X., Bloom, J. S., Wright, J. T., Butler, R. P., Chen, H. W., Vogt, S. S., & Marcy, G. W. 2005b, GRB Coordinates Network, 3833, 1
- Prochaska, J. X., Foley, R., Tran, H., Bloom, J. S., & Chen, H.-W. 2006, GRB Coordinates Network, 4593, 1
- Prochaska, J. X., Thoene, C. C., Malesani, D., Fynbo, J. P. U., & Vreeswijk, P. M. 2007a, GRB Coordinates Network, 6698, 1
- Prochaska, J. X., Perley, D. A., Modjaz, M., Bloom, J. S., Poznanski, D., & Chen, H.-W. 2007b, GRB Coordinates Network, 6864, 1
- Pugliese, G., et al. 2005, A&A, 439, 527
- Quimby, R., Fox, D., Hoeflich, P., Roman, B., & Wheeler, J. C. 2005, GRB Coordinates Network, 4221, 1

- Racusin, J. L., & Barthelmy, S. D. 2007, GCNR, 84, 1 (2007), 84, 1
- Racusin, J., Cummings, J., & Schady, P. 2007, GCNR, 98, 2 (2007), 98, 2
- Rau, A., et al. 2004, A&A, 427, 815
- Rau, A., Salvato, M., & Greiner, J. 2005, A&A, 444, 425
- Reichart, D. E., et al. 1999, ApJ, 517, 692
- Resmi, L., et al. 2005, A&A, 440, 477
- Retter, A., Kennea, J., Burrows, D., Grupe, D., Nousek, J., & Gehrels, N. 2006, GRB Coordinates Network, 4434, 1
- Rhoads, J., Wilson, A., Storchi-Bergmann, T., & Fruchter, A. 2000, GRB Coordinates Network, 564, 1
- Rhoads, J. E., & Fruchter, A. S. 2001, ApJ, 546, 117
- Rol, E., Salamanca, I., Kaper, L., Vreeswijk, P., Lacerda, P., Hodgkin, S., Tzanavaris, P., & Tanvir, N. 2001, GRB Coordinates Network, 955, 1
- Rol, E., & Page, K. L. 2006, GRB Coordinates Network, 5406, 1
- Rol, E., Tanvir, N., & Mundell, C. 2006a, GRB Coordinates Network, 4855, 1
- Rol, E., Jakobsson, P., Tanvir, N., & Levan, A. 2006b, GRB Coordinates Network, 5555, 1
- Rol, E., et al. 2007a, MNRAS, 374, 1078
- Rol, E., et al. 2007b, ApJ, 669, 1098
- Rol, E., et al. 2007c, GRB Coordinates Network, 6221, 1
- Rol, E., Levan, A., Tanvir, N., Schirmer, M., & Castro-Tirado, A. J. 2007d, GRB Coordinates Network, 6174, 1
- Roy, R., Misra, K., & Pandey, S. B. 2007e, GRB Coordinates Network, 6880, 1
- Rumyantsev, V., Biryukov, V., Pozanenko, A., & Ibrahimov, M. 2005a, GRB Coordinates Network, 4094, 1
- Rumyantsev, V., Biryukov, V., Pozanenko, A., & Ibrahimov, M. 2005b, GRB Coordinates Network, 4087, 1

- Rumyantsev, V., & Pozanenko, A. 2007, GRB Coordinates Network, 6874, 1
- Rykoff, E. 2004a, GRB Coordinates Network, 2915, 1
- Rykoff, E. 2004b, GRB Coordinates Network, 2919, 1
- Rykoff, E. S., et al. 2004a, ApJ, 601, 1013
- Rykoff, E., McKay, T., & Swan, H. 2004b, GRB Coordinates Network, 2912, 1
- Rykoff, E. S., Rujopakarn, W., Yost, S. A., & Yuan, F. 2005, GRB Coordinates Network, 3779, 1
- Rykoff, E. S., et al. 2006, ApJ, 638, L5
- Rykoff, E. S., Yuan, F., & Yost, S. A. 2007, GRB Coordinates Network, 6497, 1
- Sahu, K. C., et al. 2000, ApJ, 540, 74
- Sakamoto, T., et al. 2005a, GRB Coordinates Network, 3189, 1
- Sakamoto, T., et al. 2005b, ApJ, 629, 311
- Sakamoto, T., Marshall, F., Stratta, G., Perri, M., Barthelmy, S. D., Burrows, D., Roming, P., & Gehrels, N. 2006, GCNR, 19, 1 (2006), 19, 1
- Sakamoto, T., Parsons, A., Page, K., Barthelmy, S. D., Burrows, D. N., Roming, P., & Gehrels, N. 2007, GCNR, 95, 2 (2007), 95, 2
- Sakamoto, T., et al. 2008, ApJS, 175, 179
- Salamanca, I., Rol, E., Wijers, R., Ellison, S., Kaper, L., & Tanvir, N. 2002, GRB Coordinates Network, 1611, 1
- Saracco, P., et al. 2001, GRB Coordinates Network, 1205, 1
- Sato, G., et al. 2007, GRB Coordinates Network, 7148, 1
- Sbarufatti, B., et al. 2007, GCNR, 67, 1 (2007), 67, 1
- Schady, P. 2006, GRB Coordinates Network, 5413, 1
- Schady, P., & Moretti, A. 2006, GRB Coordinates Network, 5296, 1
- Schady, P., & Parsons, A. M. 2007, GRB Coordinates Network, 6712, 1

- Schady, P., Evans, P. A., & Starling, R. L. C. 2007, GCNR, 87, 1 (2007), 87, 1
- Schaefer, B. E., et al. 1999, ApJ, 524, L103
- Schaefer, J., Savage, S., Hwang, S., Canterna, R., Nysewander, M., & Reichart, D. 2002a, GRB Coordinates Network, 1681, 1
- Schaefer, J., Savage, S., Canterna, R., Nysewander, M., Reichart, D., Henden, A., & Lamb, D. 2002b, GRB Coordinates Network, 1776, 1
- Schaefer, J., Gibbs, D., Nysewander, M., Canterna, R., & Reichart, D. 2003, GRB Coordinates Network, 2137, 1
- Shakhovskoy, D., Rumyantsev, V., Biryukov, V., & Pozanenko, A. 2007, GRB Coordinates Network, 6485, 1
- Sharapov, D., Abdullaeva, G., Ibrahimov, M., & Pozanenko, A. 2005a, GRB Coordinates Network, 4049, 1
- Sharapov, D., Ibrahimov, M., Pozanenko, A., & Rumyantsev, V. 2005b, GRB Coordinates Network, 4185, 1
- Sharapov, D., Ibrahimov, M., Pozanenko, A., & Rumyantsev, V. 2006a, GRB Coordinates Network, 4927, 1
- Sharapov, D., Ibrahimov, M., & Pozanenko, A. 2006b, GRB Coordinates Network, 4925, 1
- Sharapov, D., Pozanenko, A., Klunko, E., Ibrahimov, M., & Rumyantsev, V. 2006c, GRB Coordinates Network, 4956, 1
- Sharapov, D., Augusteijn, T., & Pozanenko, A. 2006d, GRB Coordinates Network, 5263, 1
- Shin, M.-S., & Berger, E. 2007, ApJ, 660, 1146
- Silvey, J., Allen, D., Canterna, R., & Price, P. A. 2003, GRB Coordinates Network, 2447, 1
- Smith, D. A., Rykoff, E. S., & Yost, S. A. 2005, GRB Coordinates Network, 3021, 1
- Soderberg, A., Djorgovski, S. G., Halpern, J. P., & Mirabal, N. 2004a, GRB Coordinates Network, 2837, 1
- Soderberg, A. M., Berger, E., & Ofek, E. 2005, GRB Coordinates Network, 4186, 1
- Soderberg, A. M., et al. 2006a, ApJ, 650, 261

- Soderberg, A. M., et al. 2007, ApJ, 661, 982
- Sollerman, J., et al. 2007, A&A, 466, 839
- Soyano, T., Mito, H., & Urata, Y. 2006, GRB Coordinates Network, 5548, 1
- Stamatikos, M., et al. 2006, GRB Coordinates Network, 5760, 1
- Stamatikos, M., et al. 2007a, GRB Coordinates Network, 6711, 1
- Stamatikos, M., Evans, P. A., Brown, P. J., Barthelmy, S. D., Burrows, D. N., Roming, P., & Gehrels, N. 2007b, GCNR, 107, 2 (2007), 107, 2
- Stanek, K. Z., Garnavich, P. M., Jha, S., & Berlind, P. 2000, GRB Coordinates Network, 709, 1
- Stanek, K. Z., et al. 2005, ApJ, 626, L5
- Stanek, K. Z., et al. 2007, ApJ, 654, L21
- Starling, R., Osborne, J. P., Page, K. L., & Marshall, F. E. 2007, GRB Coordinates Network, 6852, 1
- Starling, R. L. C., et al. 2007b, GCNR, 66, 3 (2007), 66, 3
- Stefanescu, A., Schrey, F., Kanbach, G., Duscha, S., Muhlegger, M., Prymak, N., & Steinle, H. 2006a, GRB Coordinates Network, 5291, 1
- Stefanescu, A., Schrey, F., Duscha, S., Kanbach, G., Muehlegger, M., Primak, N., & Steinle, H. 2006b, GRB Coordinates Network, 5623, 1
- Stefanescu, A., Duscha, S., Kanbach, G., Schrey, F., Slowikowska, A., & Steinle, H. 2007, GRB Coordinates Network, 6723, 1
- Stern, D., Perley, D. A., Reddy, N., Prochaska, J. X., Spinrad, H., & Dickinson, M. 2007, GRB Coordinates Network, 6928, 1
- Still, M., et al. 2005, ApJ, 635, 1187
- Stratta, G., et al. 2007a, A&A, 461, 485
- Stratta, G., et al. 2007b, A&A, 474, 827
- Stratta, G., Perri, M., Krimm, H., Oates, S. R., Barthelmy, S. D., Burrows, D. N., Roming, P., & Gehrels, N. 2007c, GCNR, 104, 2 (2007), 104, 2

- Stratta, G., Perri, M., Conciatore, M., Burrows, D., & Sato, G. 2007d, GRB Coordinates Network, 6119, 1
- Stroh, M. C., et al. 2007, GCNR, 99, 1 (2007), 99, 1
- Swan, H., Smith, I., Akerlof, C., Yost, S., & Skinner, M. 2006, GRB Coordinates Network, 4491, 1
- Swan, H., Smith, I., Akerlof, C., & Skinner, M. 2007, GRB Coordinates Network, 6472, 1
- Tagliaferri, G., et al. 2005, GRB Coordinates Network, 4222, 1
- Tam, P. H., Pun, C. S. J., Huang, Y. F., & Cheng, K. S. 2005, New Astronomy, 10, 535
- Tanvir, N., Rol, E., & Hewett, P. 2006, GRB Coordinates Network, 5216, 1
- Terada, H., Pyo, T.-S., Aoki, K., Hattori, T., & Kawai, N. 2007, GRB Coordinates Network, 6976, 1
- Terra, F., et al. 2006, GRB Coordinates Network, 5659, 1
- Terra, F., et al. 2007, GRB Coordinates Network, 6458, 1
- Thone, C., et al. 2005, GRB Coordinates Network, 4291, 1
- Thoene, C. C., Nilsson, K., Jensen, B. L., & Fynbo, J. 2006a, GRB Coordinates Network, 5003, 1
- Thoene, C. C., Jensen, B. L., Fynbo, J., & Solheim, J.-E. 2006b, GRB Coordinates Network, 5094, 1
- Thoene, C. C., et al. 2006c, GRB Coordinates Network, 5373, 1
- Thoene, C. C., Fynbo, J. P. U., Jakobsson, P., Vreeswijk, P. M., & Hjorth, J. 2006d, GRB Coordinates Network, 5812, 1
- Thoene, C. C., Malesani, D., Fynbo, J. P. U., Henriksen, C., & Sharapov, D. 2006e, GRB Coordinates Network, 5807, 1
- Thoene, C. C., Perley, D. A., & Bloom, J. S. 2007a, GRB Coordinates Network, 6663, 1
- Thoene, C. C., Kann, D. A., Augusteijn, T., & Reyle-Laffont, C. 2007b, GRB Coordinates Network, 6154, 1

- Thoene, C. C., Jaunsen, A. O., Fynbo, J. P. U., Jakobsson, P., & Vreeswijk, P. M. 2007c, GRB Coordinates Network, 6379, 1
- Thoene, C. C., Jakobsson, P., Fynbo, J. P. U., Malesani, D., Hjorth, J., & Vreeswijk, P. M. 2007d, GRB Coordinates Network, 6499, 1
- Thoene, C. C., Perley, D. A., Cooke, J., Bloom, J. S., Chen, H.-W., & Barton, E. 2007e, GRB Coordinates Network, 6741, 1
- Thorstensen, J., Uglesich, R., Halpern, J., Mirabal, N., Costa, E., Feroci, M., & Piro, L. 1999, GRB Coordinates Network, 423, 1
- Tiengo, A., Mereghetti, S., Ghisellini, G., Rossi, E., Ghirlanda, G., & Schartel, N. 2003, *A&A*, 409, 983
- Tinney, C., et al. 1998, IAU Circ., 6896, 1
- Tristram, P., Jelinek, M., de Ugarte Postigo, A., Gorosabel, J., Castro-Tirado, A. J., Castro Cerón, J. M., & Yock, P. 2005a, GRB Coordinates Network, 3151, 1
- Tristram, P., Jelinek, M., Castro-Tirado, A. J., de Ugarte Postigo, A., Guziy, S., Gorosabel, J., Yock, P., & Krimm, H. 2005b, GRB Coordinates Network, 4055, 1
- Uglesich, R., Mirabal, N., Halpern, J. P., Vanlandingham, K., Noel-Storr, J., Wagner, R. M., & Eskridge, P. 2000, GRB Coordinates Network, 663, 1
- Ukwatta, T. N., et al. 2007, GCNR, 106, 2 (2007), 106, 2
- Updike, A. C., Garimella, K. V., & Hartmann, D. H. 2006, GRB Coordinates Network, 5738, 1
- Updike, A. C., Puls, J., Hartmann, D. H., Wood, M., Cardenzana, J., & Pederson, S. 2007, GRB Coordinates Network, 6530, 1
- Urata, Y., et al. 2004, GRB Coordinates Network, 2662, 1
- Valle, M. D., et al. 2006, Nature, 444, 1050
- Vergani, S. D., et al. 2007, GCNR, 39, 2 (2007), 39, 2
- Vetere, L., Cummings, J., & Immler, S. 2007a, GCNR, 29, 1 (2007), 29, 1
- Vetere, L., Cummings, J., Holland, S. T., Bartthelmy, S. D., Burrows, D. N., Roming, P., & Gehrels, N. 2007b, GCNR, 55, 1 (2007), 55, 1

- Villasenor, J. S., et al. 2005, *Nature*, 437, 855
- Vrba, F. J., et al. 2000, *ApJ*, 528, 254
- Vreeswijk, P. M., et al. 1999a, *ApJ*, 523, 171
- Vreeswijk, P. M., et al. 1999b, *GRB Coordinates Network*, 324, 1
- Vreeswijk, P. M., et al. 1999c, *GRB Coordinates Network*, 496, 1
- Vreeswijk, P., Rol, E., Packham, C., Tanvir, N., Kouveliotou, C., Wijers, R., & Knapen, J. 2000, *GRB Coordinates Network*, 886, 1
- Vreeswijk, P. M., et al. 2001, *ApJ*, 546, 672
- Vreeswijk, P., Fruchter, A., Hjorth, J., & Kouveliotou, C. 2003, *GRB Coordinates Network*, 1785, 1
- Vreeswijk, P. M., et al. 2004, *A&A*, 419, 927
- Vreeswijk, P., & Jaunsen, A. 2006, *GRB Coordinates Network*, 4974, 1
- Vreeswijk, P. M., et al. 2006, *A&A*, 447, 145
- Wiersema, K., Starling, R. L. C., Rol, E., Vreeswijk, P., & Wijers, R. A. M. J. 2004, *GRB Coordinates Network*, 2800, 1
- Wiersema, K., Thoene, C. C., & Rol, E. 2006, *GRB Coordinates Network*, 5552, 1
- Wiersema, K., Rol, E., & Thoene, C. C. 2007, *GRB Coordinates Network*, 6188, 1
- Wiersema, K., et al. 2008, in preparation
- Xin, L. P., Zhai, M., Qiu, Y. L., Wei, J. Y., Hu, J. Y., Deng, J. S., Urata, Y., & Zheng, W. K. 2007a, *GRB Coordinates Network*, 6747, 1
- Xin, L. P., et al. 2007b, *GRB Coordinates Network*, 6965, 1
- Xin, L. P., et al. 2007c, *GRB Coordinates Network*, 6956, 1
- Xin, L. P., Zhai, M., Qiu, Y. L., Wei, J. Y., Hu, J. Y., Deng, J. S., Wang, J., & Zheng, W. K. 2007d, *GRB Coordinates Network*, 7015, 1
- Yanagisawa, K., Toda, H., & Kawai, N. 2006a, *GRB Coordinates Network*, 4496, 1
- Yanagisawa, K., Toda, H., & Kawai, N. 2006b, *GRB Coordinates Network*, 4517, 1

- Yoshida, A., et al. 2002, GRB Coordinates Network, 1686, 1
- Yoshida, M., Yanagisawa, K., & Kawai, N. 2007a, GRB Coordinates Network, 6123, 1
- Yoshida, M., Yanagisawa, K., Shimizu, Y., Nagayama, S., Toda, H., & Kawai, N. 2007b,
GRB Coordinates Network, 7119, 1
- Yost, S. A., et al. 2006, ApJ, 636, 959
- Zheng, W. K., et al. 2007, GRB Coordinates Network, 6250, 1
- Ziaeepour, H., Barthelmy, S. D., Parsons, A., Page, K. L., de Pasquale, M., & Schady, P.
2007a, GCNR, 74, 2 (2007), 74, 2
- Ziaeepour, H., Barthelmy, S. D., Sakamoto, T., Evans, P. A., Page, K. L., & Schady, P.
2007b, GCNR, 72, 2 (2007), 72, 2
- Zimmerman, N., & Tyagi, S. 2006, GRB Coordinates Network, 4440, 1
- Zhu, J. 2000, GRB Coordinates Network, 904, 1
- Zhu, J. 2001, GRB Coordinates Network, 946, 1